(Brief Remarks on) Baryon Spectroscopy

Michael Döring

THE GEORGE WASHINGTON UNIVERSITY
WASHINGTON, DC

Jefferson Lab

Hadronic Physics with Lepton and Hadron Beams

Jefferson Lab, September 5-8

Thanks for slides:
Rönchen, Mai, Landay, Nakayama, Burkert,...

Supported by

National Science Foundation

HPC support by JSC grant *jikp07*

JÜLICH FORSCHUNGSZENTRUM

DOE DE-AC05-06OR23177 & DE-SC0016582; NSF PIF 1415459 & CAREER PHY-1452055

Outline

- (Theoretical) Motivation
- Phenomenology: Kaon photoproduction, model selection, ...
- [Form factors]

Motivation and overview

The Missing Resonance Problem

Overview: Int.J.Mod.Phys. E22 (2013) 1330015

Experimental study of hadronic reactions

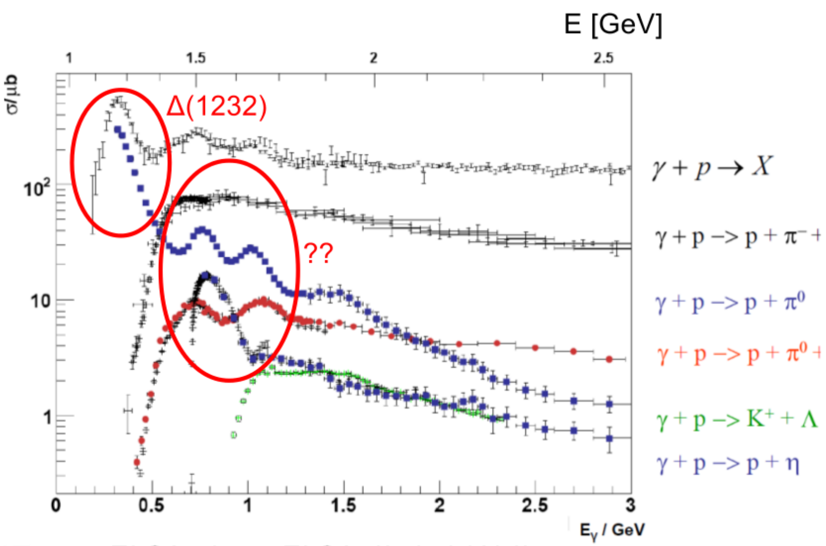

source: ELSA; data: ELSA, JLab, MAMI

$\Longleftrightarrow$

Theoretical predictions of excited hadrons
e.g. from lattice calculations:

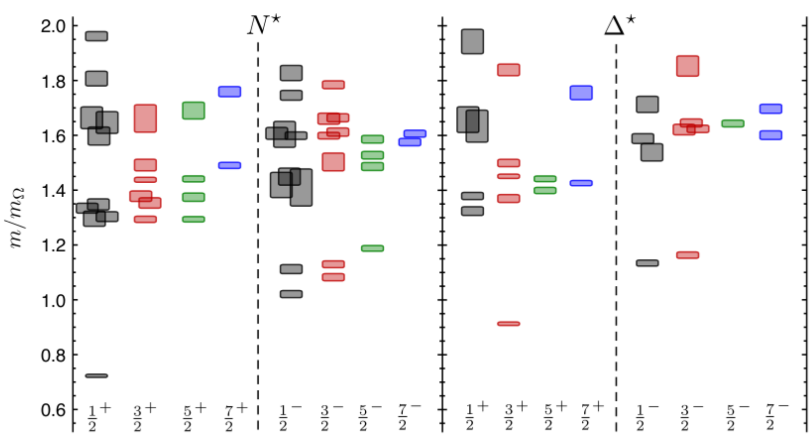

$m_\pi = 396$ MeV [Edwards *et al.*, Phys.Rev. D84 (2011)]

$\Rightarrow$ Partial wave decomposition:
decompose data with respect to a conserved quantum number: J^P

Missing resonance problem

→ Simultaneously analyze pion- and photon-induced reactions

Hybrid Baryons

J.J. Dudek and R.G. Edwards, PRD85 (2012) 054016

Unusual transition FF?

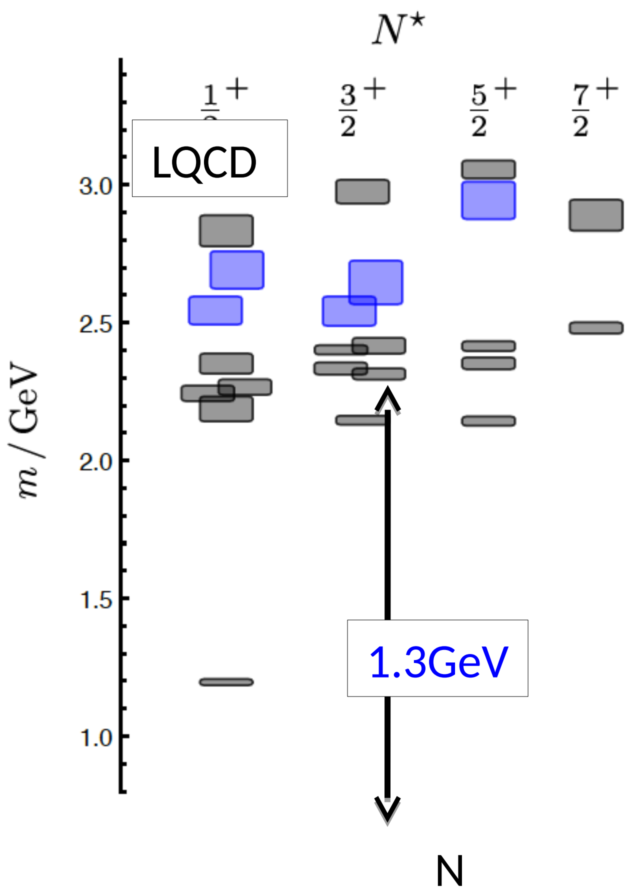

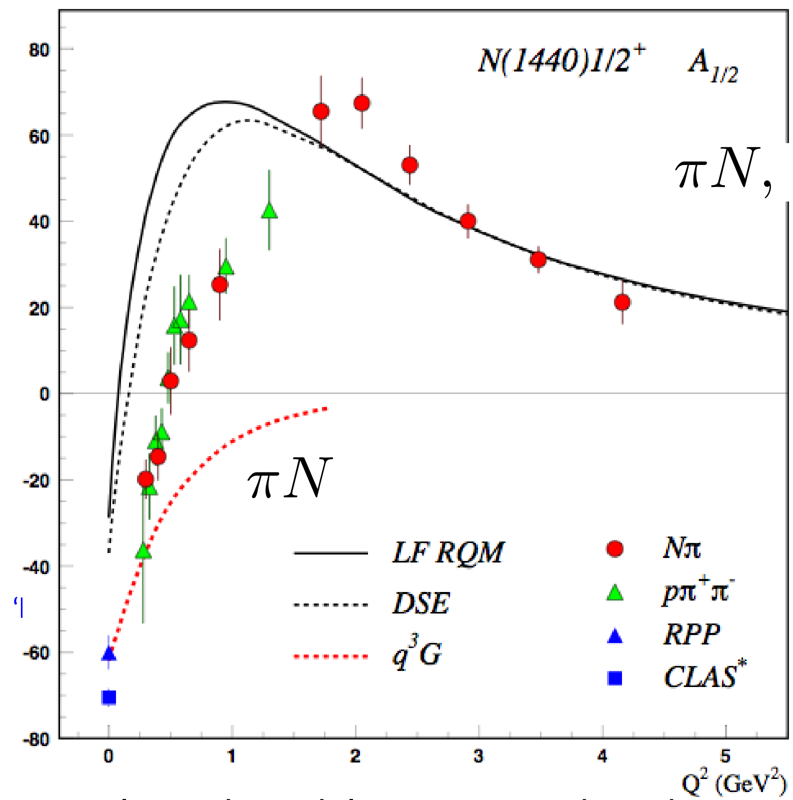

$\pi N,\ \sigma(\pi\pi)N,\ \pi\Delta(\pi N)$

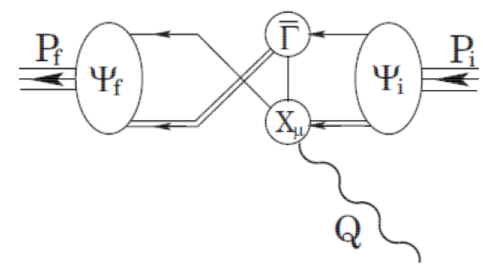

[source: Int. J. Mod. Phys. (2013)]

Rel. quark model: Aznauryan (2007)
Dyson-Schwinger: Wilson, Cloet, Chang, C. D. Roberts (2012)

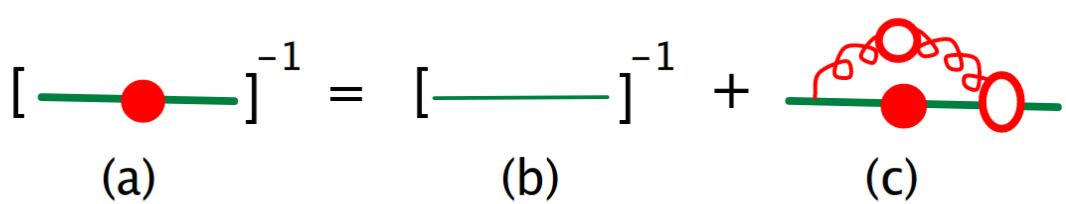

Hybrid states have same J^P values as q^3 baryons. How to identify them? → Measure Q^2 dependence of electro-couplings (CLAS 12)

Using ONLY meson-baryon degrees of freedom (no explicit quark dynamics):

Manifestly gauge invariant approach based on full BSE solution

[M. Mai, P.C. Bruns, U.-G. Meissner PRD 86 (2012) 094033 [arXiv:1207.4923]

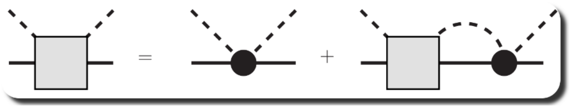

Gauge invariance

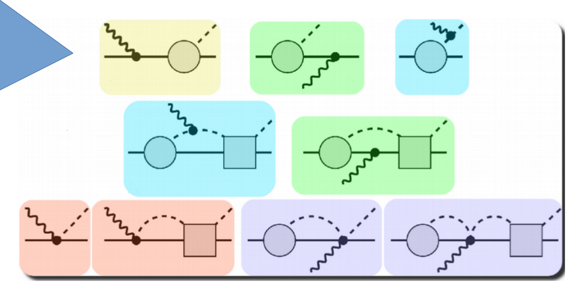

Fit

Prediction

- Exact unitary meson-baryon scattering amplitude T with parameters, fixed to reproduce:
  - πN-partial wave S_{11} and S_{31} for $\sqrt{s} < 1560$ MeV

    Arndt et al. (2012)
  - $\pi^- p \to \eta n$ differential cross sections

    Prakhov et al. (2005)

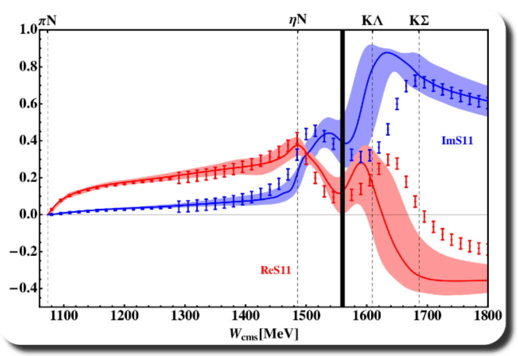

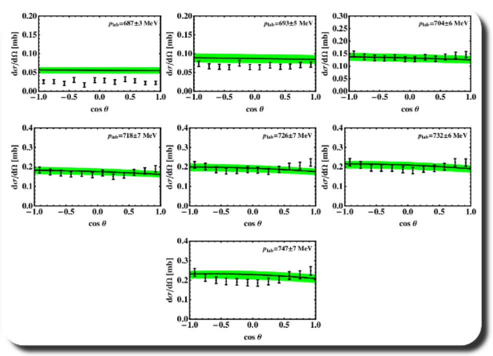

II. $E_{0+}(\pi N)$ to be compared with SAID and MAID2007 analyses:

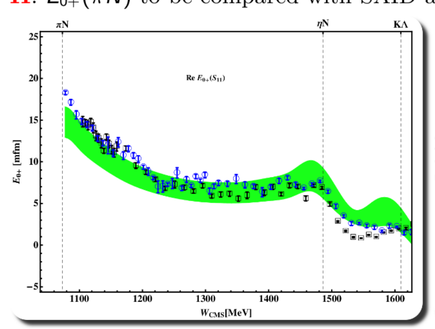

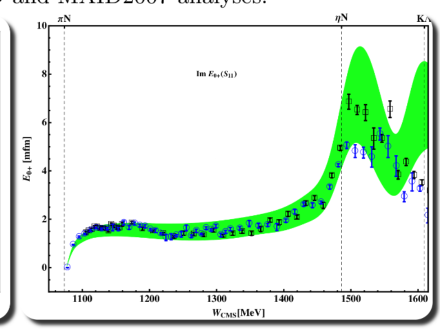

→ Making the “Missing resonance problem” worse ?!

Measured reactions (incomplete)

- Bonn-Gatchina: $(\pi N \to \pi N), \to \eta N, K\Lambda, K\Sigma, \pi\pi N, \omega N$
  $\gamma p \to \pi N; \to \eta N, K\Lambda, K\Sigma, \pi\pi N, \omega N, \eta' N$
  $\gamma n \to \pi N$
- Giessen: $(\pi N \to \pi N), \to \eta N, K\Lambda, K\Sigma, (\pi\pi N), \omega N$
  $\gamma p \to \pi N; \to \eta N, K\Lambda, K\Sigma, \omega N$
- SAID: $\pi N \to \pi N; \to \eta N,\ \gamma p \to \pi N,\ \gamma n \to \pi N; \gamma^* p \to \pi N$
- MAID: $(\pi N \to \pi N);\ \gamma p \to \pi N,\ (\to \eta N, \to K\Lambda),\ \gamma n \to \pi N; \gamma^* p \to \pi N$
- ANL-Osaka: $(\pi N \to \pi N), \to \eta N, K\Lambda, K\Sigma, \pi\pi N$
  $\gamma p \to \pi N; \to \eta N, K\Lambda, \pi\pi N; (\gamma^* p \to \pi N)$
- Jülich-Bonn: $(\pi N \to \pi N), \to \eta N, K\Lambda, K\Sigma$
  $\gamma p \to \pi N; \to \eta N, K\Lambda$
- JLAB-MSU: $\gamma^* N \to \pi\pi N$

Mindmap

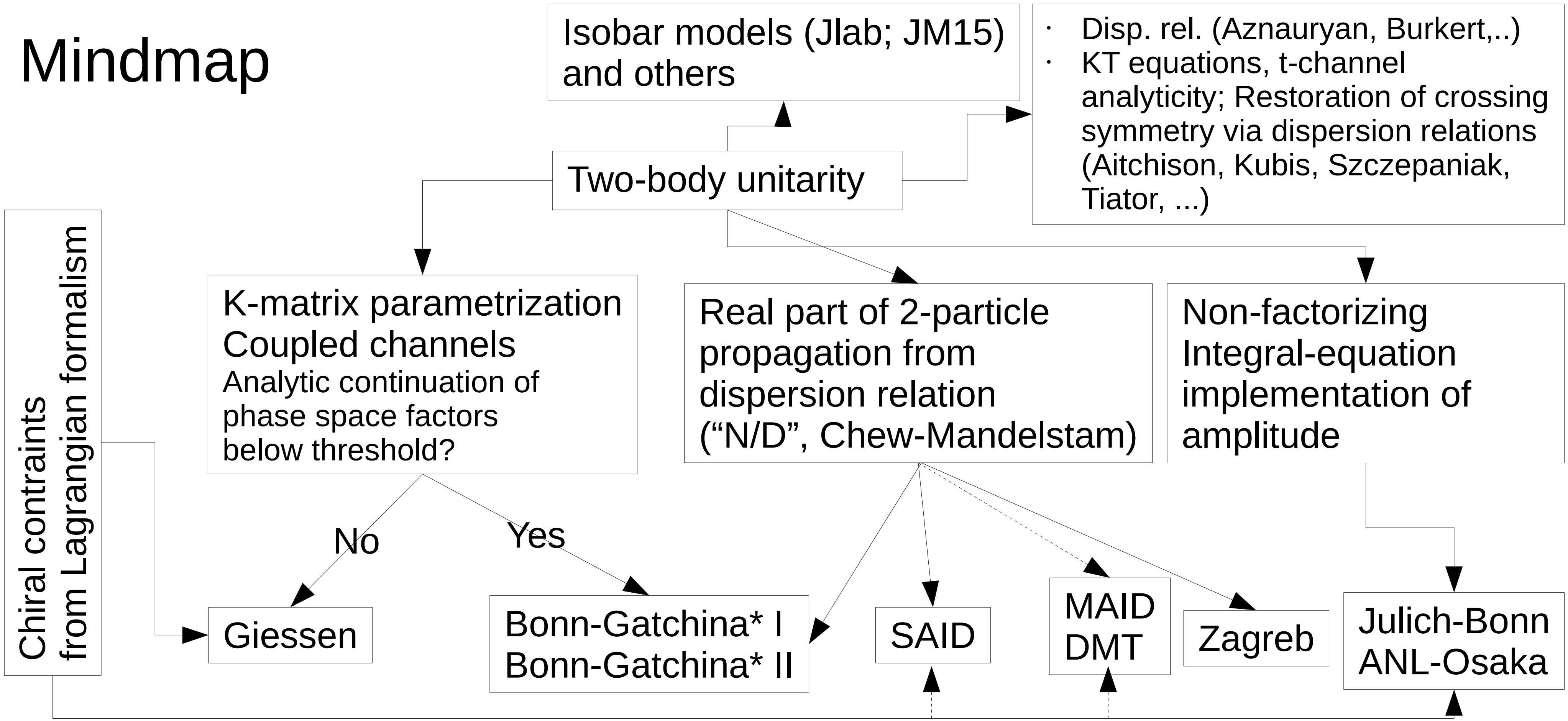

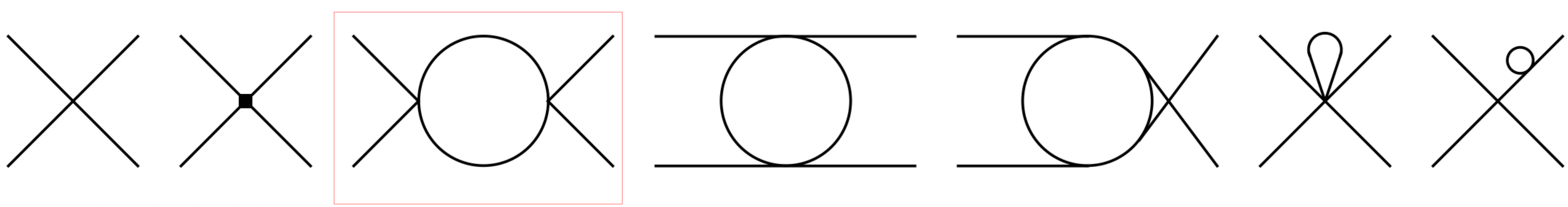

Unitarity loop

vs.

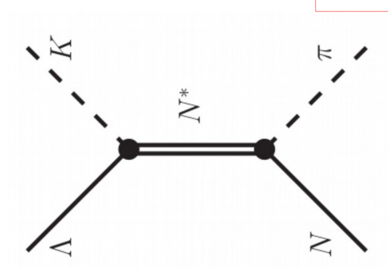

* largest set of analyzed reactions

Mindmap

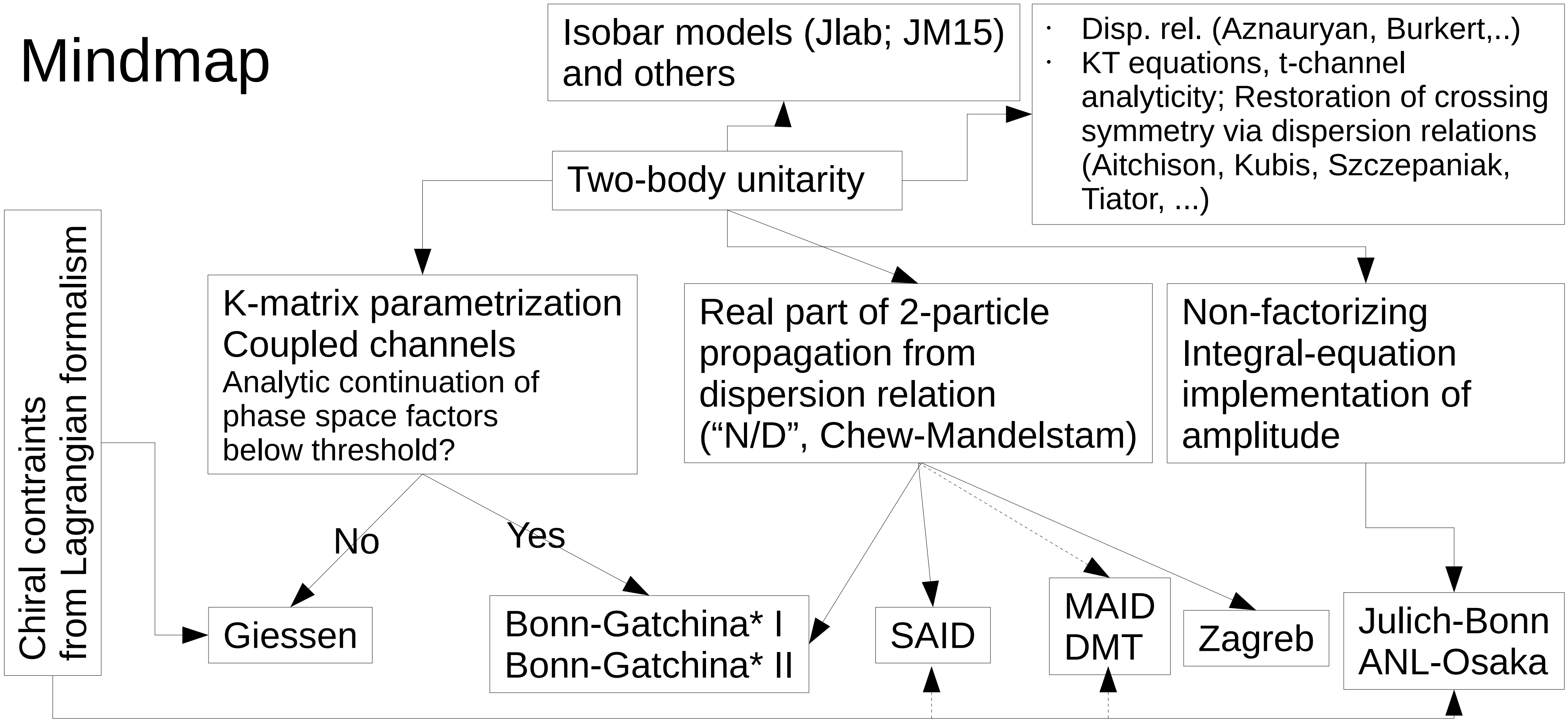

<table>
<tr><th></th><th>Giessen</th><th>Bonn-Gatchina</th><th>SAID</th><th>MAID / DMT</th><th>Zagreb</th><th>Julich-Bonn / ANL-Osaka</th></tr>
<tr><td>Explicit resonance Terms?</td><td>Yes</td><td>Yes</td><td>No</td><td>(Yes)</td><td>Yes</td><td>Yes/No</td></tr>
<tr><td>Analyticity (math.)</td><td>No</td><td>Yes</td><td>Yes</td><td>Yes</td><td>Yes</td><td>Yes</td></tr>
<tr><td>Analyticity (disp.)</td><td>No</td><td>No/Yes</td><td>Yes</td><td></td><td></td><td>Yes</td></tr>
<tr><td>Effective $\pi\pi N$?</td><td colspan="6">Yes</td></tr>
<tr><td>Three-body unitarity?</td><td colspan="5">No</td><td>Yes</td></tr>
</table>

* largest set of analyzed reactions

One aspect: Three-Body Unitarity

[**GWU & JPAC** (Mai, Hu, M.D., Pilloni, Szczepaniak) EPJA (2017), arXiv: 1706.06118 [nucl-th]]

Unitary isobar parametrization

2→ 2 scattering input for isobars ($\pi\pi$)
(not necessarily resonant)

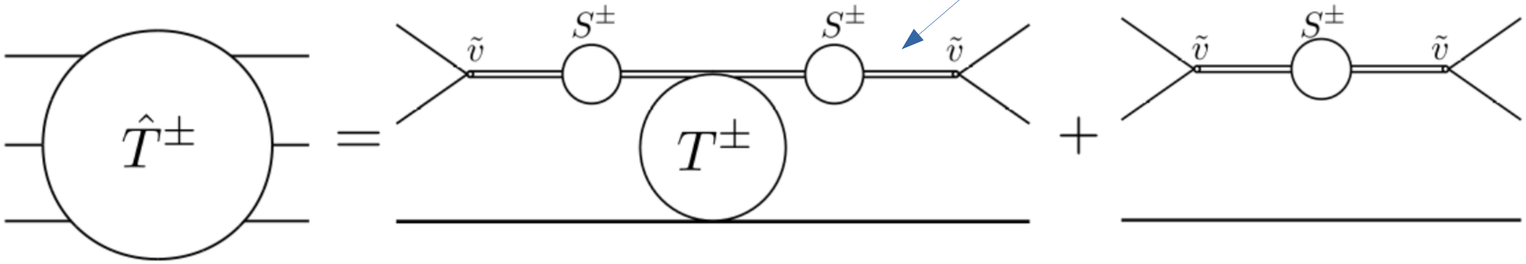

Unitarity

$$\langle q_1, q_2, q_3|(\hat{T}^{+} - \hat{T}^{-})|p_1, p_2, p_3\rangle = i\int \left(\prod_{\ell=1}^{3} \frac{\mathrm{d}^4 k_\ell}{(2\pi)^4}\,(2\pi)\delta^{+}(k_\ell^2 - m^2)\right)(2\pi)^4\delta^4\left(P - \sum_{\ell=1}^{3} k_\ell\right)$$

$$\times\,\langle q_1, q_2, q_3|\hat{T}^{-}|k_1, k_2, k_3\rangle\,\langle k_1, k_2, k_3|\hat{T}^{+}|p_1, p_2, p_3\rangle\,,$$

Bethe-Salpeter Eq. (BSE) ansatz

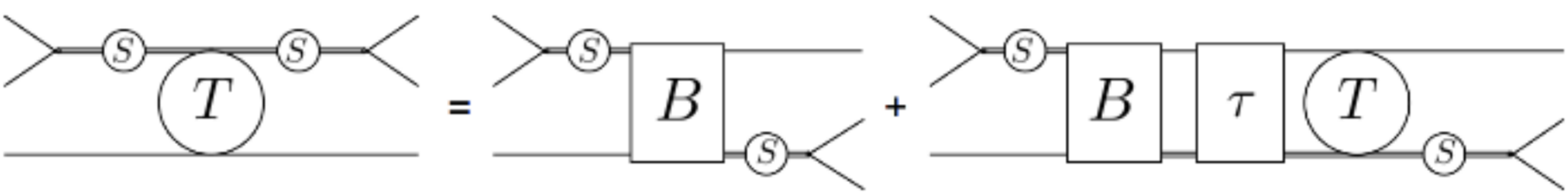

Strategy: To obtain a 3-body unitary amplitude, compare the right-hand sides of unitarity relation, both for generic isobar structure and BSE [Aaron, Amamdo, Young, PR (1969)]

Unitarity above breakup

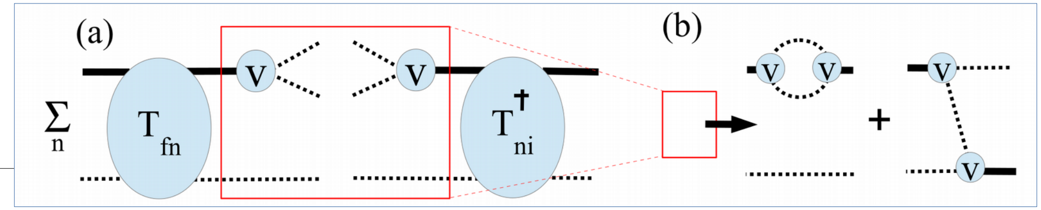

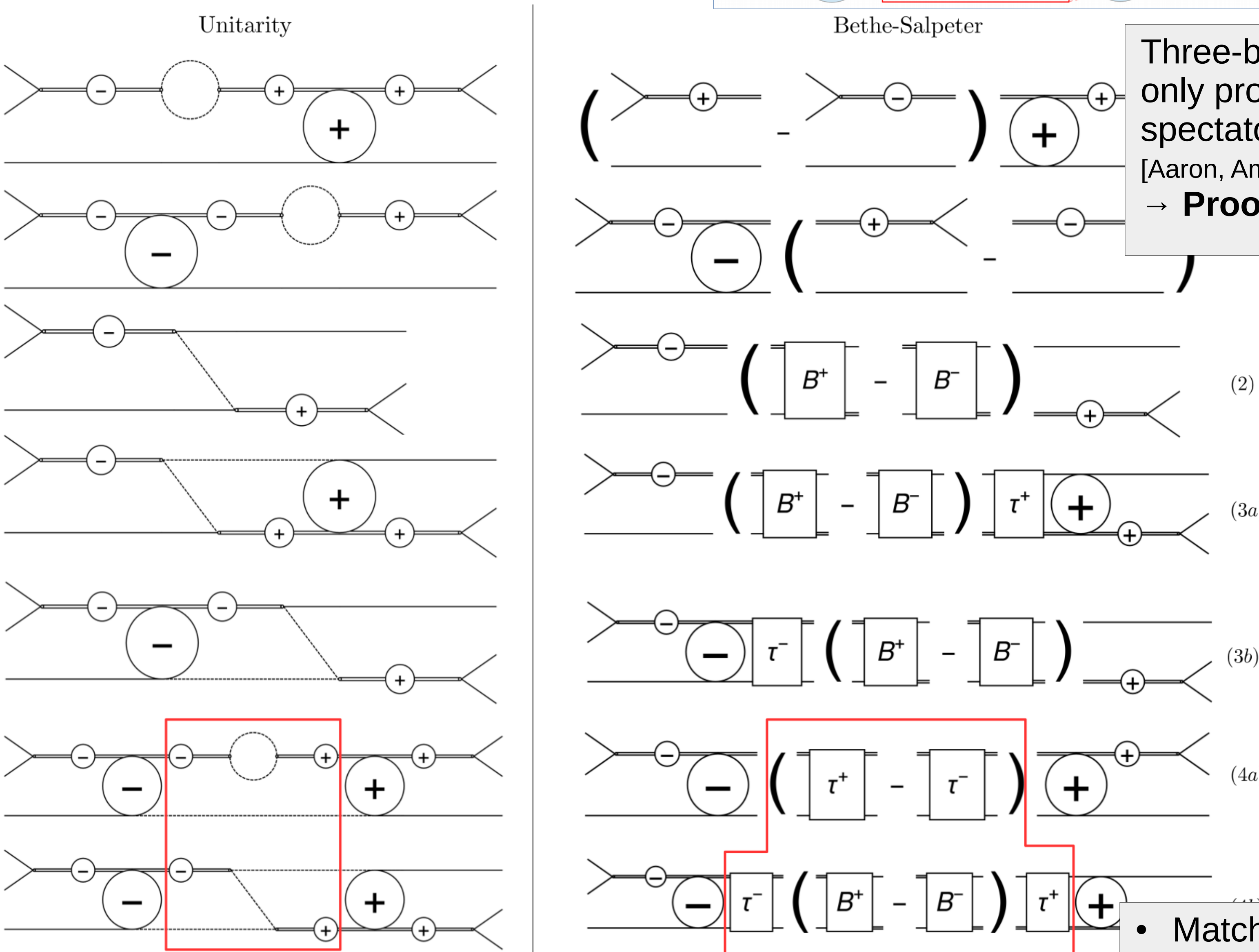

Three-body unitarity for isobars only proven for bound state-spectator scattering
[Aaron, Amamdo, Young, PR (1969)]
→ **Proof above breakup needed**!

Bound-state particle scattering requires only comparing these.

- Match Ansatz to unitarity
- Determine three-body amplitude
- Consistency of matching relations shown.
- Proof finished

Solution

"Diagrammatic" illustration:

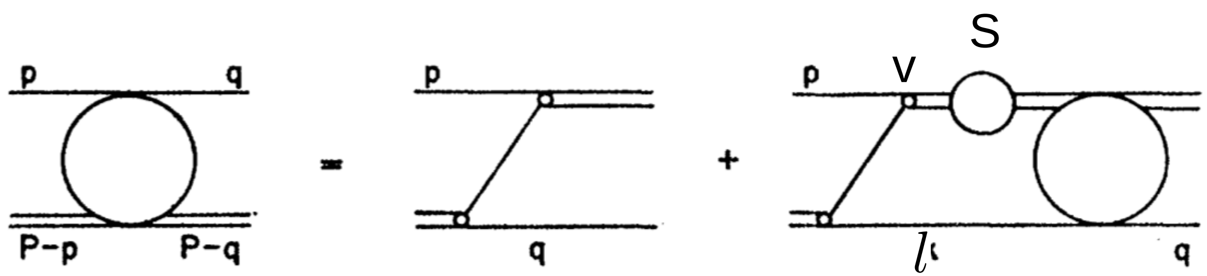

$$\langle p|T(s)|q\rangle = \frac{v(P-p-q,q)v(P-p-q,p)}{(P-p-q)^2-m^2} + \int \frac{\mathrm{d}^3 l}{(2\pi)^3}\frac{1}{2E_l}\frac{v(P-p-l,l)v(P-p-l,p)}{(P-p-l)^2-m^2}\frac{1}{D(\sigma(l))}\langle l|T(s)|q\rangle$$

- Three-body unitarity induces two-body unitarity of the sub-amplitude

- Re-arranging gives solution of 3→3 scattering in terms of on-shell 2→2 amplitude $T_{22} = vSv$

$$\langle q_1, q_2, q_3|\hat{T}_c(s)|p_1, p_2, p_3\rangle = \frac{1}{3!}\sum_{n=1}^{3}\sum_{m=1}^{3} T_{22}(\sigma_{\mathbf{q}_n})\tilde{T}_{\mathbf{q}_n\mathbf{p}_m}(s)T_{22}(\sigma_{\mathbf{p}_m})$$

$$\tilde{T}_{\mathbf{qp}}(s) = \frac{1}{(P-p-q)^2-m^2} + \int \frac{\mathrm{d}^3\boldsymbol{\ell}}{(2\pi)^3}\frac{1}{2E_{\boldsymbol{\ell}}}\frac{T_{22}(\sigma_{\boldsymbol{\ell}})}{(P-p-\ell)^2-m^2}\tilde{T}_{\boldsymbol{\ell}\mathbf{q}}(s)$$

- 3-body equation is of integral type; not further reducible like in 2-body.

- Three-body forces can (and have to be) be included straightforwardly.
- Not an approximation in description of physical on-shell three-body states, rather an organization scheme in terms of quantum numbers – resonant or non-resonant.
- May be parametrized in terms of microscopic description (→ ANL/Osaka, Julich-Bonn) or be left at dispersive level (choice).
- Three-body unitarity fully dictates the imaginary parts of the amplitude in the physical region.

→ dictates the divergences in finite volume.

→ How to relate excited baryons to lattice QCD simulations?

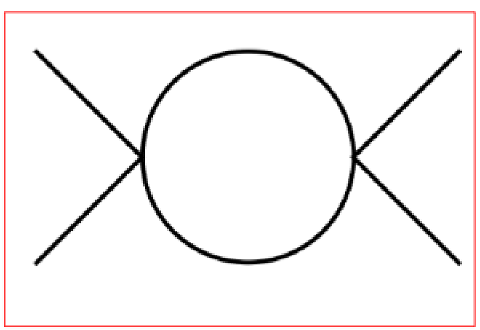

↔

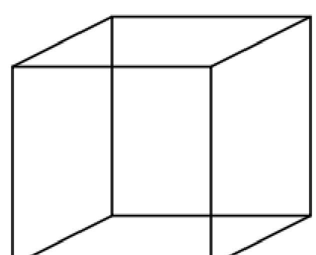

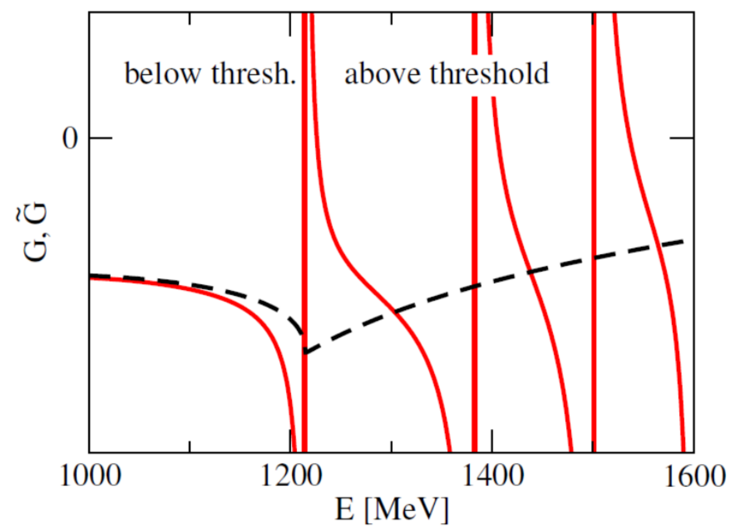

- Extensive effort in recent years (very non-complete list):

K. Polejaeva and A. Rusetsky, Eur. Phys. J. A **48** (2012) 67

R. A. Briceno and Z. Davoudi, Phys. Rev. D **87** (2013) 094507

L. Roca and E. Oset, Phys. Rev. D **85** (2012) 054507

S. Kreuzer and H. W. Grießhammer, Eur. Phys. J. A **48** (2012) 93

P. Guo, Phys. Rev. D **95** (2017) 054508

R. A. Briceño, M. T. Hansen and S. R. Sharpe, arXiv:1701.07465 [hep-lat]

H.-W. Hammer, J.-Y. Pang and A. Rusetsky, arXiv:1707.02176 [hep-lat]

- Roper on lattice from BGR group [Lang et al., Phys.Rev. D95 (2017), 014510]

$M_\pi \approx 156\,\mathrm{MeV}$

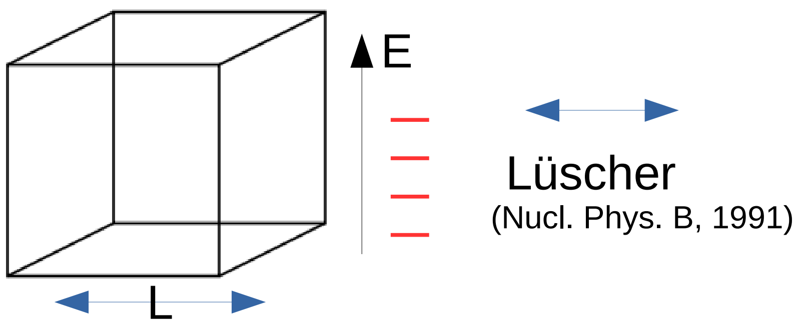

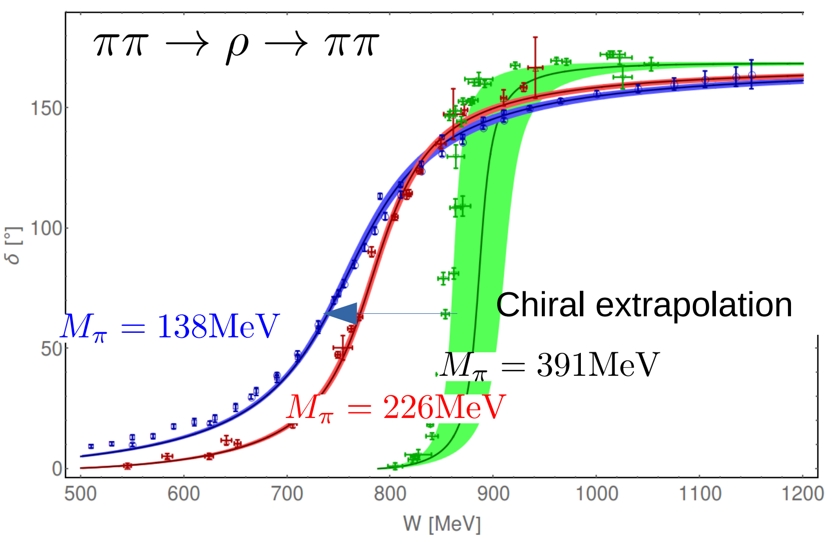

Data: HadronSpectrum (Dudek, PRD 2013,Briceño PRL 2016);
Analysis: M.D., B. Hu, M. Mai, arXiv 1610.10070
See also: Bolton, Briceno, Wilson, Phys.Lett. B757 (2016) 50

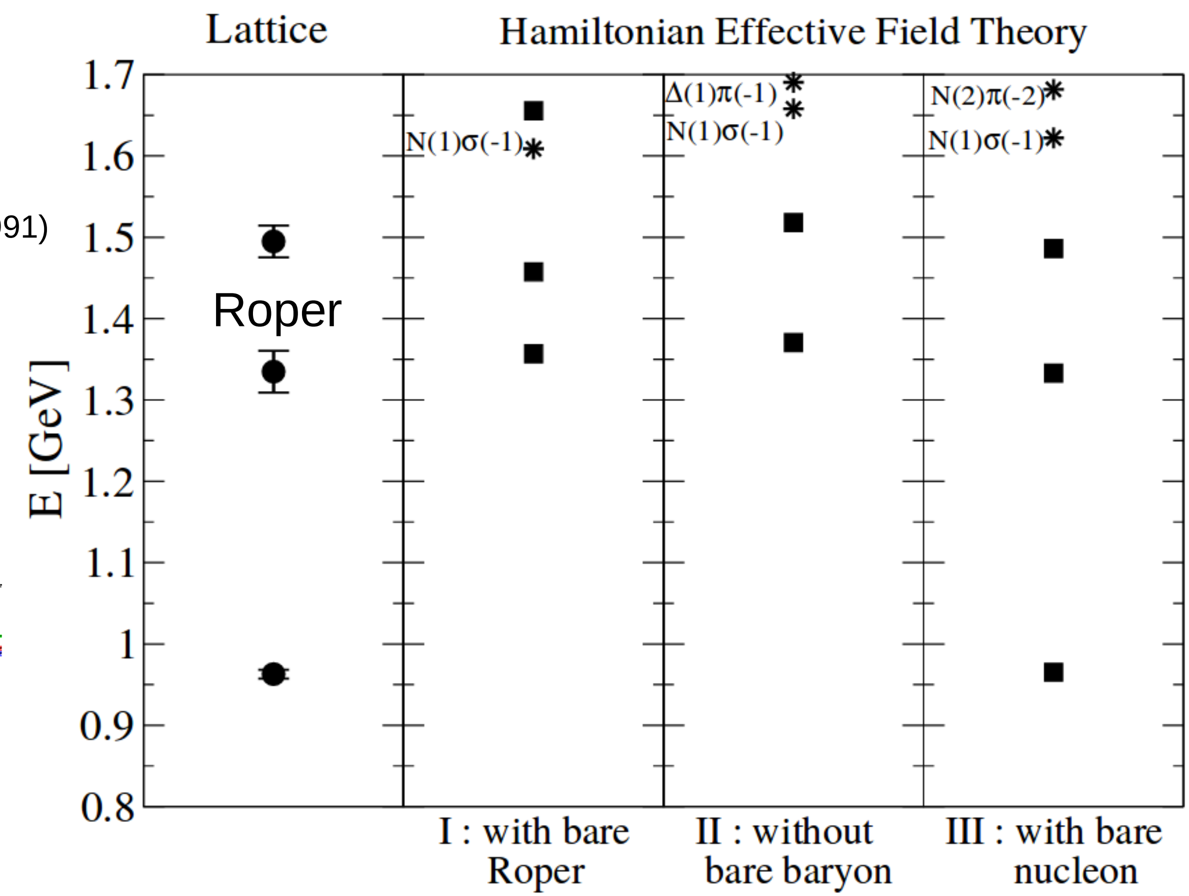

Hamiltonian finite volume approach [Liu et al., Phys.Rev. D95 (2017) 034034]; **stable** sigma meson

Channels:
$\pi N, \eta N, \pi\pi N(\sigma N, \pi\Delta, \dots)$
Genuine three-body dynamics

3 Bodies in finite volume

M. Mai, M.D., in progress

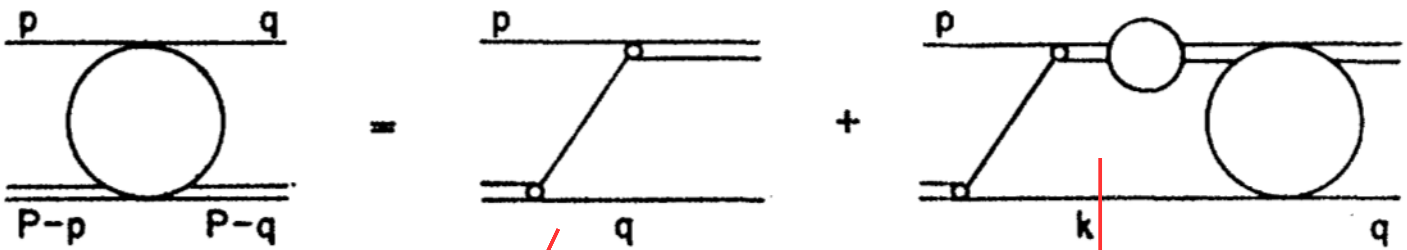

S-wave infinite volume vs. A_1^+ finite volume

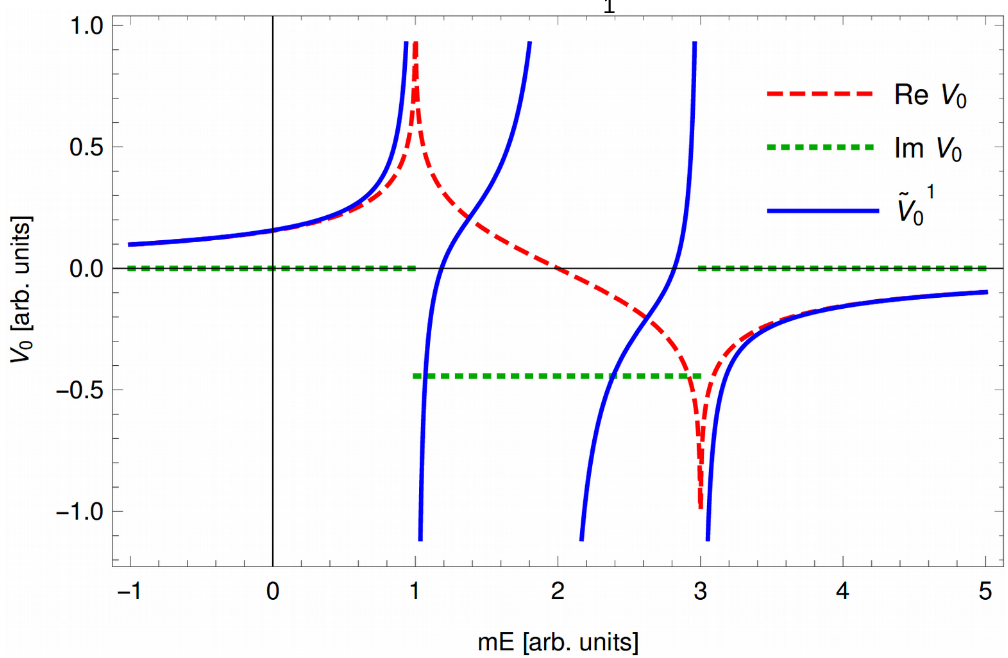

Tower of boosted $2 \to 2$ amplitudes to implement 3-body quantization condition

Power-law finite-volume effects dictated by three-body unitarity

Finite volume spectrum

M. Mai, M.D., in progress

- Spinless particles; isobar S-wave decay

Lattice measures poles

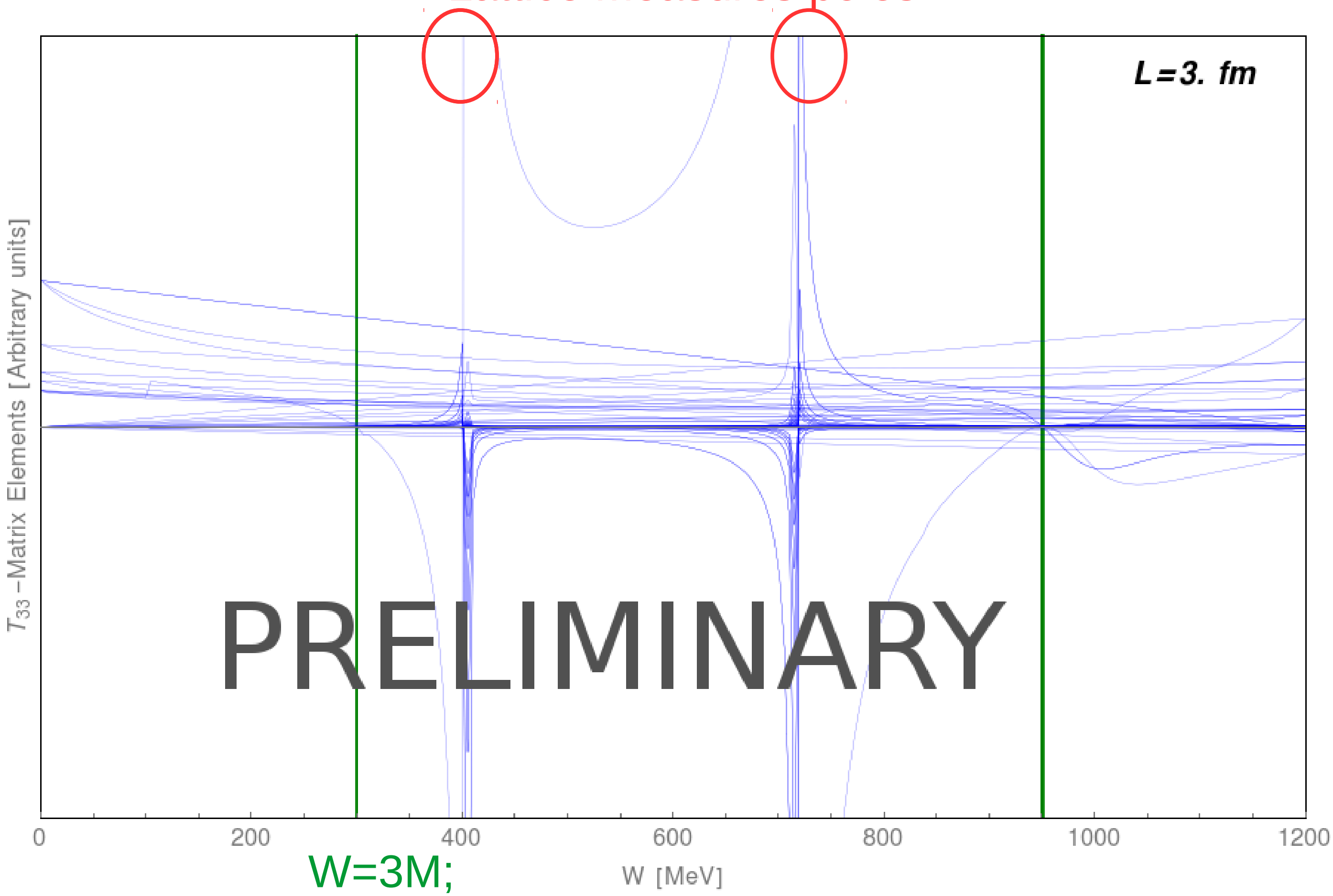

W=3M; threshold

- Isobar-spectator in A_1
- Organization of amplitude in shells |**p**|=n
- Each blue line is a transition from shell i ↔ j (i,j=0,…,8)
- Genuine three-body poles in T(3→3) give the finite-volume eigenvalues
- Green lines are free 3-body energies

Phenomenology

Convergence in Baryon Spectroscopy

Common analysis of BnGa, JuBo, MAID, SAID groups to assess systematic uncertainties

[A.V. Anisovich, R. Beck, M.D. *et al.*, EPJA(2016)]

Data:
J. Hartmann et al. [CBELSA/TAPS Collaboration], Phys. Lett. B 748, 212 (2015).
A. Thiel et al. [CBELSA/TAPS Collaboration], arXiv:1604.02922 [nucl-ex]
M. Gottschall et al. [CBELSA/TAPS Collaboration], in preparation.

- How do differences in Partial-Wave Analyses behave once a set of new high-precision polarization measurements is included?
  →
- Compare “Before” and “After” including sets of new high-precision polarization observables
- Calculate variance(s) of multipoles

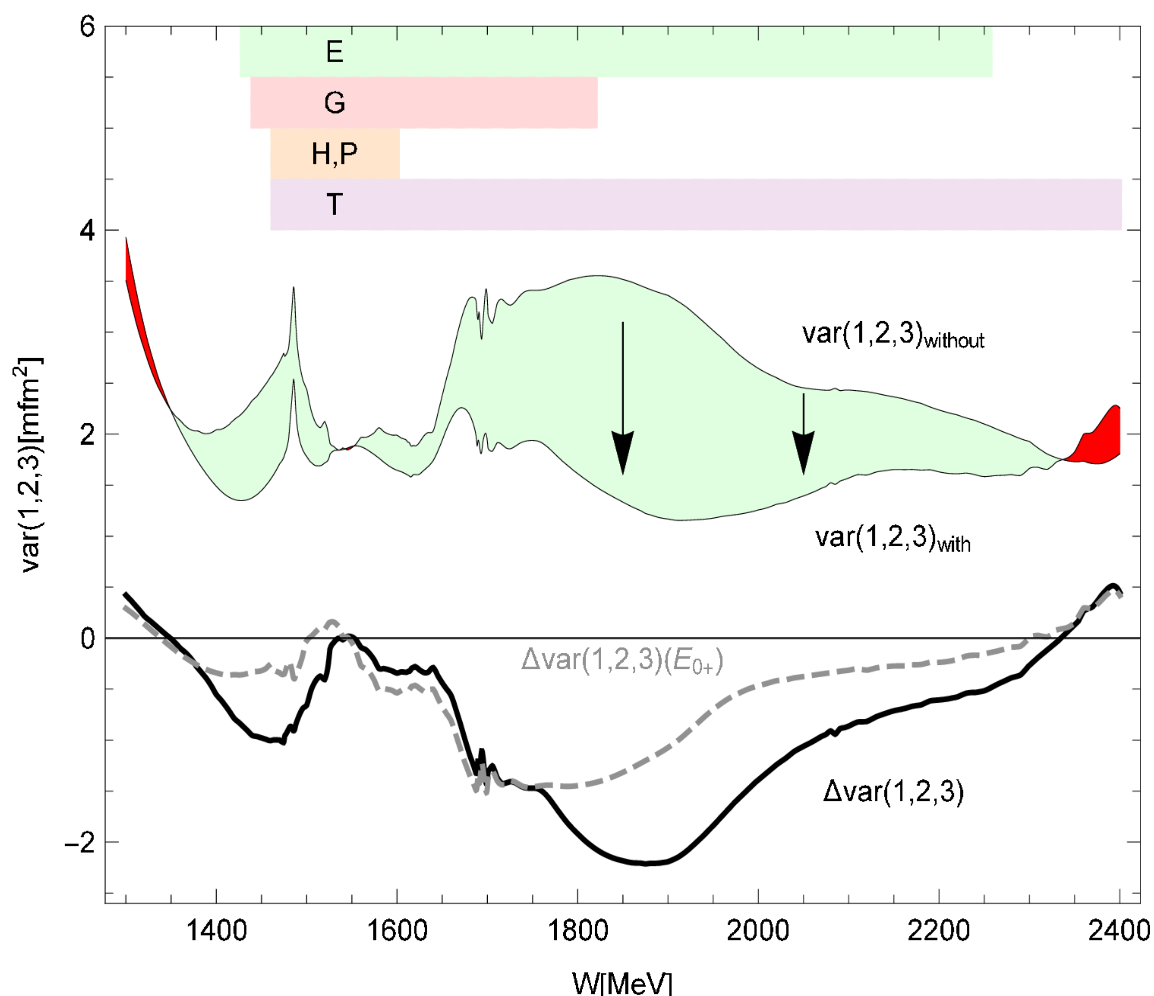

The Julich-Bonn Dynamical Coupled-Channel Approach

e.g. EPJ A 49, 44 (2013)

Dynamical coupled-channels (DCC): **simultaneous** analysis of different reactions

The scattering equation in partial-wave basis

$$\langle L'S'p'|T^{IJ}_{\mu\nu}|LSp\rangle = \langle L'S'p'|V^{IJ}_{\mu\nu}|LSp\rangle + \sum_{\gamma,L''S''}\int_0^\infty dq\quad q^2 \quad \langle L'S'p'|V^{IJ}_{\mu\gamma}|L''S''q\rangle \frac{1}{E-E_\gamma(q)+i\epsilon}\langle L''S''q|T^{IJ}_{\gamma\nu}|LSp\rangle$$

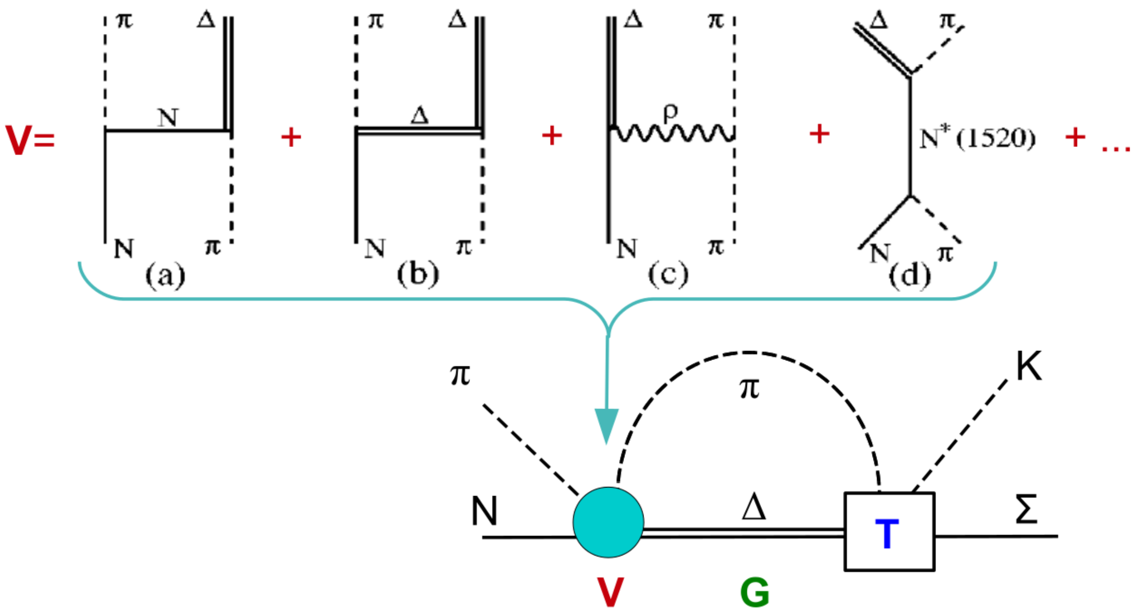

- potentials V constructed from effective $\mathcal{L}$
- s-channel diagrams: T^P

  genuine resonance states
- t- and u-channel: T^{NP}

  dynamical generation of poles

  partial waves strongly correlated

Analytic structure

[M.D. et al, NPA (2009)]

Resonance states: **Poles in the T-matrix** on the 2^{nd} Riemann sheet

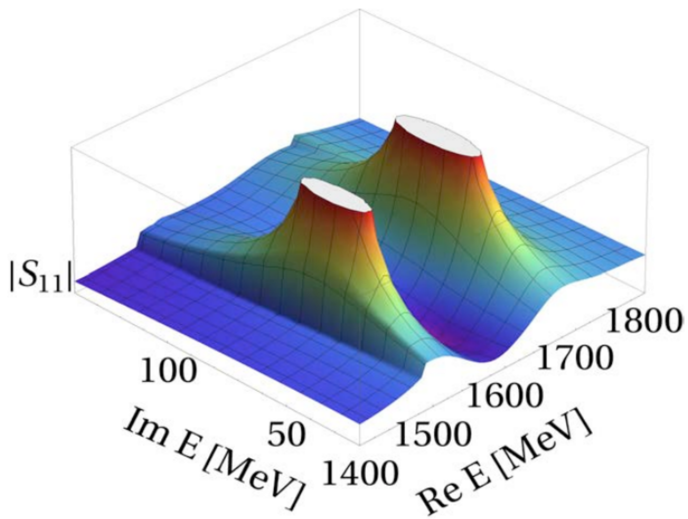

$\mathrm{Re}(E_0)$ = "mass", $-2\mathrm{Im}(E_0)$ = "width"

- pole position E_0 is the same in all channels
- residues$\rightarrow$ branching ratios

- (2-body) unitarity and analyticity respected
- 3-body $\pi\pi N$ channel:
  - parameterized effectively as $\pi\Delta$, σN, ρN
  - $\pi N/\pi\pi$ subsystems fit the respective phase shifts

  ↳ branch points move into complex plane

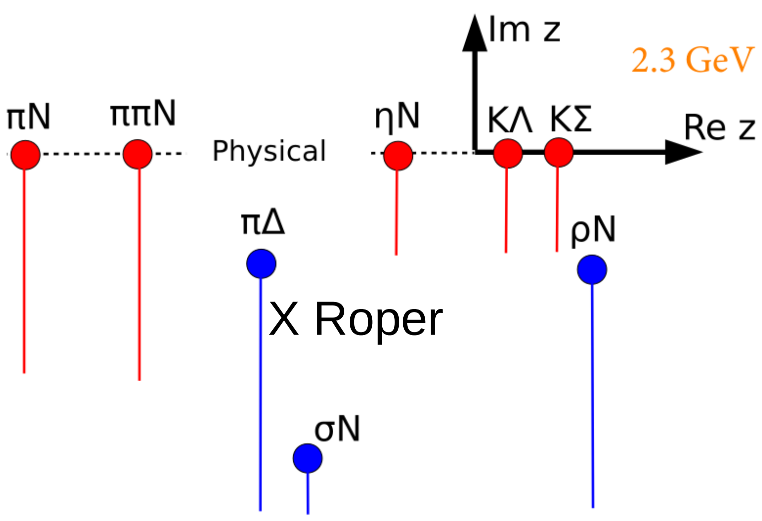

Photon-induced Reactions

- **simultaneous** fit of $\gamma p \to \pi^0 p\,,\ \pi^+ n\,,\ \eta p,\ K^+\Lambda$ & $\pi N \to \pi N\,,\ \eta N\,,\ K\Lambda\,,\ K\Sigma$
- $\sim$ 40.000 data points, $\sim$ 500 free parameters
  ↳ fit with JURECA supercomputer: parallelization in energy ($\sim$ 300 - 400 processes)

Kaon-photoproduction

Measurement of **recoil polarization** easier due to self-analysing decay of hyperons

→ more recoil and beam-recoil data available

→ possibility of finding new, so far missing states? (**“missing resonances problem”**)

$N(1440)$ PHOTON DECAY AMPLITUDES AT THE POLE

$N(1440) \to p\gamma$, helicity-1/2 amplitude $A_{1/2}$

MODULUS ($GeV^{-1/2}$)	*PHASE ($^\circ$)*	*DOCUMENT ID*		*TECN*	*COMMENT*
-0.044 ± 0.005	-40 ± 8	SOKHOYAN	15A	DPWA	Multichannel
$-0.054^{+0.004}_{-0.003}$	5^{+2}_{-5}	ROENCHEN	14	DPWA	

Preliminary: $K^+\Lambda$ photoproduction in the JüBo model

simultaneous fit of $\gamma p \to \pi^0 p$, $\pi^+ n$, ηp, $K^+\Lambda$ and $\pi N \to \pi N$, ηN , $K\Lambda$, $K\Sigma$

$\gamma p \to K^+\Lambda$:

D. Rönchen et al., in progress

- Differential cross section

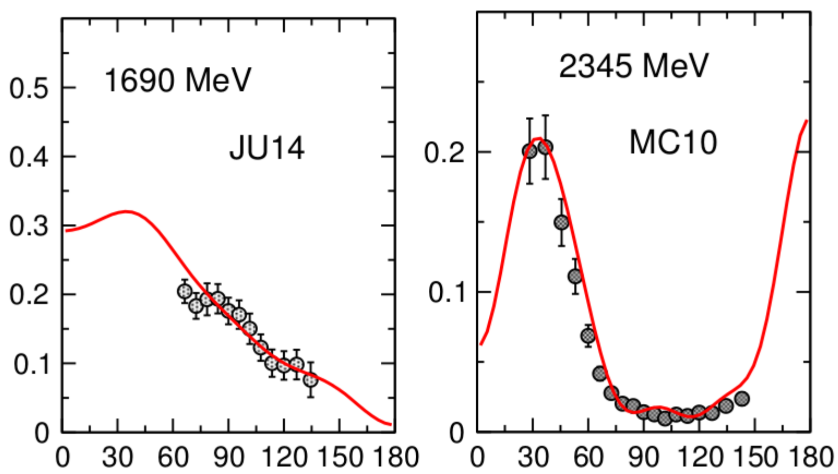

JU14: Jude PLB 735 (2014), MC10: McCracken PRC 81 (2010)

- Recoil polarization

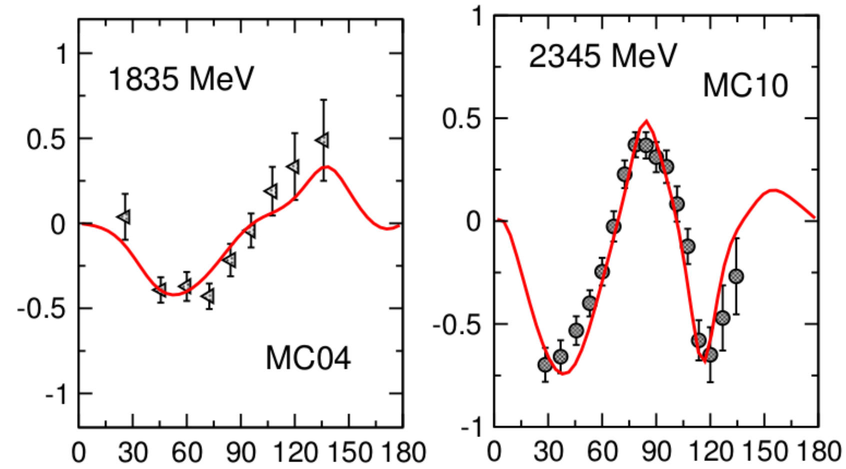

MC04: McNabb PRC 69 (2004), MC10: McCracken PRC 81 (2010)

- Beam asymmetry

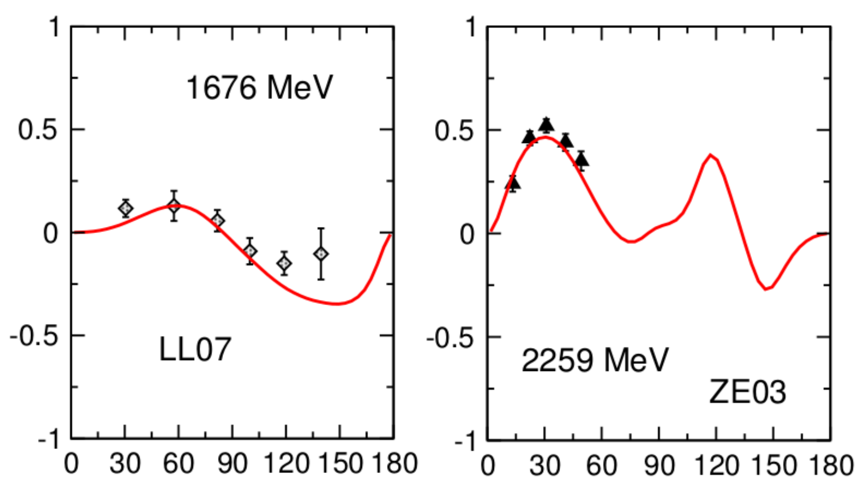

LL07: Lleres EPJA 31 (2007), ZE03: Zegers PRL (2003)

- Target asymmetry

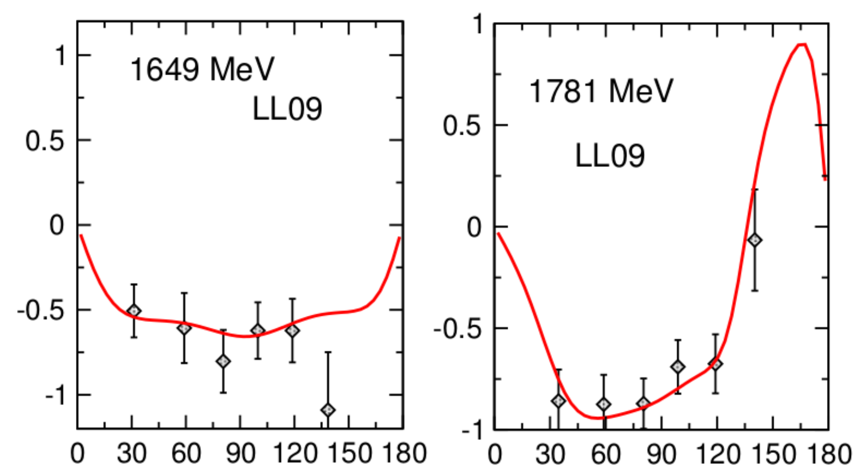

LL09: Lleres EPJA 39 (2009)

Preliminary: $K^+\Lambda$ photoproduction in the JüBo model

simultaneous fit of $\gamma p \to \pi^0 p$, $\pi^+ n$, ηp, $K^+\Lambda$ and $\pi N \to \pi N$, ηN, $K\Lambda$, $K\Sigma$

$\gamma p \to K^+\Lambda$:

- C_x

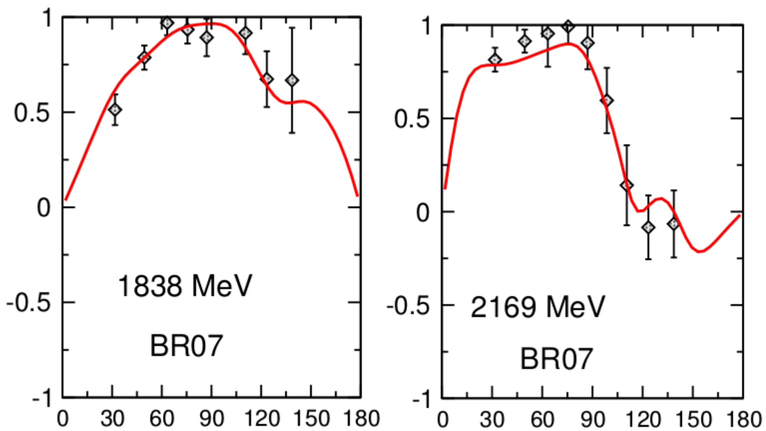

BR07: Bradford PRC 75 (2007)

- C_z

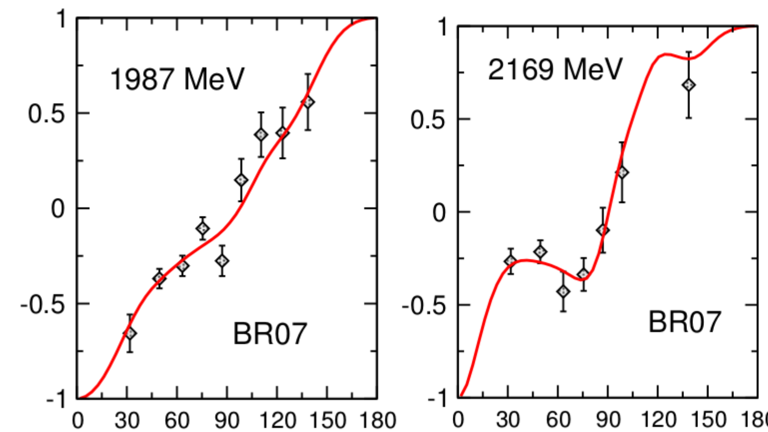

BR07: Bradford PRC 75 (2007)

- O_x

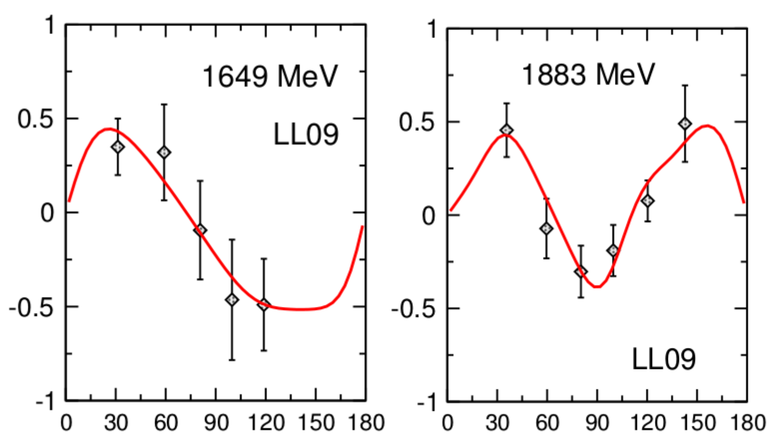

LL09: Lleres EPJA 39 (2009)

- O_z

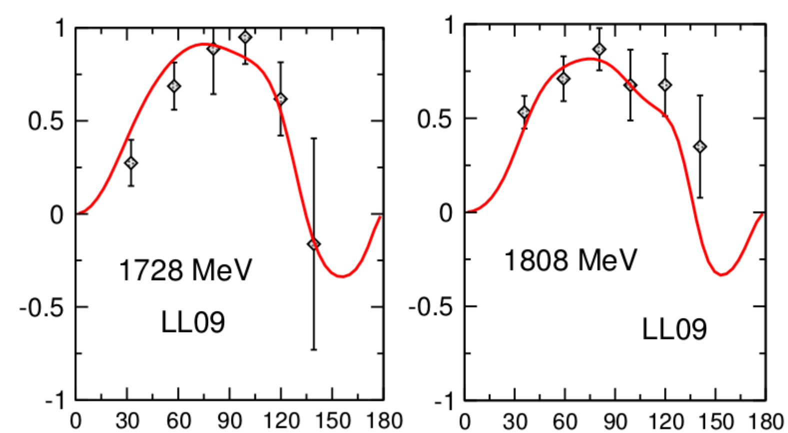

LL09: Lleres EPJA 39 (2009)

Introducing a *P_{13}(1900)* resonance improves fit significantly, as well.

Preliminary: $K^+\Lambda$ photoproduction in the JüBo model

simultaneous fit of $\gamma p \to \ \pi^0 p\ ,\ \pi^+ n\ ,\ \eta p,\ K^+\Lambda$ and $\pi N \to\ \pi N\ ,\ \eta N\ ,\ K\Lambda\ ,\ K\Sigma$

Influence of new CLAS data (Paterson *et al.* Phys. Rev. C 93, 065201 (2016)):

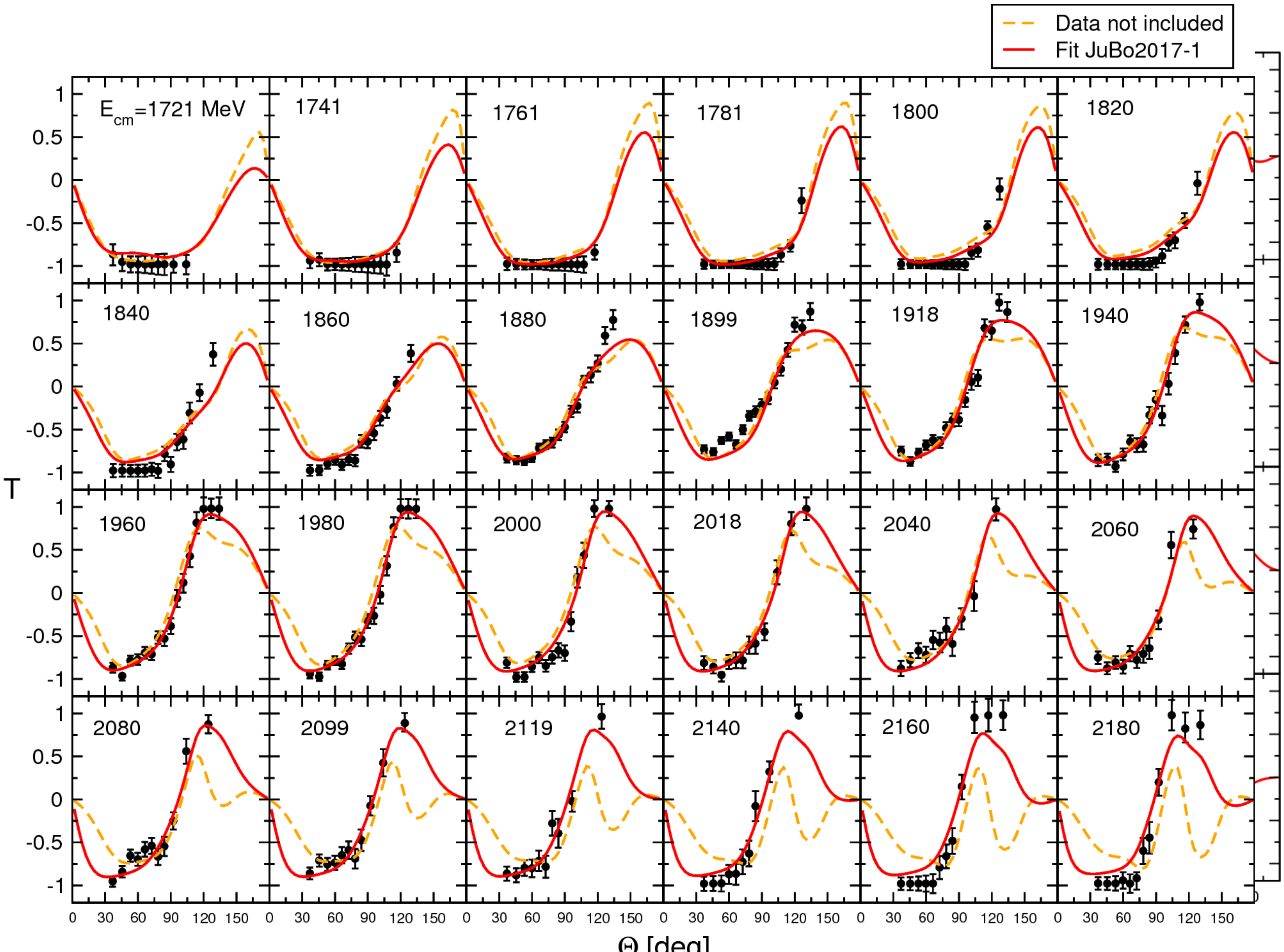

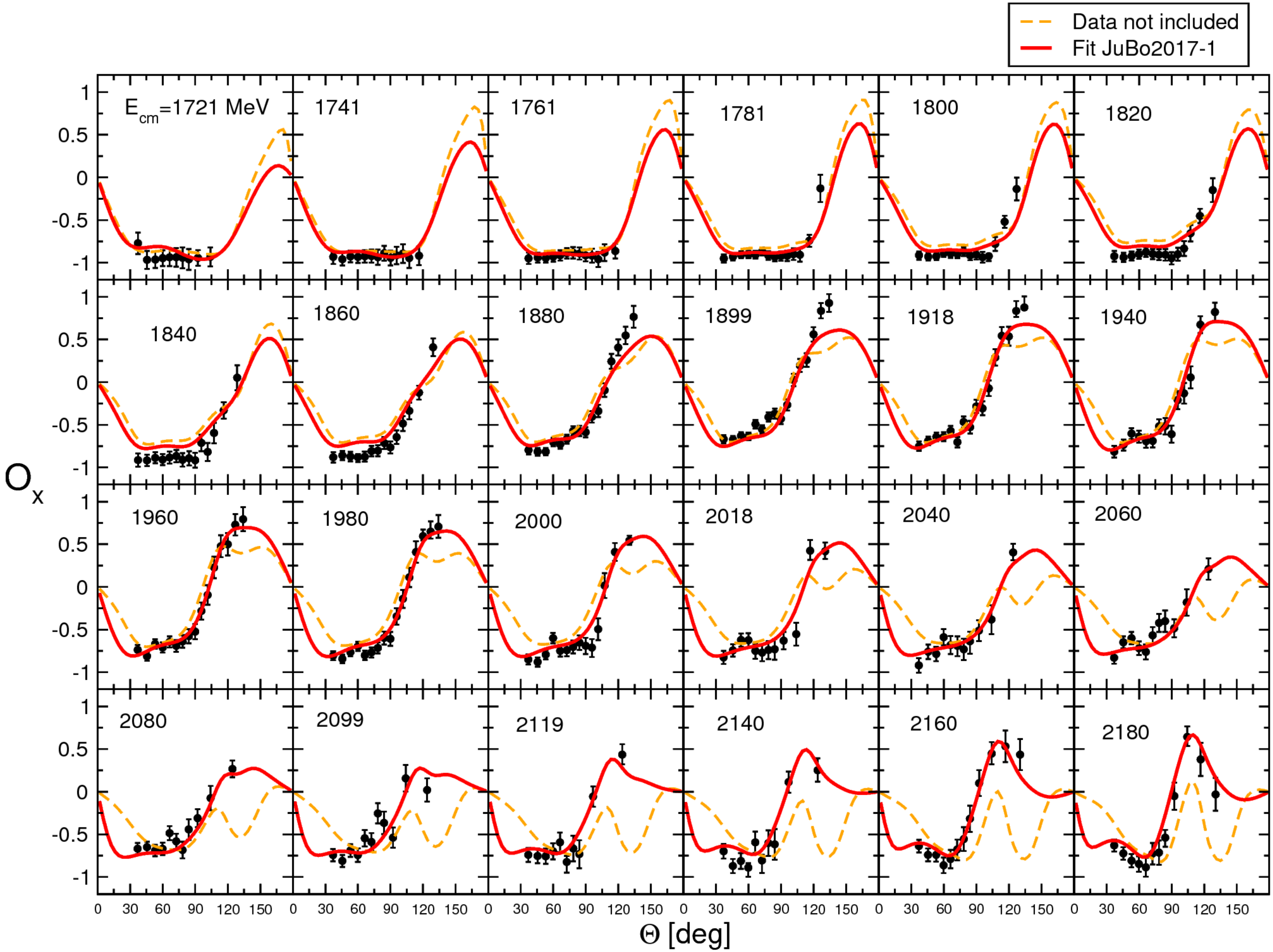

Data not included
Fit JuBo2017-1
E_{cm}=1721 MeV
1741
1761
1781
1800
1820
1840
1860
1880
1899
1918
1940
1960
1980
2000
2018
2040
2060
2080
2099
2119
2140
2160
2180
O_x
Θ [deg]

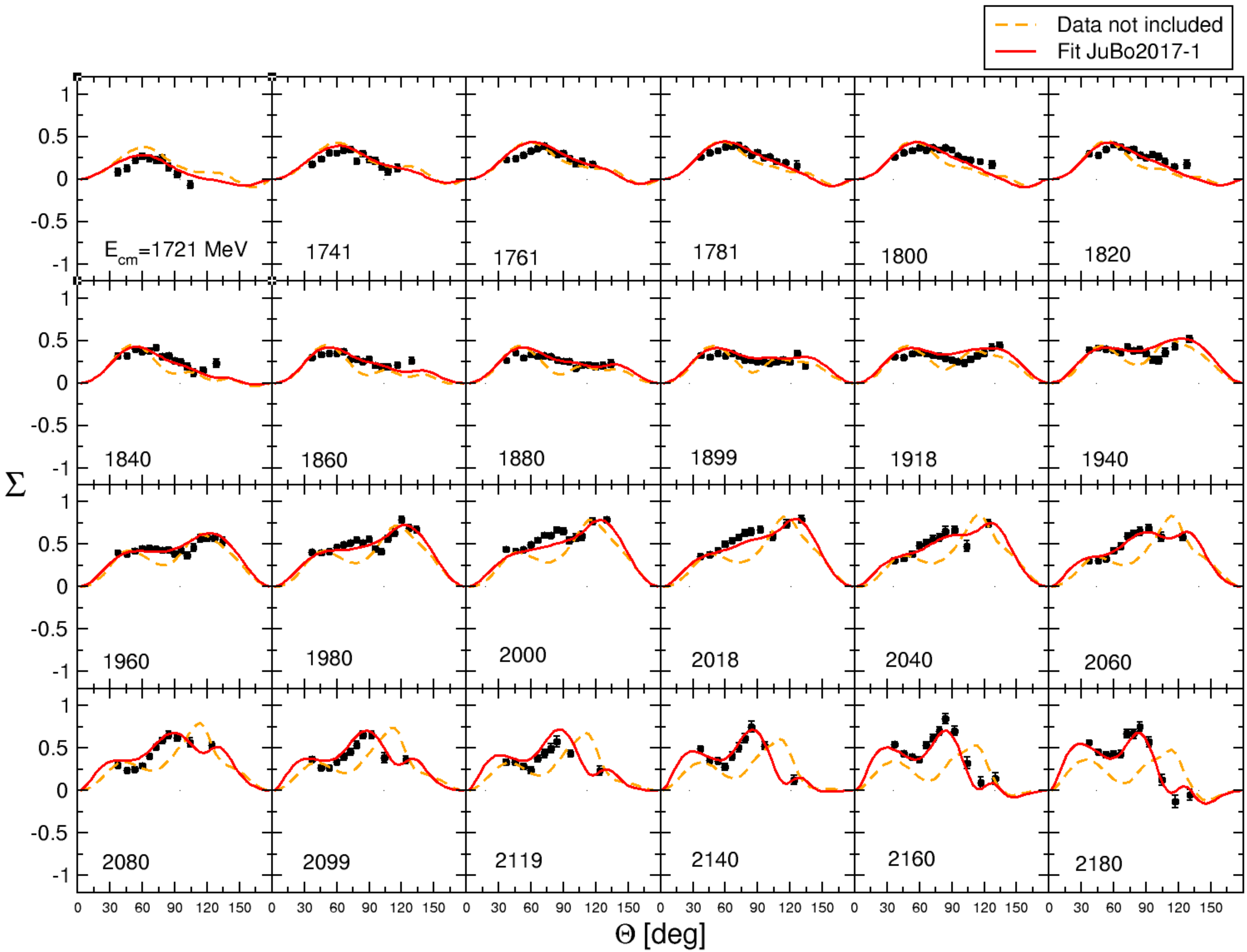

Data not included
Fit JuBo2017-1
E_{cm}=1721 MeV
1741
1761
1781
1800
1820
1840
1860
1880
1899
1918
1940
1960
1980
2000
2018
2040
2060
2080
2099
2119
2140
2160
2180
Σ
Θ [deg]

Resonance content (preliminary)

Previous JüBo analyses of photoproduction:

- resonances included in studies of pion-induced reactions sufficient to describe $\gamma p \to \pi N$, ηN
- no additional dynamically generated poles

Inclusion of $\gamma p \to K^+\Lambda$ in JüBo ("JuBo2017-1"): 3 additional states

	z_0 [MeV]	$\frac{\Gamma_{\pi N}}{\Gamma_{\text{tot}}}$	$\frac{\Gamma_{\eta N}}{\Gamma_{\text{tot}}}$	$\frac{\Gamma_{K\Lambda}}{\Gamma_{\text{tot}}}$	$\frac{\Gamma_{K\Sigma}}{\Gamma_{\text{tot}}}$	
N(1900)$3/2^+$	$1923 - i\,108.4$	1.5 %	0.78 %	2.99 %	69.5 %	
N(2060)$5/2^-$	$1924 - i\,100.4$	0.35 %	0.15 %	13.47 %	27.02 %	
Δ(*2190*)$1/2^+$	$2191 - i\,103.0$	33.12 %			3.78 %	
(N(*1730*)$1/2^-$	$1731 - i\,78.73$	1.86 %	1.30 %	56.43 %	1.11 %	)
(N(*1750*)$1/2^-$	$1750 - i\,158.8$	1.80 %	0.29 %	0.57 %	5.63 %	)

- N(1900)$3/2^+$: s-channel resonances, seen in many other analyses of kaon photoproduction (BnGa), 3 stars in PDG
- N(2060)$5/2^-$: dynamically generated, 2 stars in PDG, seen e.g. by BnGa
- Δ(*2190*)$3/2^+$: dyn. gen., no equivalent PDG state
- N(*1730*)$1/2^-$, N(*1750*)$1/2^-$: dyn. gen., no equivalent PDG state
  previous JüBo solutions: **one** dyn. N(*1750*)$1/2^-$ with $z_0 \sim 1745 - i\,155$ MeV

Visible influence of new states

$\Delta(2190)3/2^+$ in πN PW

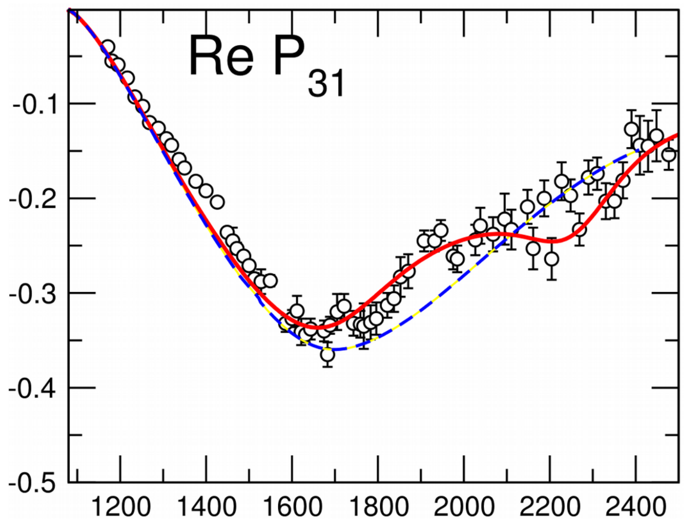

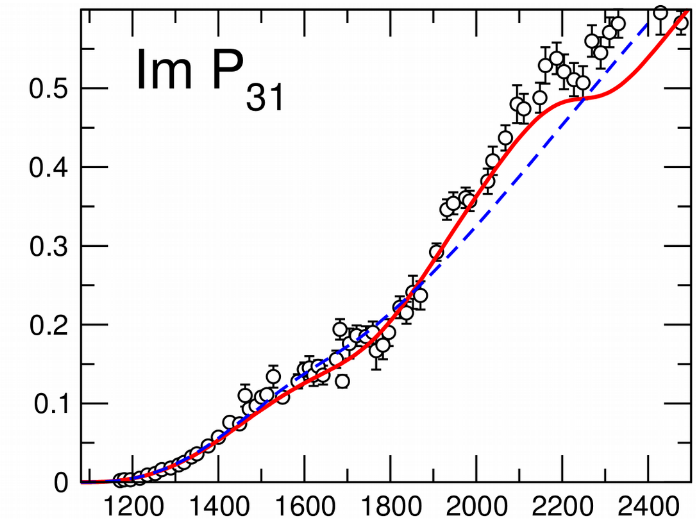

N(1900)$3/2^+$, N(2060)$5/2^-$ in σ_{tot} in $\pi^- p \to K^+\Sigma^-$

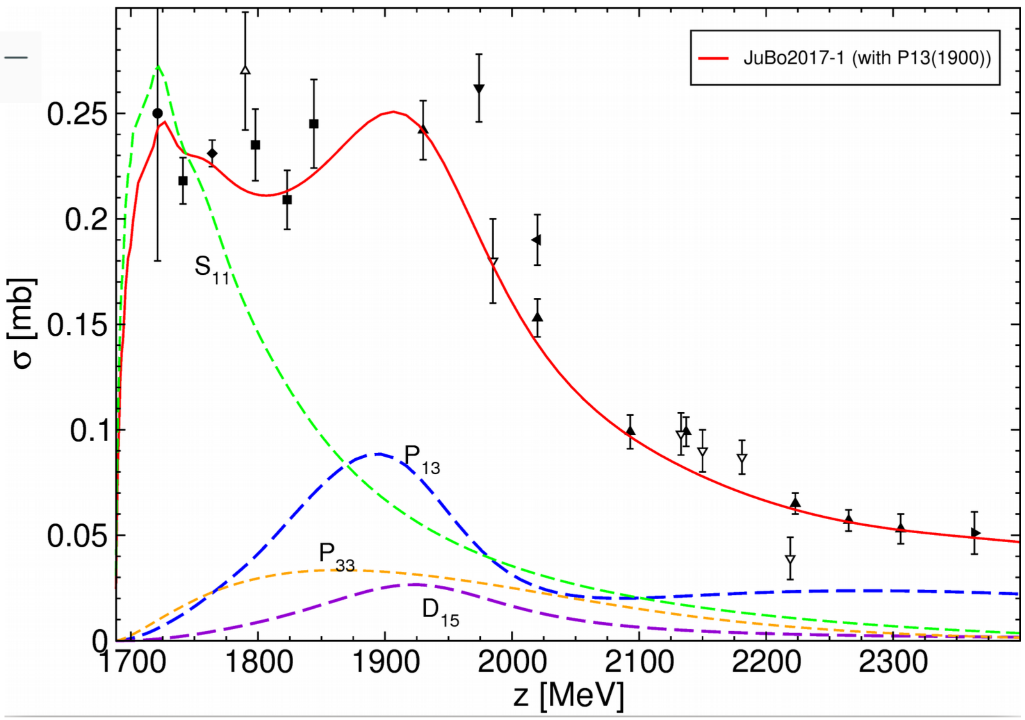

FROST/CLAS

CLAS/JuBo (M. D., D. Rönchen), Phys.Lett. B755 (2016)

- First-ever measurement of observable E in η photo-production, enabled through the FROST target

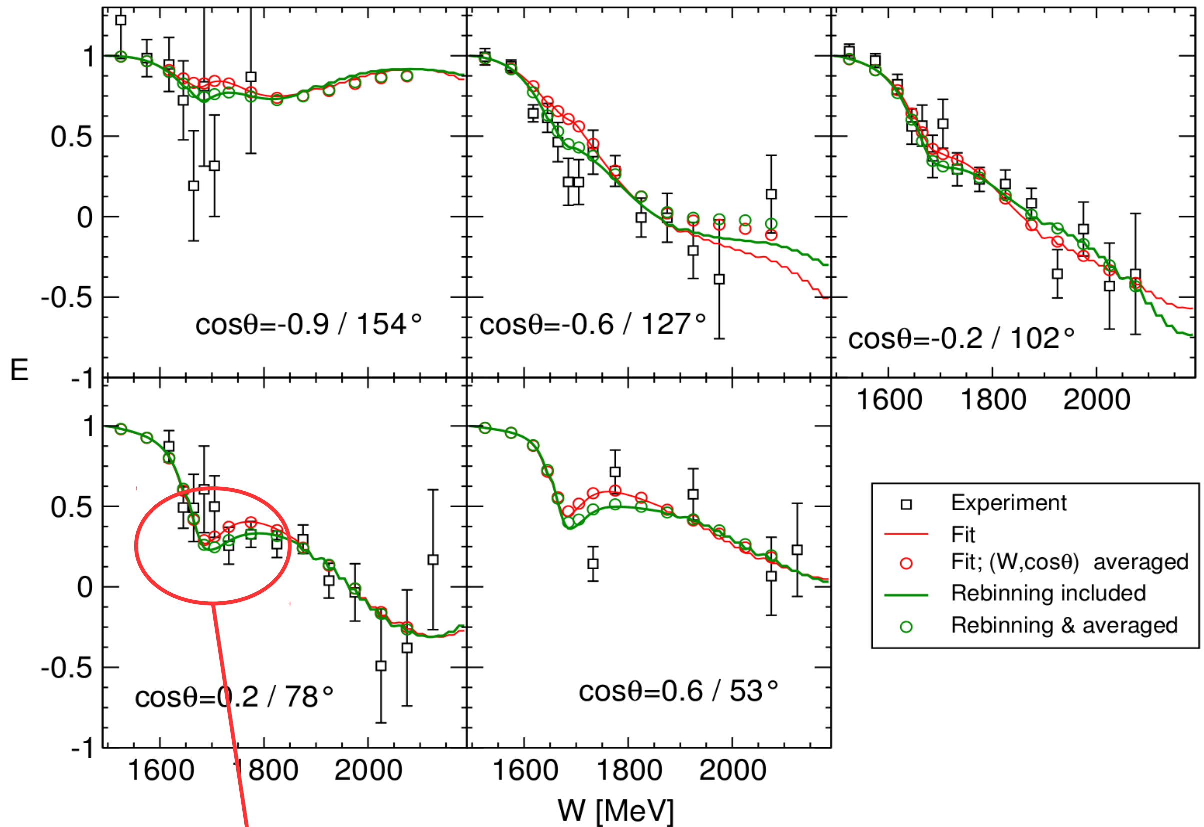

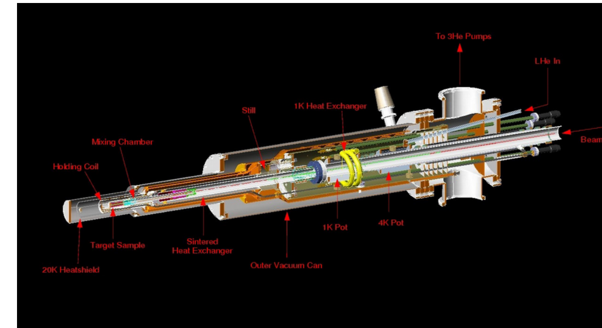

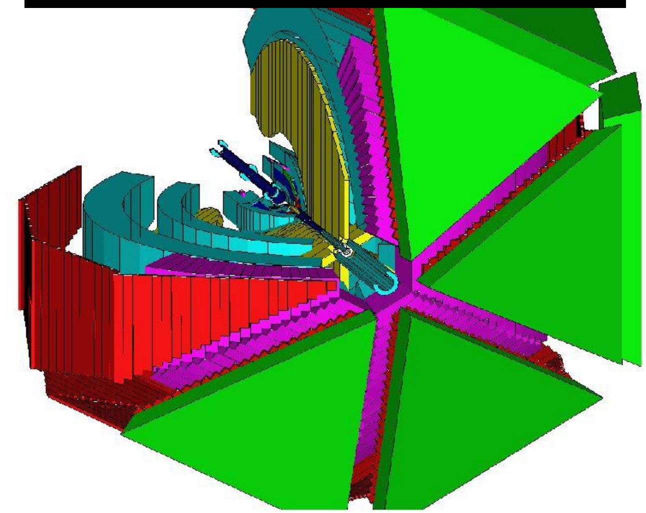

Is this a new narrow baryonic resonance?
→ Conventional explanation in terms of interference effects.

LASSO is capable of setting coefficients exactly to zero

$$\sum_{i=1}^{n}\underbrace{\frac{(y_i - f(x_i,\beta_j))^2}{\sigma_i^2}}_{\text{Normal } X^2} + \lambda\underbrace{\sum_{j=1}^{m}|\beta_j|}_{\text{Penalty Term}}$$

$\hat{\beta}_i$: Best parameters without penalty
$\beta_i = 0$: Best parameters only penalty

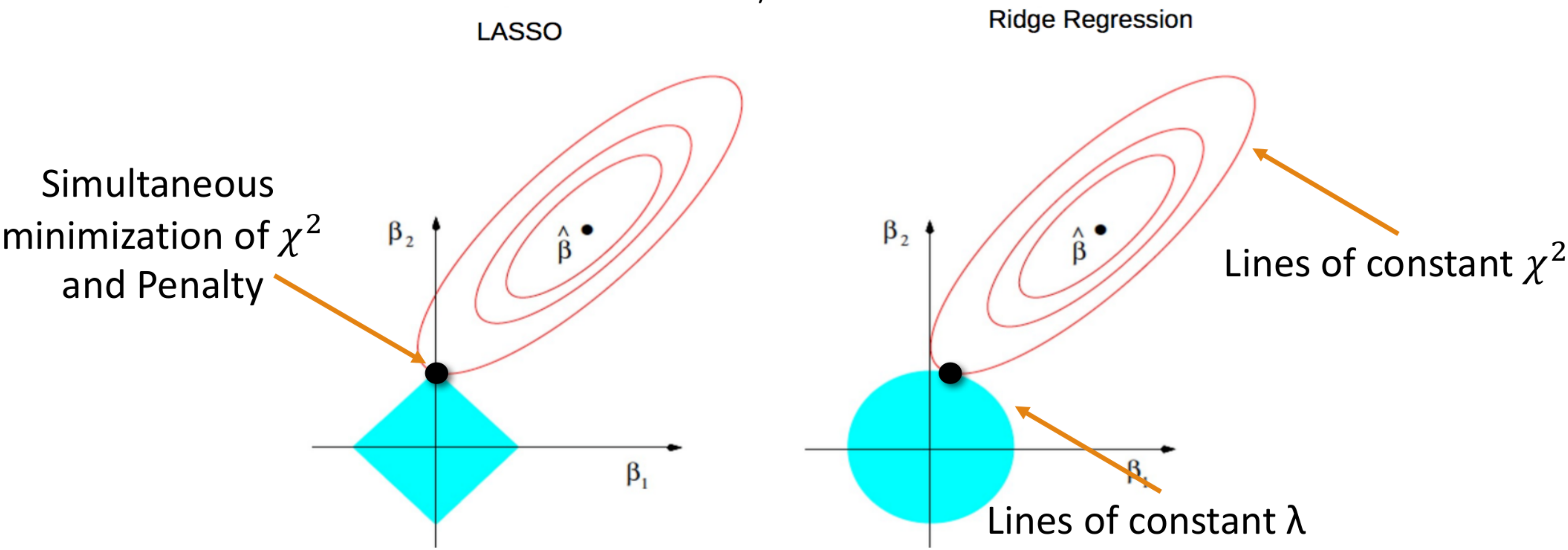

(Least Absolute Shrinkage and Selection Operator LASSO)

Different models can give satisfactory fits. How do we determine the optimal one?

[J. Landay, M.D., B. Hu. R. Molina, EPJA 2017]

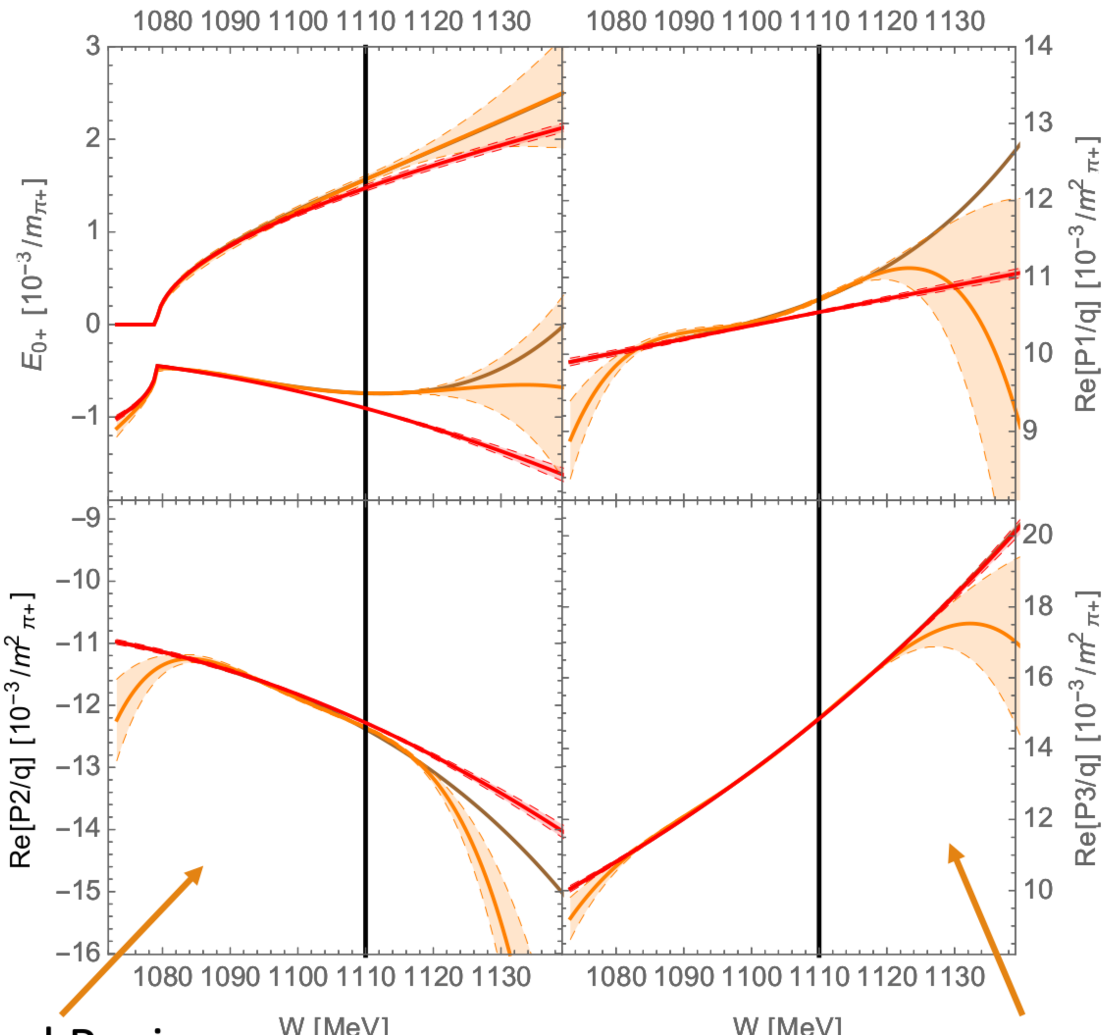

Fitted Region

Predicted Region

All solutions pass Pearson's Chi-Squared test.

Orange Solution- 23 parameters

Red Solution – 13 parameters

LASSO:

$$\chi^2 = \chi^2_{\text{stat.}} + \lambda \sum_i |a_i|$$

Lasso Example: Fit to data from toy model with known best parameters

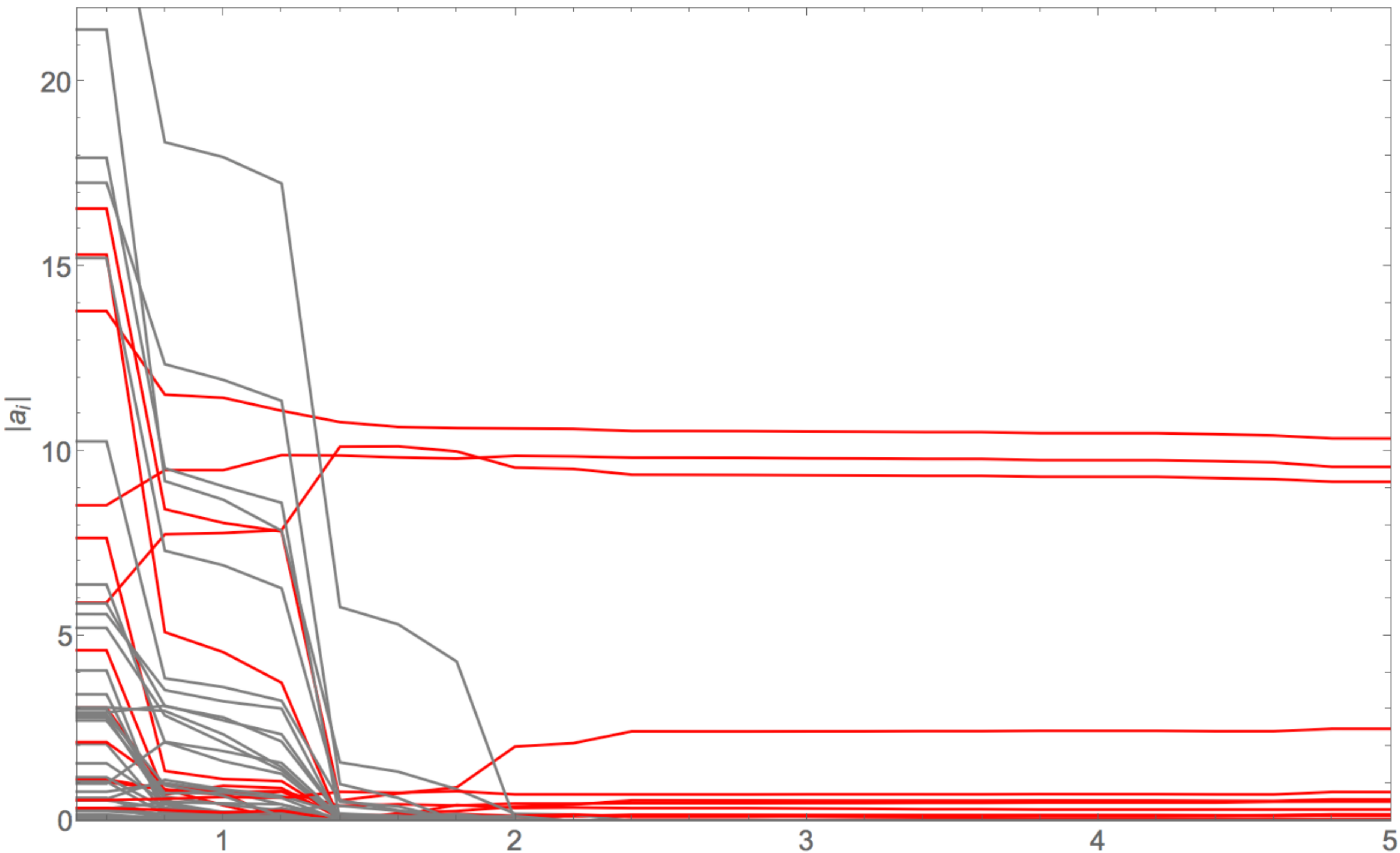

Red- Non-Zero Parameters λ Gray- Zero-Parameters

Resonance selection

[M.D., J. Landay, H. Haberzettl, M. Mai, K. Nakayama, in progress]

Synthetic data with hidden resonances

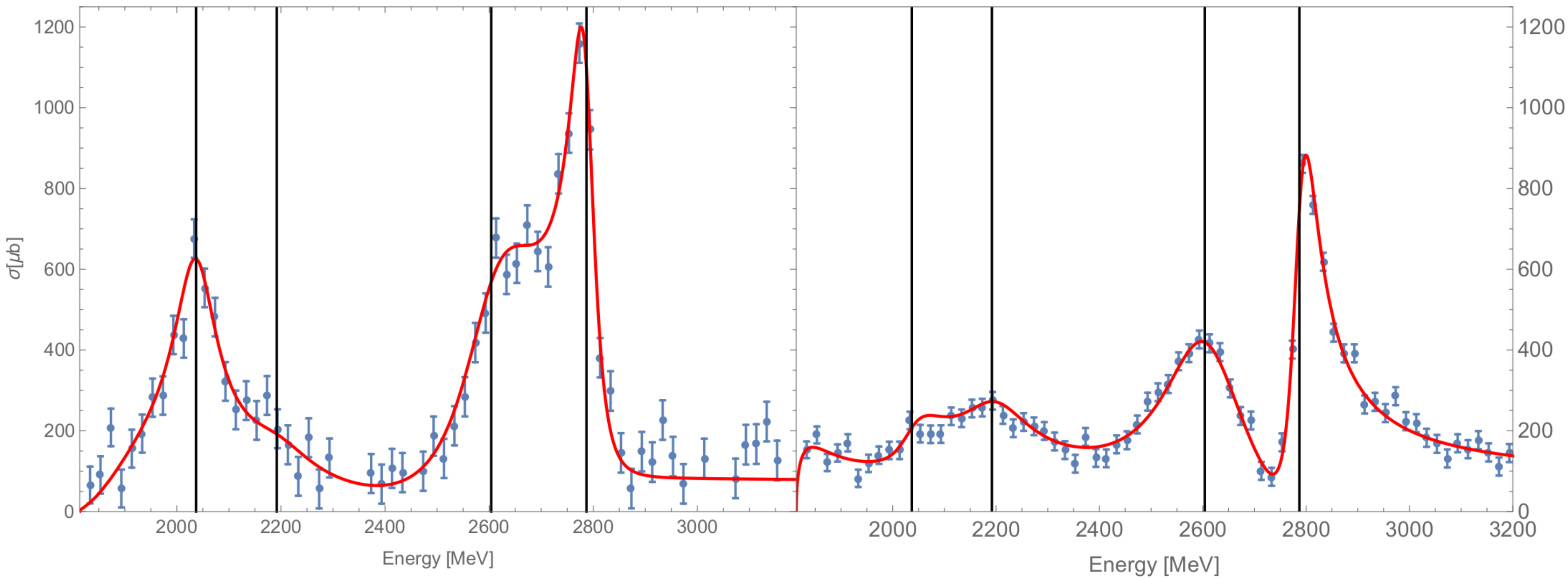

Total cross section + diff cs (not shown) + Polarization P (not shown) assuming Reaction kinematics of $K^{-}p \to K\Xi$

Monotonous LASSO

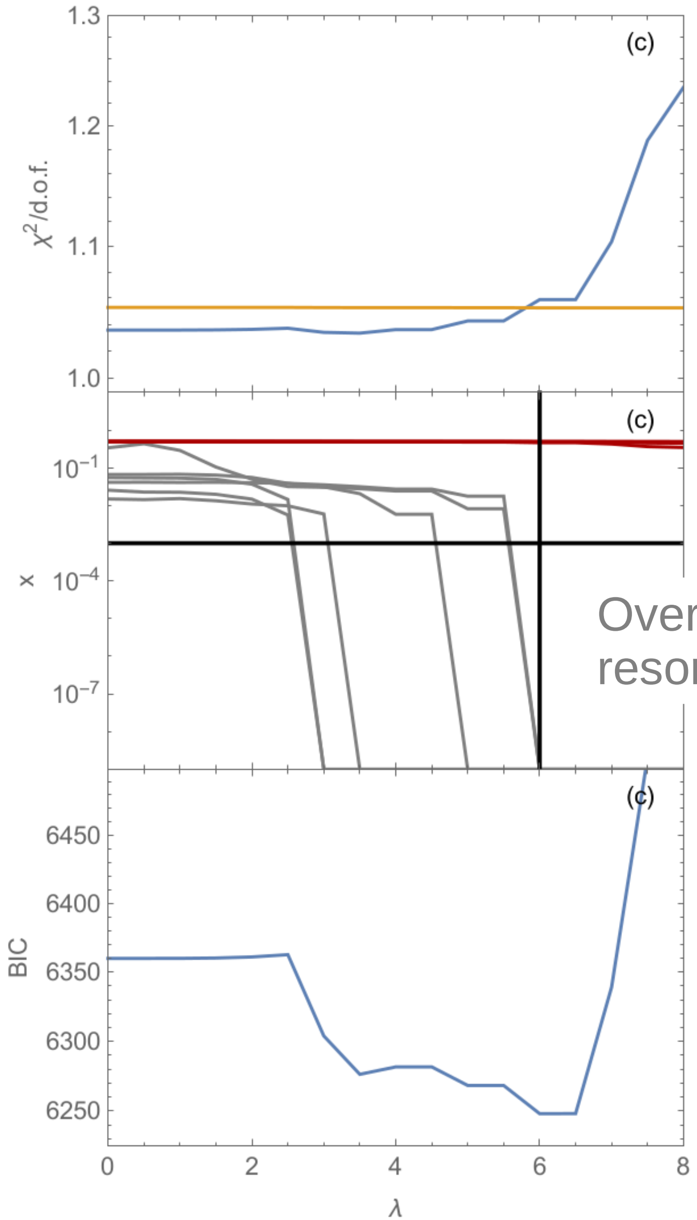

Pearson's Chi-square limit

True resonances

Overpopulated resonances

Partial-wave parametrization:

$$\tau(W) = \left(a\, e^{-\alpha^2 \left(\frac{k_f(W)}{\Lambda}\right)^2} - x\, e^{i\Phi} \frac{\Gamma}{2(W - M + i\frac{\Gamma}{2})} \right) \left(\frac{k_f(W)}{\Lambda} \right)^{L+\frac{1}{2}} \left(e^{i\phi}\right)$$

- Penalize resonance coupling
- Ten partial waves; 10 resonances in Ansatz
- LASSO picks the 4 correct ones

Other penalties

$$P(\lambda) = \lambda^5 \sum_{i=0}^{9} \int_{m_K+m_\Xi}^{3200} \frac{\partial^2}{\partial W^2} \left(\left| - x_i\, e^{i\Phi_i} \frac{\Gamma_i}{2(W - M_i + i\frac{\Gamma_i}{2})} \right|^2 \right) dW$$

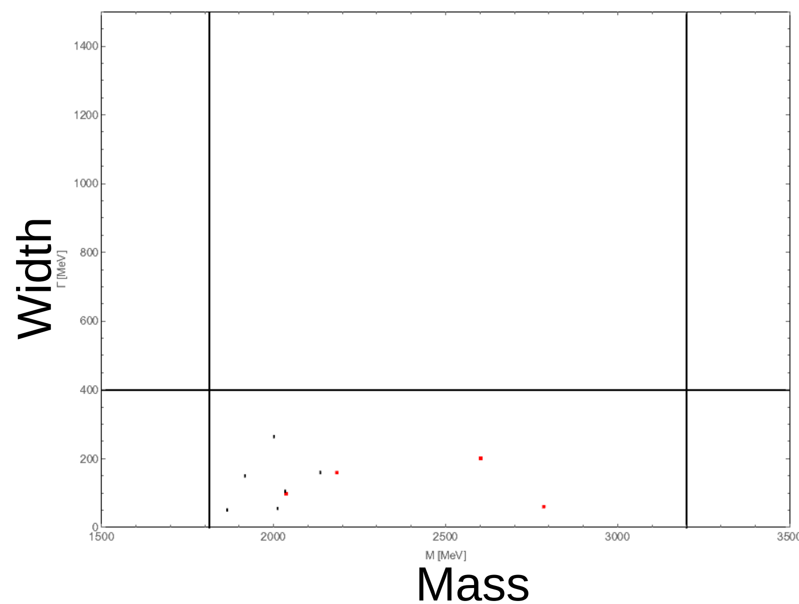

Consequences for data analysis

- LASSO + information theory criteria/cross validation provide **relative** model comparison/selection. Models do **not** have to be good in frequentist's statistical sense.

  → Robust method for problematic data.

  → Additional confidence for newly found states in different analyses (Implementation in full codes needed).

Form factors

Electroproduction - SAID

- Energy dependent SM08 and associated SES & SQS
- W = 1080 – 2000 MeV $\quad Q^2 = 0 – 6\ GeV^2$
- PWs = 60 [multipoles] $\quad [J < 6]$
- Prms = 171
- Constraint: πN + Pion Photo PWAs [no theoretical input]

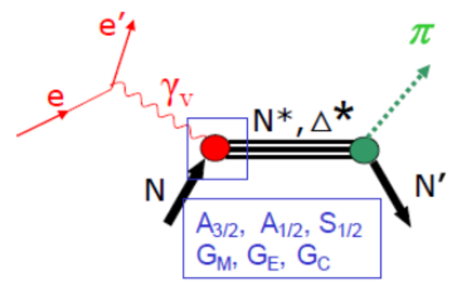

- 0.85 World Electro Prod from JLab CLAS

- **PWA Problems:**
  - Additional [S] Multipoles
  - Q^2 dependence

- **Database Problems:**
  - Most of data are unPolarized measurements
  - There are no $\pi^0 n$ data and very few $\pi^- p$ [no Pol measurements] That does not allow to determine n-couplings at $Q^2 > 0$

Reaction	Data	χ^2
$\gamma^* p \to \pi^0 p$	55,766	81,284
$\gamma^* p \to \pi^+ n$	51,312	80,004
Redundant	14,772	17,375
Total	121,850	178,663
$\gamma N \to \pi N$	25,358	53,458
All Photo*	147,208	232,121
$\pi N \to \pi N$	31,479	57,157
All πN	178,687	289,278
$\gamma^* n \to \pi^- p$	801	
$\gamma^* n \to \pi^0 n$	No Data	

Q^2-Data

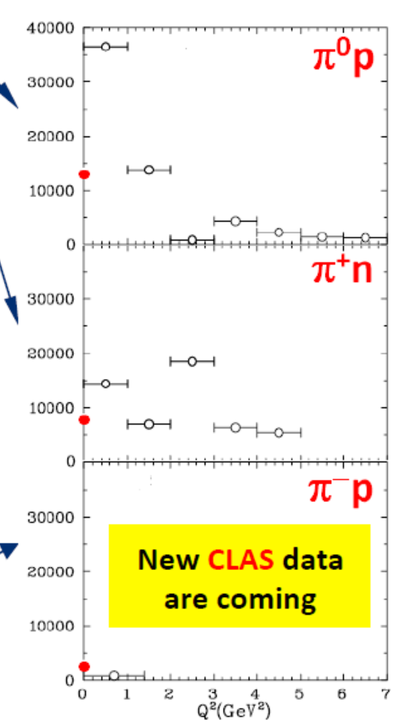

Transition form factors @ CLAS 12

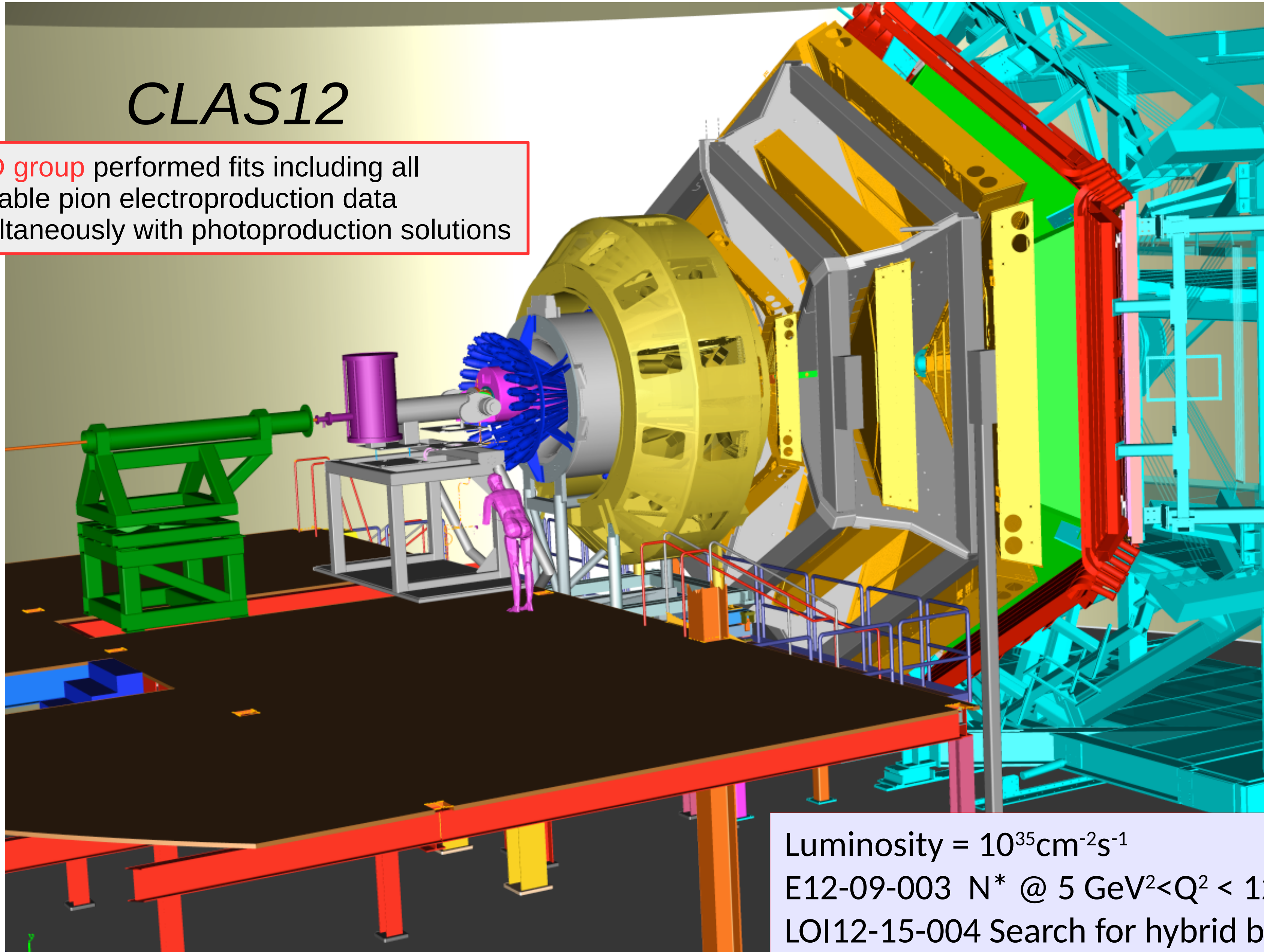

SAID group performed fits including all available pion electroproduction data simultaneously with photoproduction solutions

Luminosity = $10^{35}cm^{-2}s^{-1}$

E12-09-003 N* @ 5 $GeV^2 < Q^2 < 12\ GeV^2$

LOI12-15-004 Search for hybrid baryons

E12-06-108A KY Electroproduction with CLAS

Transition Form Factors at the Pole

Common effort MAID/SAID/Zagreb/JuBo
[Tiator, M.D., R. Workman, et al., PRC (2017)]

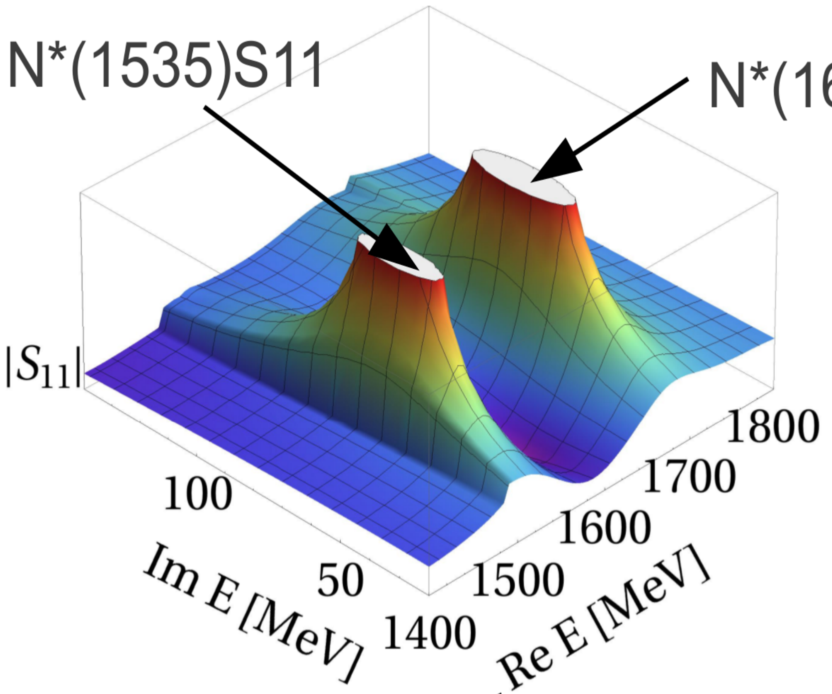

Definition of a resonance:
Pole in the complex plane of the scattering energy E (≡ z ≡ W);
- Pole position (“mass & width”)
- Residues (“branching ratios”)

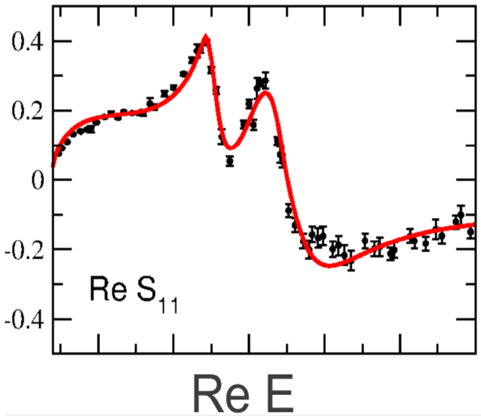

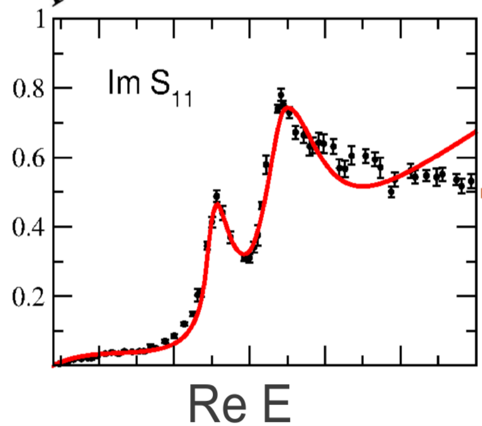

Also $\gamma^{(*)}NN^*$ transition form factors are complex quantities if defined at pole (background-inde-pendent definition)

Pole: point of comparison for (unitary) chiral models & lattice [Jido, M.D., Oset, PRC77 (2008); for lattice: A. Agadjanov, Bernard, Meissner, Rusetsky, NPB886 (2014)]

First Results for $\Delta(1232)P33$

[Tiator, M.D., R. Workman, et al. PRC (2017)]

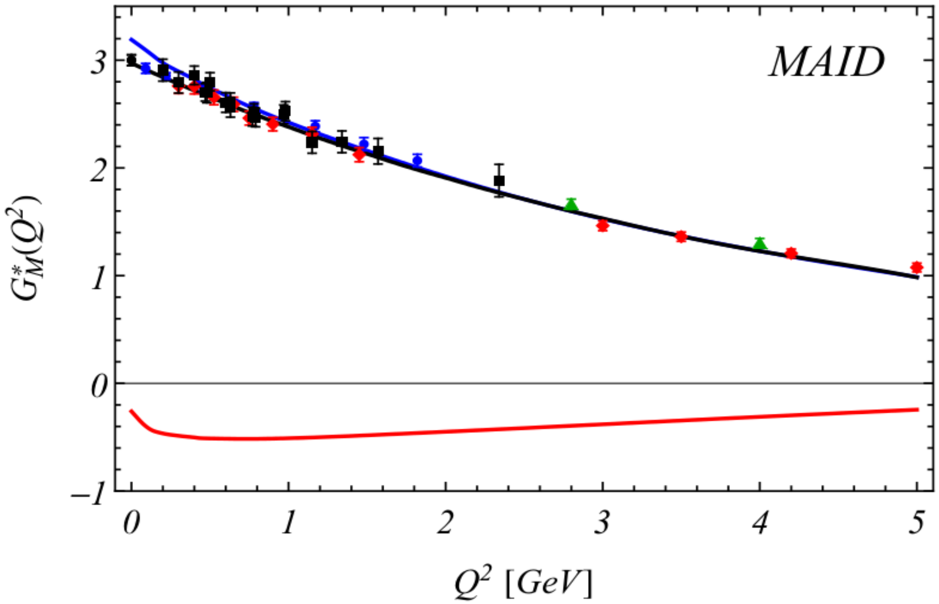

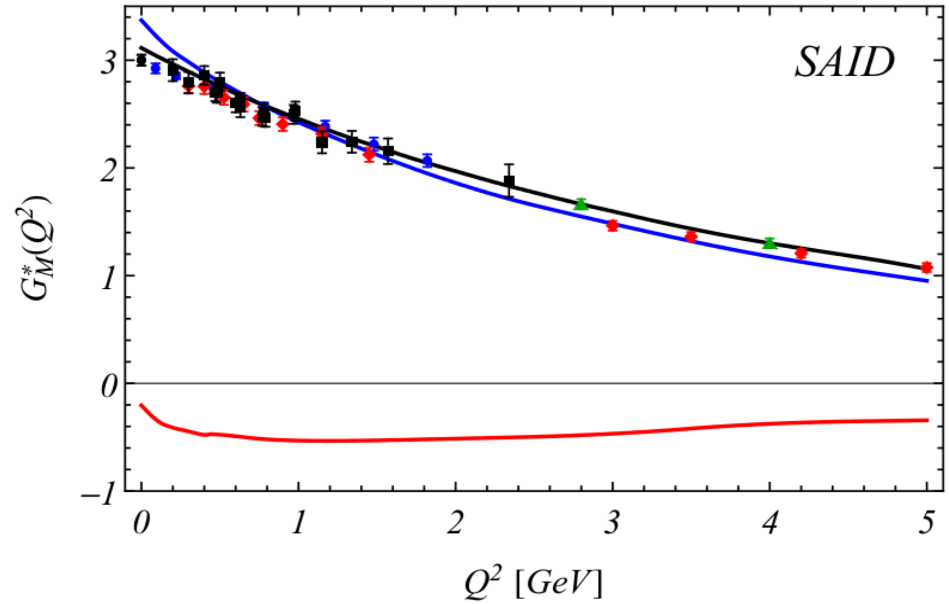

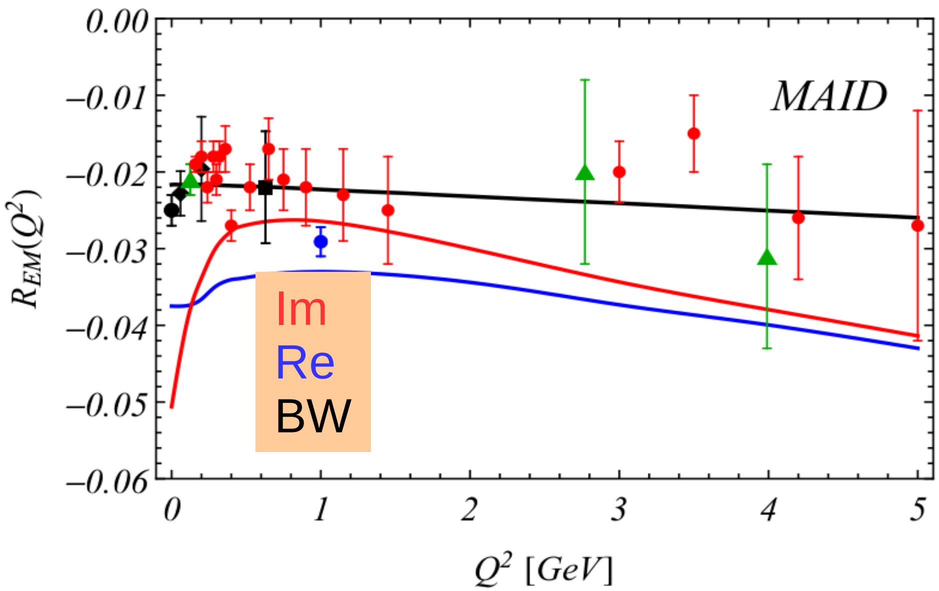

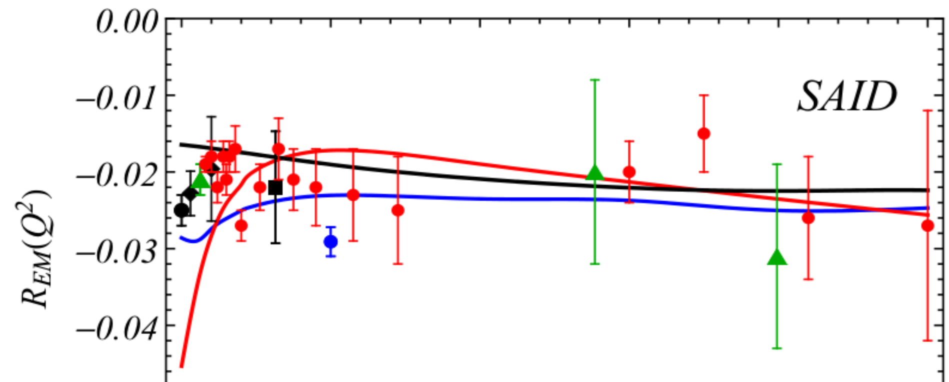

SAID: existing fit of pion electro-
Production data up to 6 GeV^2. Challenges:

- Unified formulation with photoproduction (CM12)
- Update with future data from Jlab

“Data points”: Aznauryan *et al.*

Comparison with ChPT at the pole

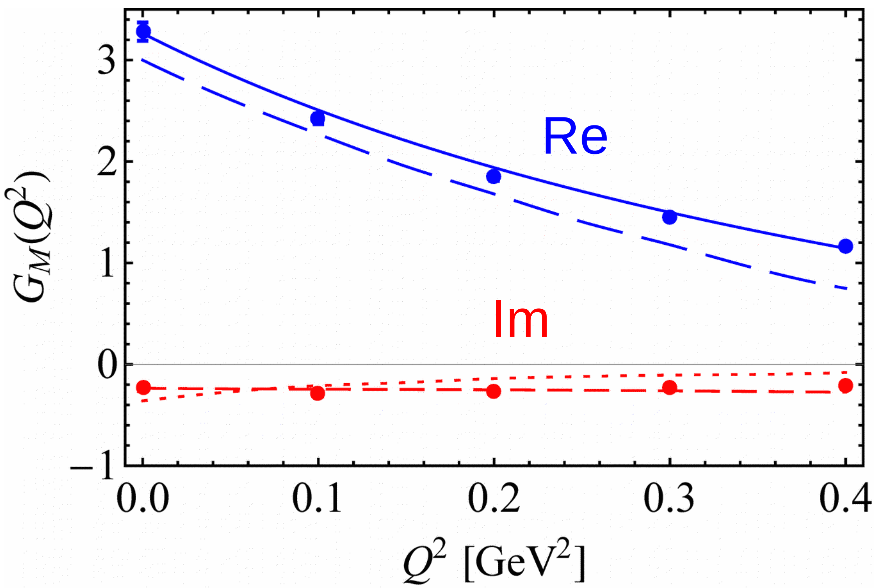

data points: average MAID+SAID (2016)

Baryon χPT (Scherer et al, 2017)

HB χPT (Gail, Hemmert, 2006)

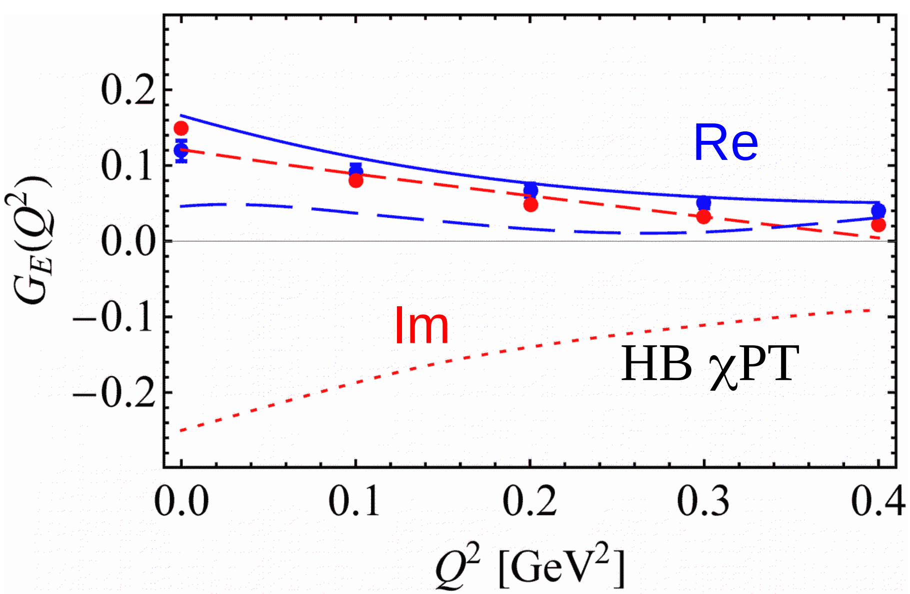

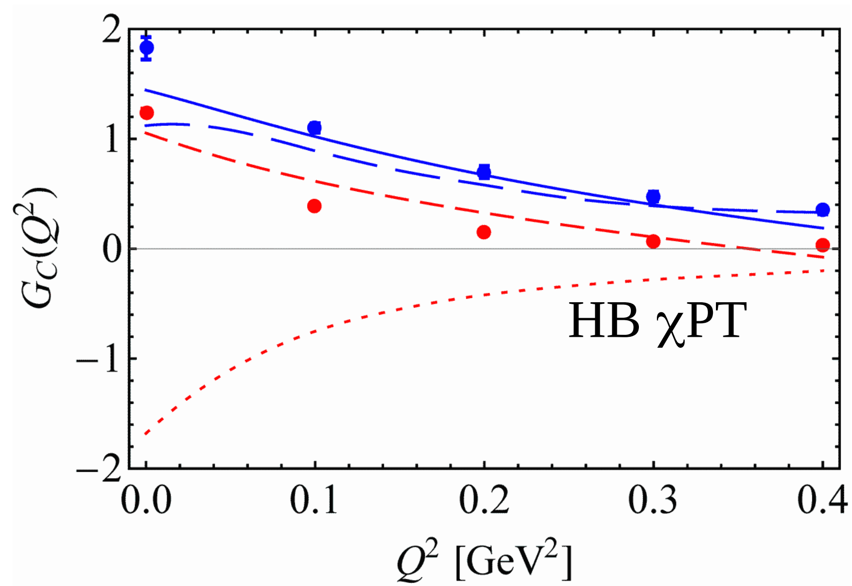

Outlook

- Precision spectroscopy seems to benefit from
  - Systematic search for new resonances (model selection techniques)
  - Extension to Electroproduction planned, building on existing SAID analyses.
  - Extensions of analysis tools to finite volume to analyze lattice QCD data

Fit to world data on $\pi N \to \pi N, \eta N, K\Lambda, K\Sigma$ ($\sim 10^5$ exp. points)

[Rönchen, M.D. *et al.*, EPJA 49 (2013)]

Selected results for $\pi^- p \to K^0\Lambda$ [almost complete experiment]

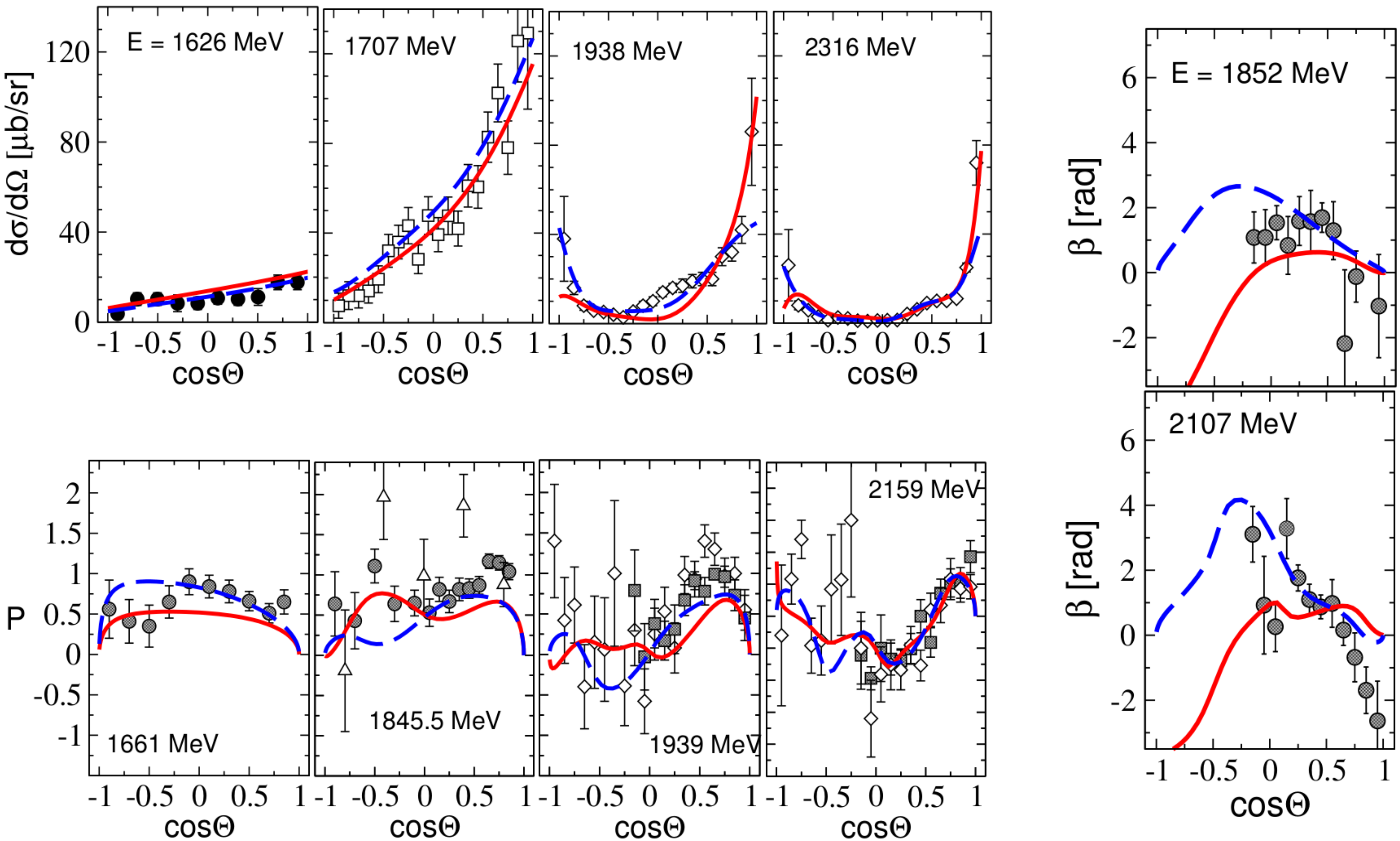

Re-measuring hadron-induced reactions

Fits: D. Rönchen, M.D., et al., EPJ A**49** (2013)

$\pi^- p \to K^0 \Sigma^0$

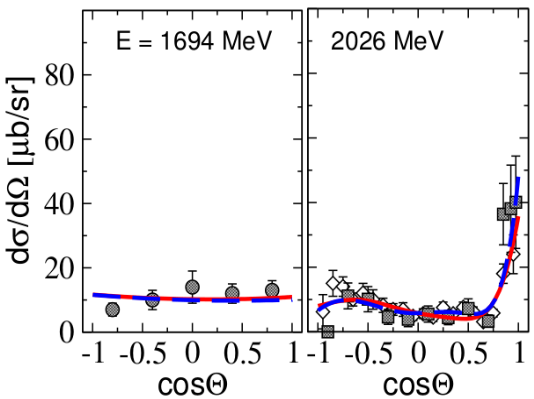

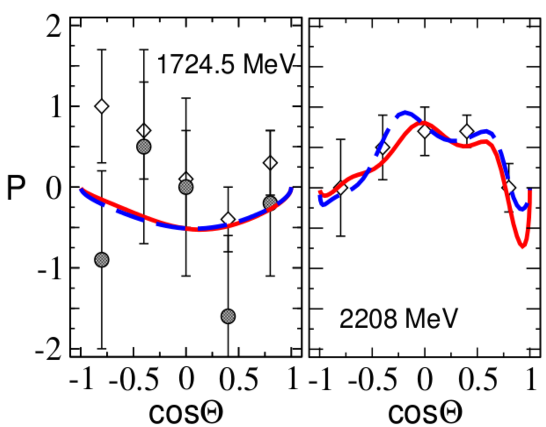

$\pi^- p \to K^+ \Sigma^-$

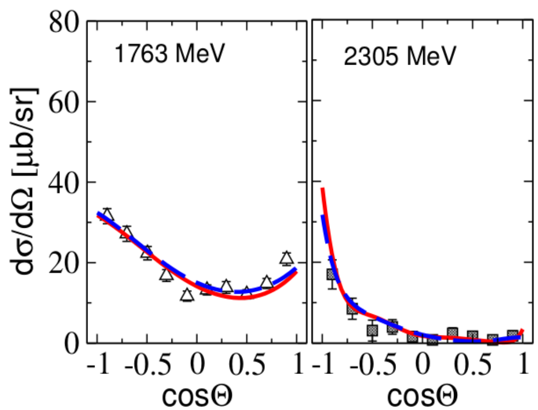

No polarization data!

$\pi^+ p \to K^+ \Sigma^+$

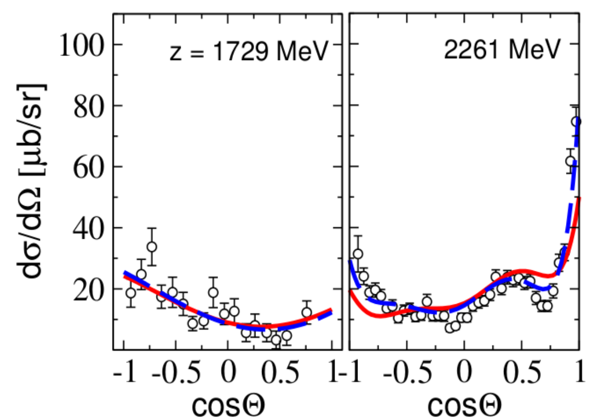

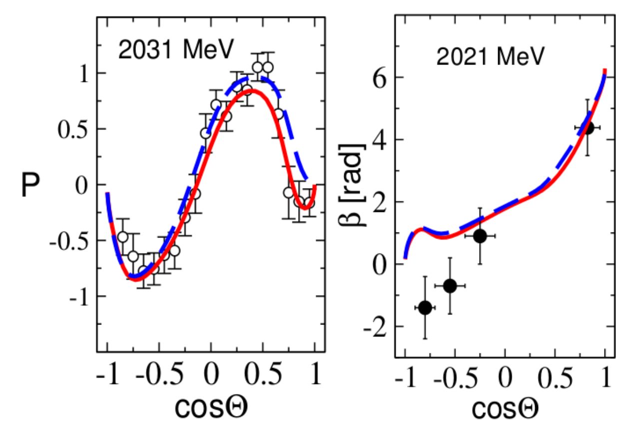

→ *Physics Opportunities with meson beams*,
Briscoe, M.D., Haberzettl, Manley, Naruki, Strakovsky, Swanson, EPJ A**51** (2015)

Improvement in Modern Experimental Facilities: $\pi N \to \pi N$

EPECUR & GWU/SAID, Alekseev *et al.*, PRC91, 2015

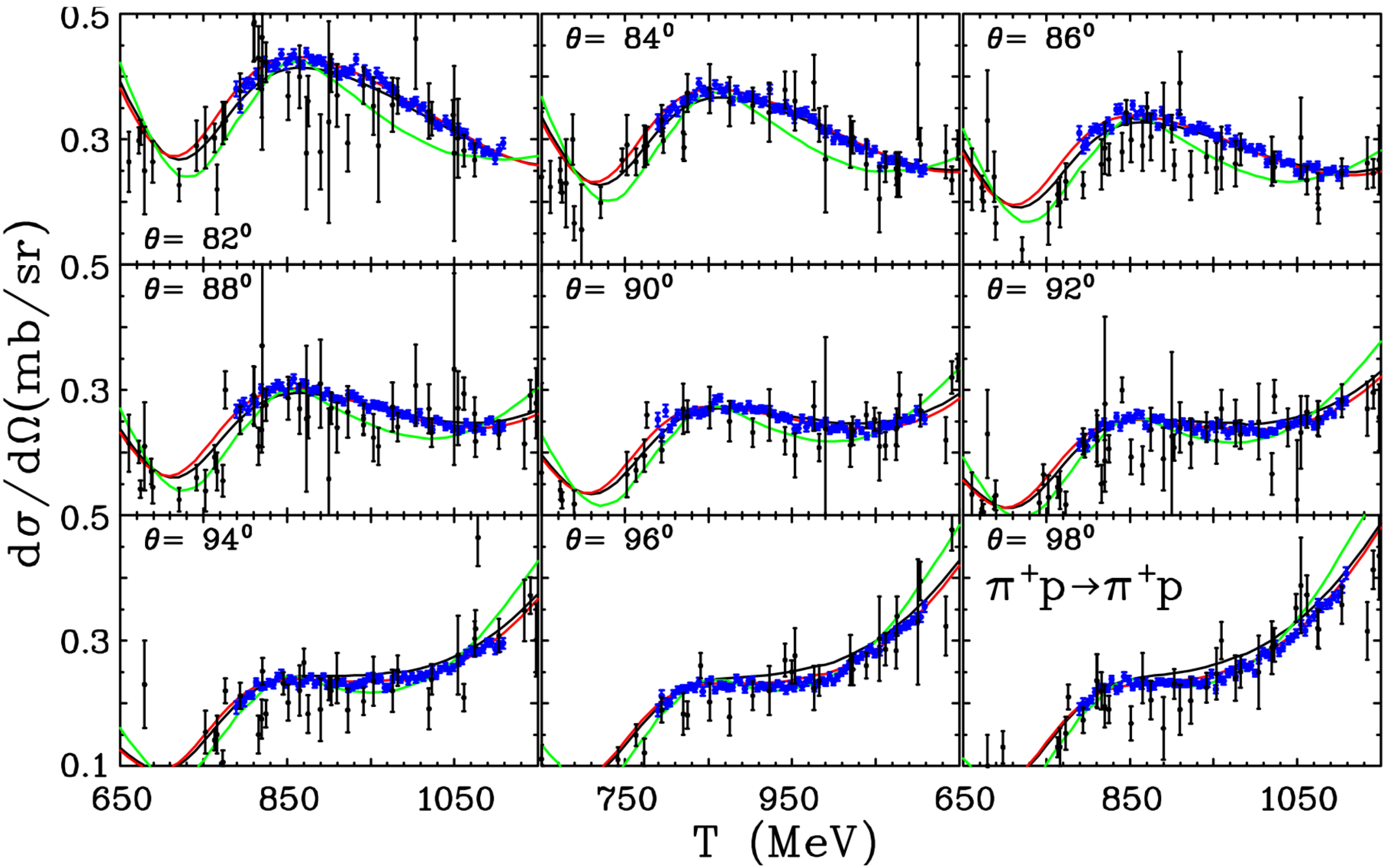

Black: WI08 prediction; Red: WI14 fit; green: KA84.

SAID Analysis of New Data

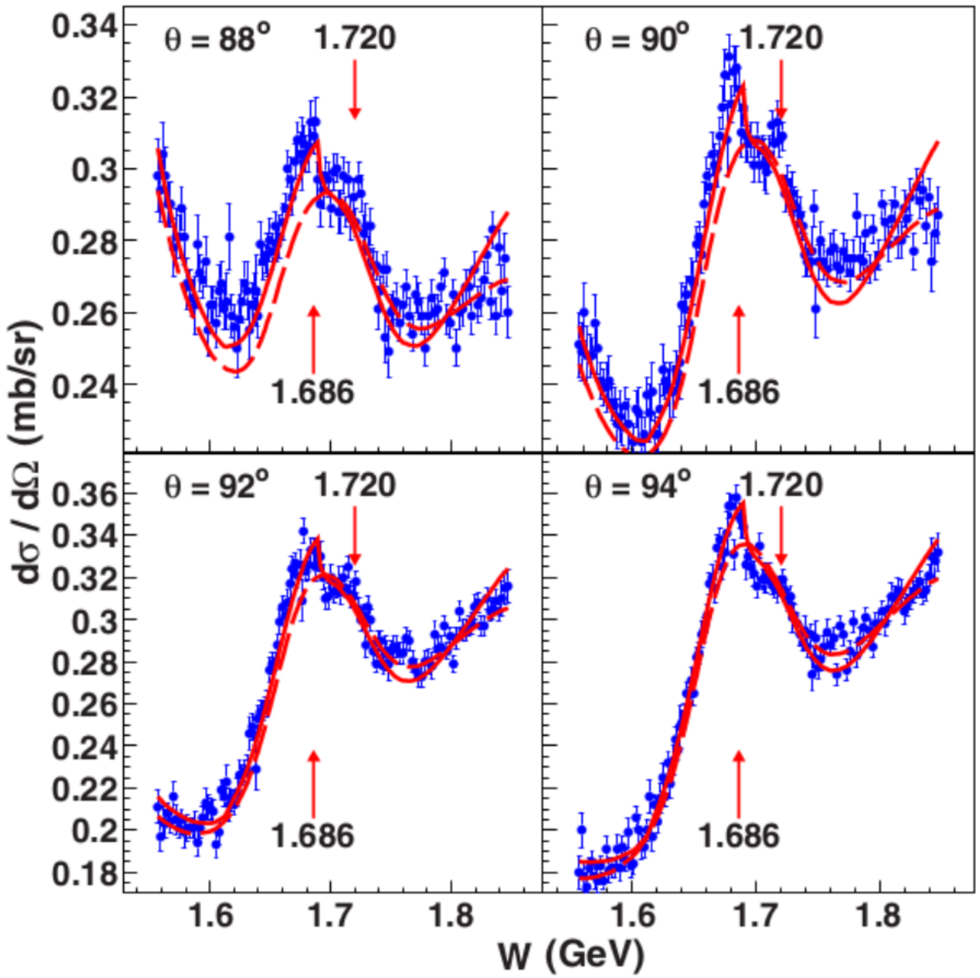

FIG. 2. $\pi^- p$ elastic scattering. Red solid lines correspond to the present calculations. Dashed lines lines are the XP15 solution.

Fit (no KΣ , KΛ channel)

Dashed Line

Fit including KΣ , KΛ channels

Solid Line

Narrow structures largely accounted for by threshold cusp effects.

Phys Rev C93 (2016) 062201

How to decide best value of λ?

$$AIC = 2k + \chi^2$$

$$AICc = AIC + \frac{2k(k+1)}{(n-k+1)}$$

$$BIC = k \log n + \chi^2$$

k : Number of parameters
n : Number of data points

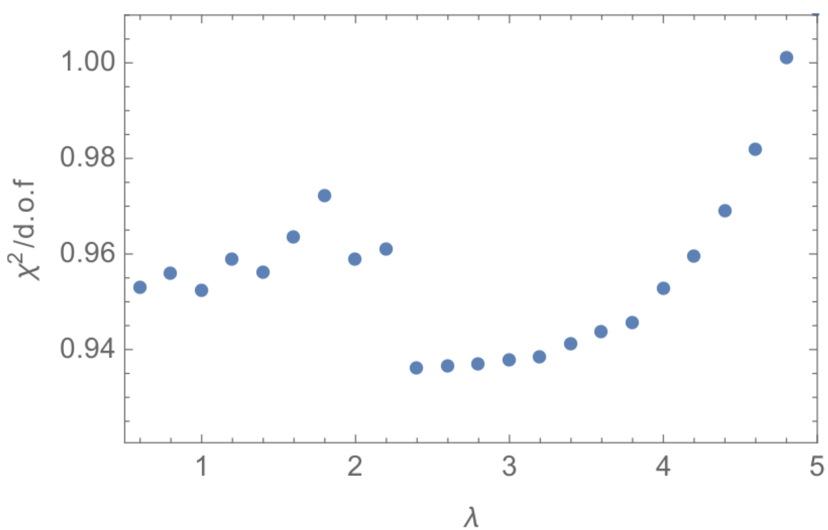

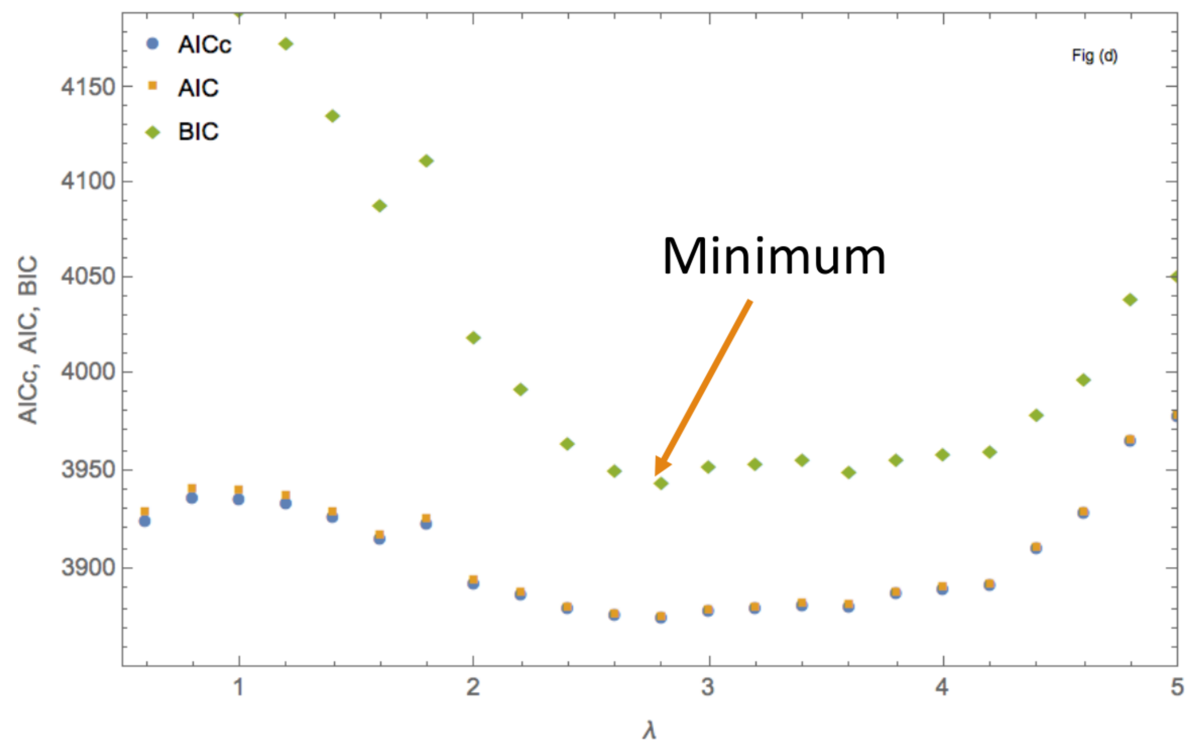

Toy Model Results

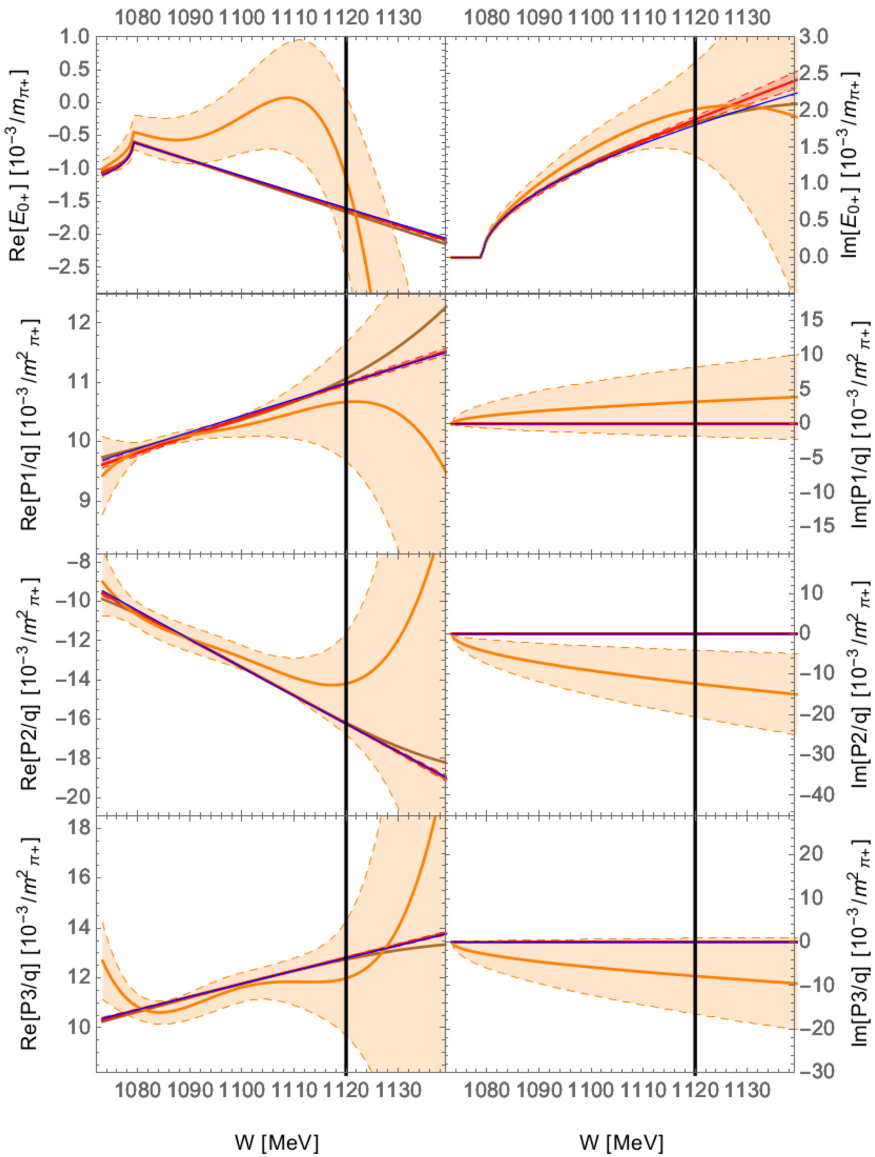

- Generate data from a toy model using a 9 parameter model (2 real S-waves, 1 imaginary S-wave, and 2 real $P_{1,2,3}$ –waves shown in blue
- LASSO (red) eliminates 36 parameters from a 46 parameter fit (orange) and reconstructs the true solution (blue) quite accurately
- LASSO sets all imaginary parts of P-waves and D- waves correctly to 0
- LASSO solution predicts true solution quite accurately beyond the fitted W_{max} =1120 MeV

Model selection with real data

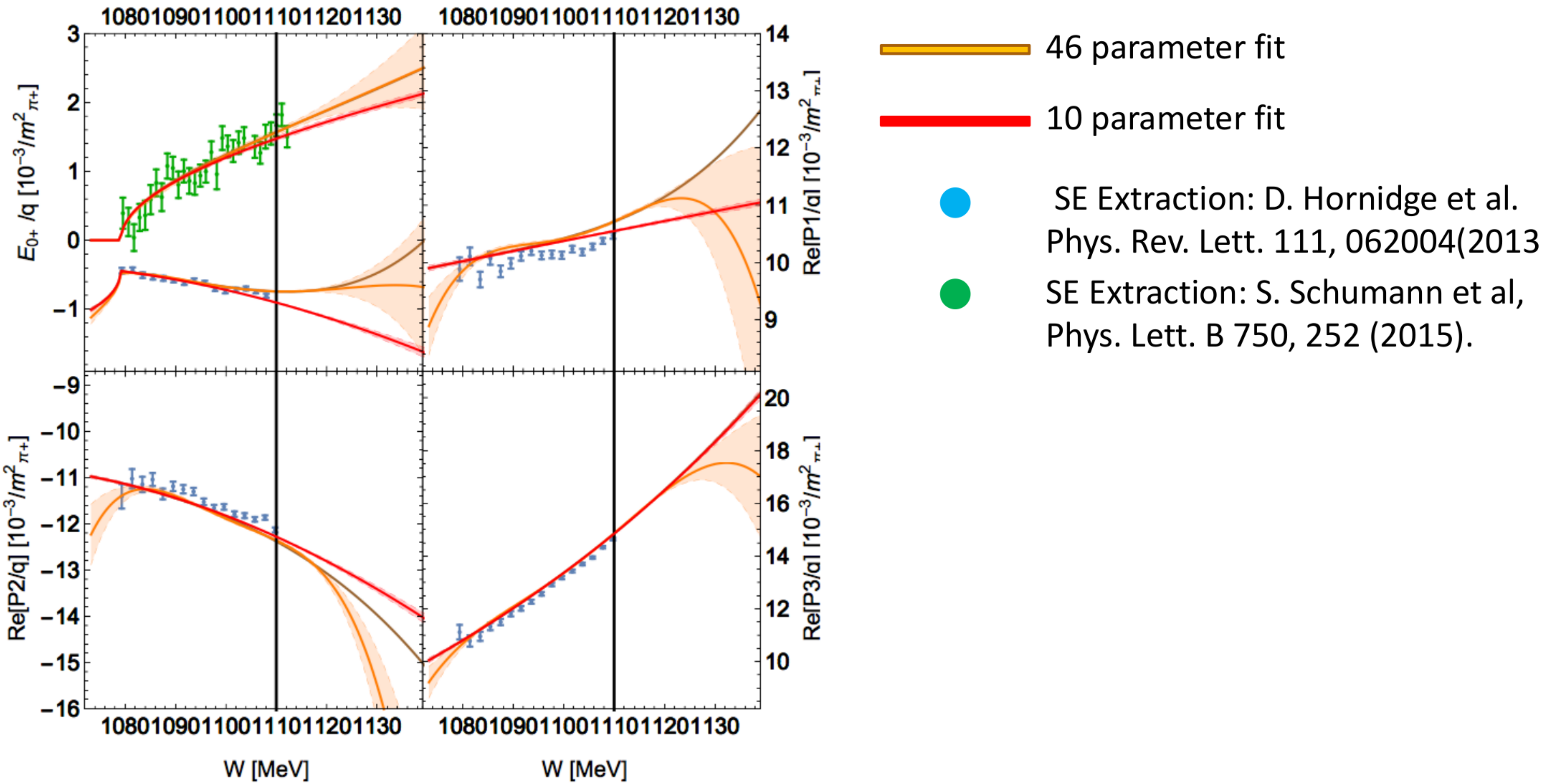

→ Selection of relevant partial waves in fit of scarce lattice QCD data

Details 3→ 3 formalism

$$
\begin{aligned}
\langle q_1, q_2, q_3 | \hat{T}(s) | p_1, p_2, p_3 \rangle &= \langle q_1, q_2, q_3 | \hat{T}_c(s) | p_1, p_2, p_3 \rangle + \langle q_1, q_2, q_3 | \hat{T}_d(s) | p_1, p_2, p_3 \rangle \qquad (1) \\
&= \frac{1}{3!} \sum_{n=1}^{3} \sum_{m=1}^{3} v(q_{\bar{n}}, q_{\bar{\bar{n}}}) \hat{T}(q_n, p_m; s) v(p_{\bar{m}}, p_{\bar{\bar{m}}}) \\
&:= \frac{1}{3!} \sum_{n=1}^{3} \sum_{m=1}^{3} v(q_{\bar{n}}, q_{\bar{\bar{n}}}) \left(\tau(\sigma(q_n))\, T(q_n, p_m; s)\, \tau(\sigma(p_m)) - 2E(q_n) \tau(\sigma(q_n)) (2\pi)^3 \delta^3(\mathbf{q}_n - \mathbf{p}_m) \right) v(p_{\bar{m}}, p_{\bar{\bar{m}}})
\end{aligned}
$$

$$
T(q, p; s) = B(q, p; s) - \int \frac{\mathrm{d}^3 \boldsymbol{l}}{(2\pi)^3} B(q, l; s) \frac{1}{2E(l) D(\sigma(l))} T(l, p; s) \,,
$$

$$
\frac{1}{\tau(\sigma(l))} = \sigma(l) - M_0^2 - \int \frac{d^3 \boldsymbol{k}}{(2\pi)^3} \frac{\lambda^2 (f(4\boldsymbol{k}^2))^2}{2E(k)(\sigma(l) - 4E(k)^2 + i\epsilon)} \,,
$$

$$
B(q, p; s) = -\frac{\lambda^2 f((P - q - 2p)^2) f((P - 2q - p)^2)}{2E(q + p)\, (W - E(q) - E(p) - E(q + p) + i\epsilon)}
$$

Which role do other “diagrams” play?

- Preferable to think in on-shell amplitudes (2→ 2 and 3→ 3), not in “diagrams”; if one still insists:

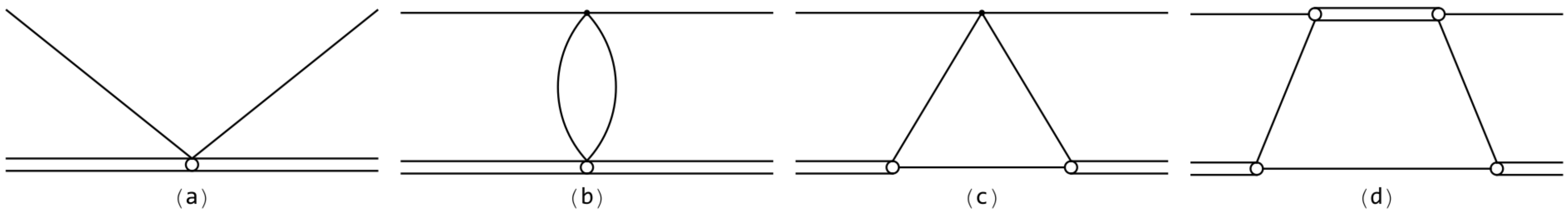

Genuine 3-body force

Non-local but real interaction

Part of isobar Insertion (d)

Cancellation mechanism of 2-body poles

2→2 boosted eigenvalues
In principle present

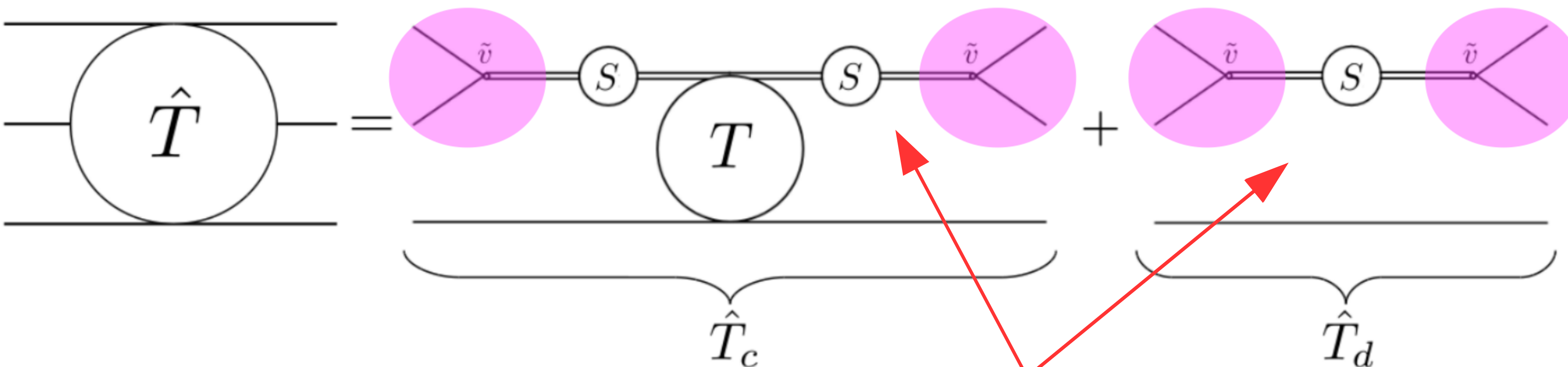

Subtle but complete cancellations involving disconnected topology

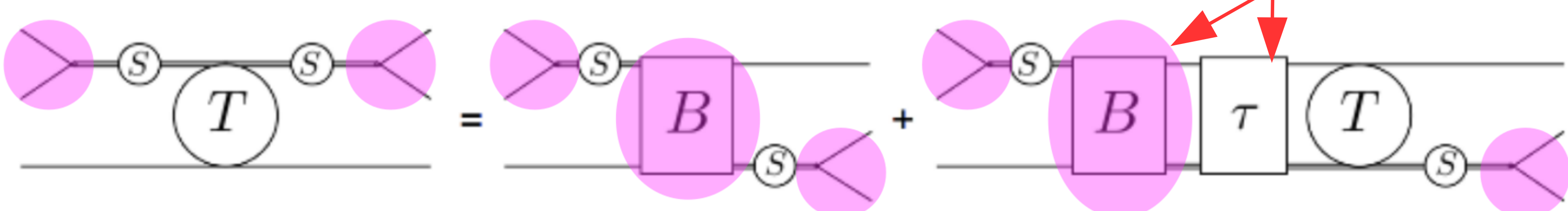

Relevance of three-body dynamics

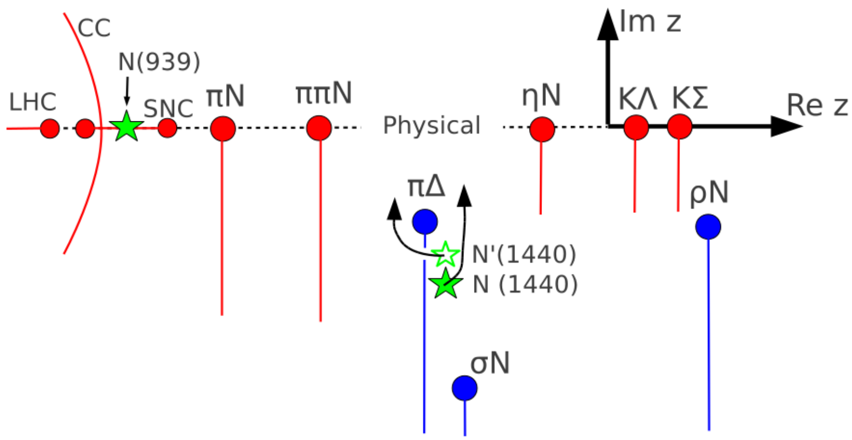

- Roper pole + $\pi\Delta$ branch point $\rightarrow$ non-standard resonance shape.
- See results by GWU/SAID data analysis center.

- Where is the 3$*$ N(1710)?
  [S. Ceci, M.D. et al, PRC84, 2011]

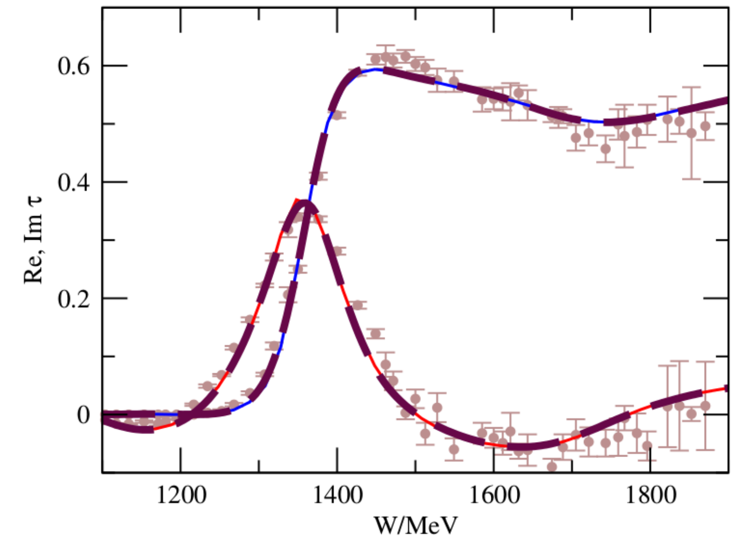

Fit of a model without ρN branch point (CMB type) [solid lines] to the Jülich amplitude [dashed lines]

- CMB fit to JM has pole at $1698 - 130\,i$ MeV, simulates missing branch point.

- Inclusion of full analytic structure important to avoid false pole signals in baryon spectroscopy.

Toward Data-driven Analyses

[M.D., Revier, Rönchen, Workman, arXiv:1603.07265, PRC 2016]

- Multi-channel analyses to detect faint resonance signals
- All groups use GW/SAID partial waves for $\pi N \to \pi N$
  - The chi-square obtained in fits to single-energy solutions is not related to chi-square of a fit to data → Statistical interpretation of resonance signals difficult.
- Provide online covariance matrices etc. to allow other groups to perform *correlated chi-square* fits.

Slight adaptation of their code allows other groups to obtain a χ^2 (almost) as if they fitted to $\pi N \to \pi N$ directly.

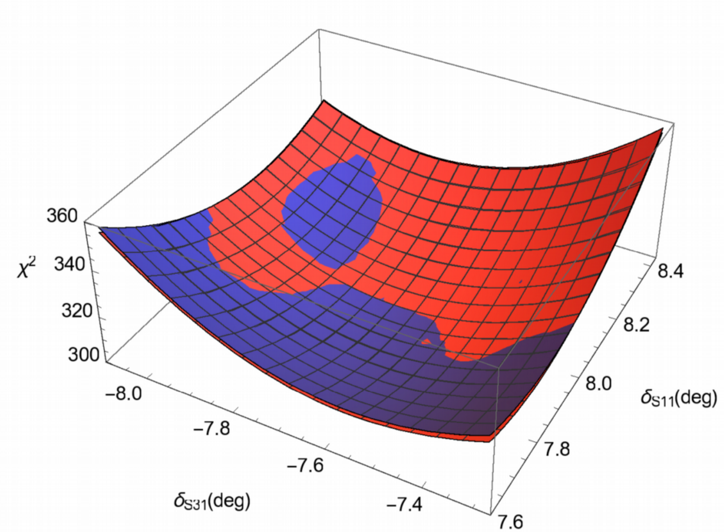

$$\chi^2(\mathbf{A}) = \chi^2(\hat{\mathbf{A}}) + (\mathbf{A} - \hat{\mathbf{A}})^T \hat{\Sigma}^{-1} (\mathbf{A} - \hat{\mathbf{A}}) + \mathcal{O}(\mathbf{A} - \hat{\mathbf{A}})^3$$

Covariance matrices etc. can be downloaded on the SAID and JPAC web pages.

$$\boxed{S = \mathbb{1} + iT}$$

Unitarity: $SS^\dagger = 1 \Leftrightarrow -i(T - T^\dagger) = T\,T^\dagger$

- 3-body unitarity:
  discontinuities from t-channel exchanges
  $\rightarrow$ Meson exchange from requirements of the S-matrix

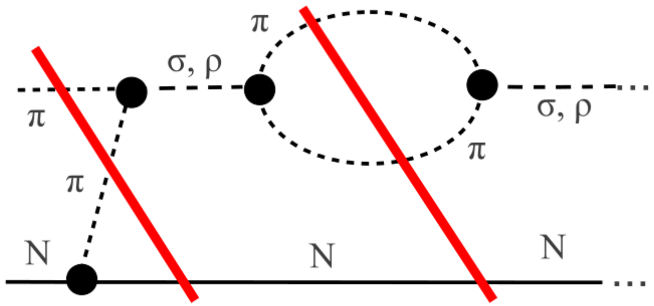

Other cuts

- to approximate left-hand cut $\rightarrow$ Baryon u-channel exchange
- σ, ρ exchanges from crossing plus analytic continuation.

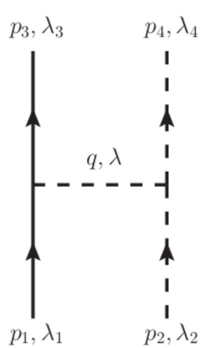

$\vec{q} = \vec{p}_1 - \vec{p}_3$

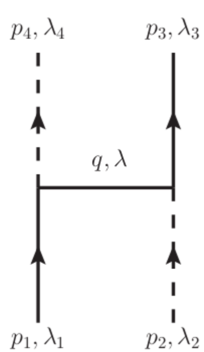

$\vec{q} = \vec{q}_1 - \vec{p}_4$

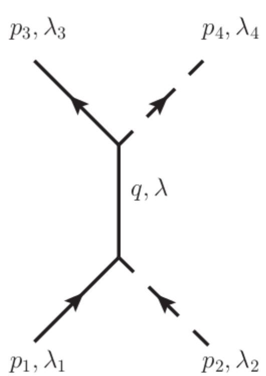

$\vec{q} = \vec{p}_1 + \vec{p}_2 = 0$

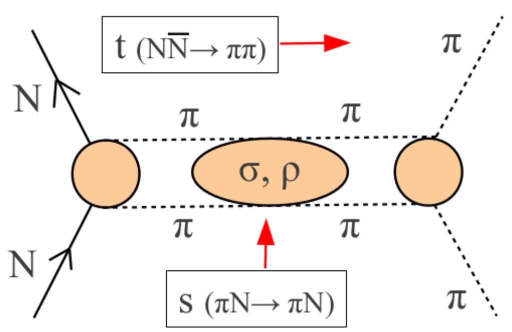

Amplitude reconstruction from complete experiments and truncated partial-wave expansions

[Workman, Tiator, Wunderlich, M.D., H. Haberzettl, PRC (2017)]

How do complete experiment and truncated partial wave complete experiment compare. Depending on which partial-wave content is admitted in the amplitude?

Set	Included Partial Waves	CEA	TPWA	Complete Sets for TPWA
1	$L=0$ (E_{0+})	1(1)	1(1)1	$I[1]$
2	$J=1/2$ (E_{0+}, M_{1-})	4(4)	4(4)1	$I[1], \check{P}[1], \check{C}_x[1], \check{C}_z[1]$
			4(3)2	$I[2], \check{P}[1], \check{C}_x[1]$
3	$L=0,1$ (E_{0+}, M_{1-}, E_{1+})	6(6)	6(6)1	$I[1], \check{\Sigma}[1], \check{T}[1], \check{P}[1], \check{F}[1], \check{G}[1]$
			6(4)2	$I[2], \check{\Sigma}[1], \check{T}[2], \check{P}[1]$
			6(3)3	$I[3], \check{\Sigma}[1], \check{T}[2]$
4	$L=0,1$ $(E_{0+}, M_{1-}, E_{1+}, M_{1+})$	†		TPWA at 1 angle not possible
	full set of 4 S, P wave multipoles		8(5)2	$I[2], \check{\Sigma}[1], \check{T}[2], \check{P}[2], \check{F}[1]$
			8(4)3	$I[3], \check{\Sigma}[1], \check{F}[2], \check{H}[2]$
5	$L=0,1,2$ $(E_{0+}, M_{1-}, E_{1+}, E_{2-})$	8(8)	8(8)1	$I[1], \check{\Sigma}[1], \check{T}[1], \check{P}[1], \check{F}[1], \check{G}[1], \check{C}_x[1], \check{O}_x[1]$
			8(4)2	$I[2], \check{\Sigma}[2], \check{T}[2], \check{P}[2]$
			8(3)3	$I[3], \check{\Sigma}[2], \check{T}[3]$
6	$J \leq 3/2$ $(E_{0+}, M_{1-}, E_{1+}, M_{1+}, E_{2-}, M_{2-})$	†		TPWA at 1 or 2 angles not possible
			12(5)3	$I[3], \check{\Sigma}[2], \check{T}[3], \check{P}[2], \check{F}[2]$
			12(4)4	$I[4], \check{\Sigma}[2], \check{F}[3], \check{H}[3]$
7	$L=0,1,2$ $(E_{0+}, \ldots, M_{2+})$	†		TPWA at 1 or 2 angles not possible
	full set of 8 S, P, D wave multipoles		16(6)3	$I[3], \check{\Sigma}[3], \check{T}[3], \check{P}[3], \check{F}[3], \check{G}[1]$
			16(5)4	$I[4], \check{\Sigma}[3], \check{T}[3], \check{P}[3], \check{F}[3]$
			$\boxed{16(4)5}$	$\boxed{I[5], \check{\Sigma}[3], \check{F}[4], \check{H}[4]}$

Four are enough!

Order:
# of different measurements,
# of different observables
# of different angles

Connecting Theory and Phenomenology at the pole

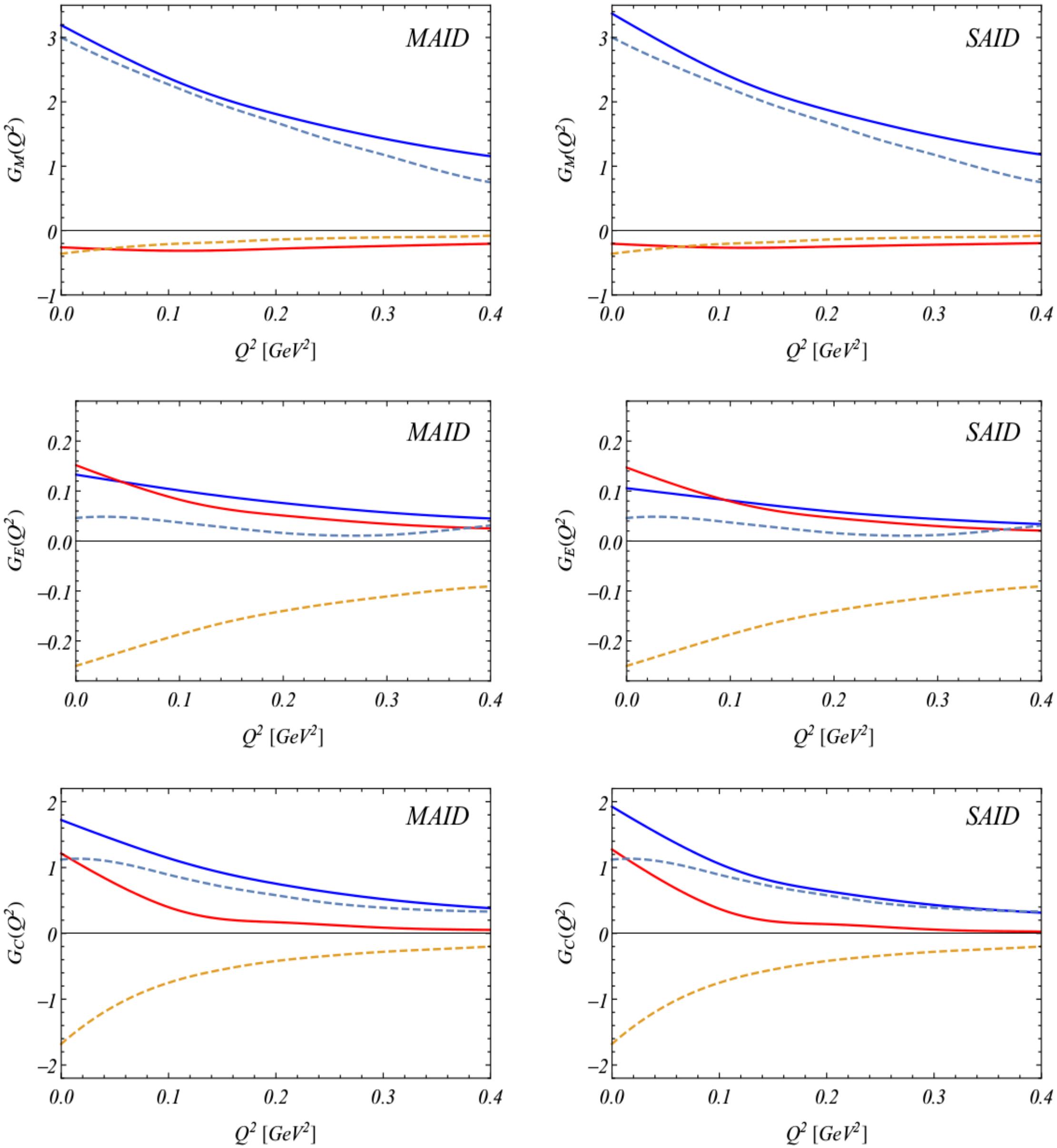

FIG. 4: Magnetic, electric and charge transition form factors compared with the Heavy Baryon chiral effective field theory of Gail and Hemmert [14] at low Q^2. The blue and red lines show real and imaginary parts of the complex pole form factors obtained from MAID and SAID. The dashed lines are the HBChEFT calculations.

T.A. Gail and T.R. Hemmert, Eur. Phys. J. A 28 (2006).

Lattice: Agadjanov, Bernard, Meißner, Rusetsky, Nucl. Phys. B 886 (2014)

New High-precision πN data

$\pi^- p \to \pi^- p$ scattering

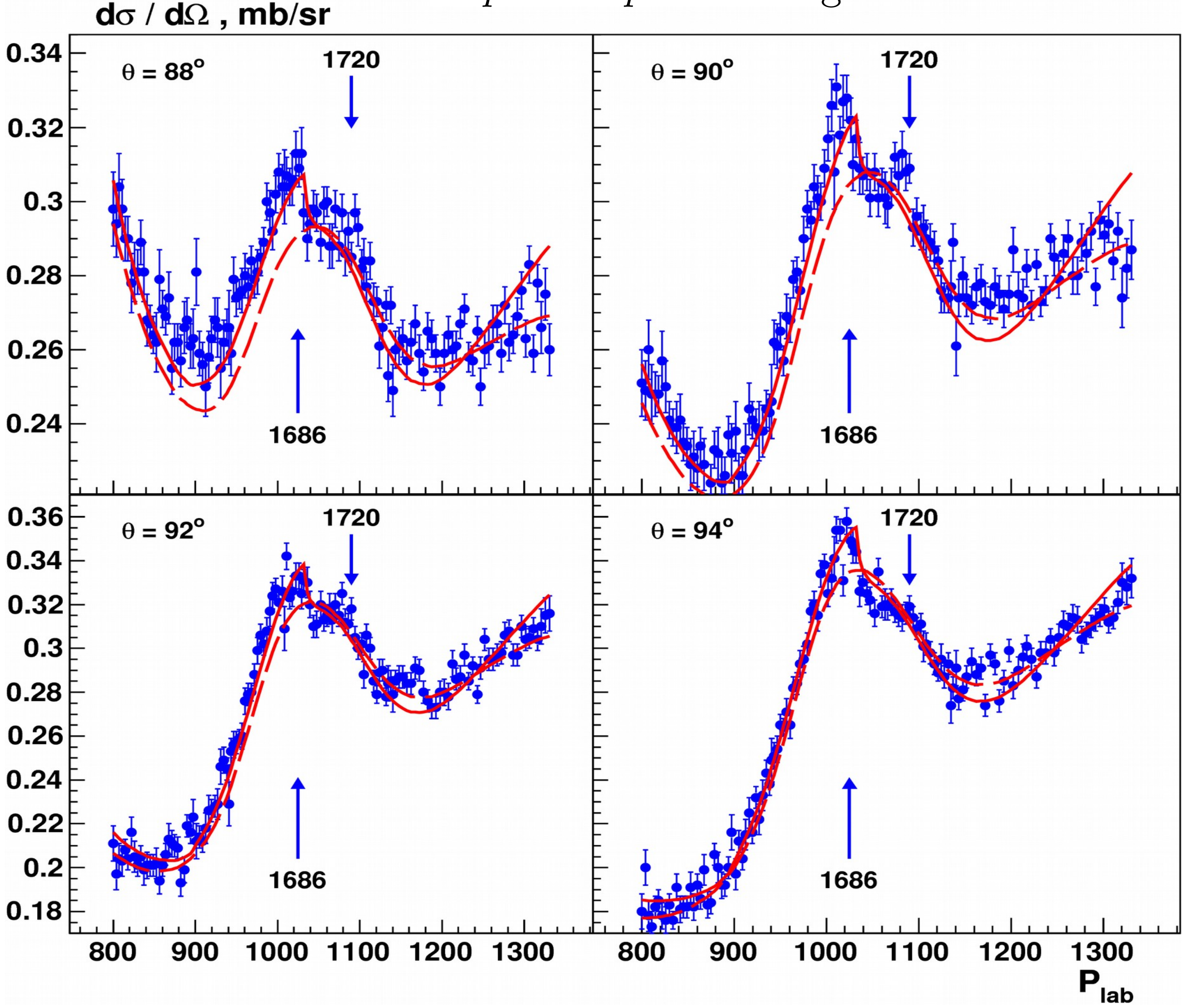

Data: EPECUR
Analysis: SAID (dashed)
Gridnev (solid)
ArXiv: 1604.02379

Sharp structures seen in EPECUR data are largely accounted for by channel-coupling ($K\Sigma$) leaving less room for narrow resonance candidates.

In general:

Hadronic data serves as “input” for many PWAs!

Photocouplings at the pole

selected results

$$\tilde{A}^h_{pole} = A^h_{pole}\, e^{i\vartheta^h}$$
$$h = 1/2,\ 3/2$$

$$\tilde{A}^h_{pole} = I_F \sqrt{\frac{q_p}{k_p} \frac{2\pi\,(2J+1)\mathrm{E_0}}{m_N\ \mathbf{r}_{\pi \mathrm{N}}}}\ \mathrm{Res}\, A^h_{L\pm}$$

I_F: isospin factor
q_p (k_p): meson (photon) momentum at the pole
$J = L \pm 1/2$ total angular momentum
E_0: pole position
$r_{\pi N}$: elastic πN residue

	$A^{1/2}_{pole}$ [10^{-3} GeV$^{-1/2}$]		$\vartheta^{1/2}$ [deg]		$A^{3/2}_{pole}$ [10^{-3} GeV$^{-1/2}$]		$\vartheta^{3/2}$ [deg]	
fit→	1	2	1	2	1	2	1	2
$N(1710)\ 1/2^+$	15	28^{+9}_{-2}	13	77^{+20}_{-9}				
$\Delta(1232)\ 3/2^+$	-116	-114^{+10}_{-3}	-27	-27^{+4}_{-2}	-231	-229^{+3}_{-4}	-15	$-15^{+0.3}_{-0.4}$

Fit 1: only **single** polarization observables included

Fit 2: also **double** polarization observables included

FROST/CLAS (I)

The E-observable in charged-pion photoproduction

CLAS/BnGa/JuBo/SAID, PLB **750** (2015)

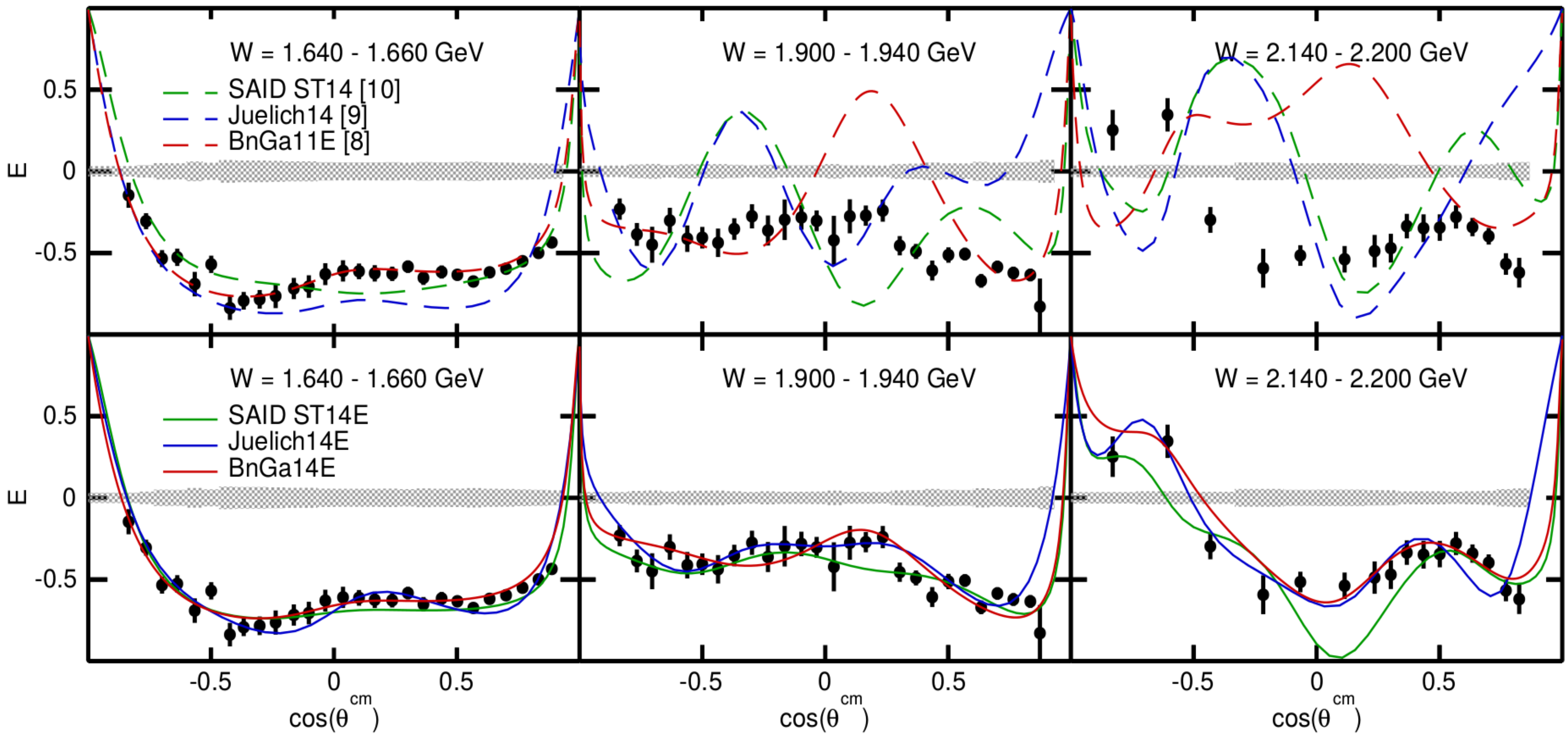

→ Significant impact on resonance parameters/
New resonance (BnGa) [$\Delta(2200)7/2^-$], arXiv: 1503.05774

T and F in $\gamma p \to \eta p$ (MAMI)

EPJA 51, 6 (2015)

Data: Akondi *et al.* (A2 at MAMI) PRL 113, 102001 (2014)

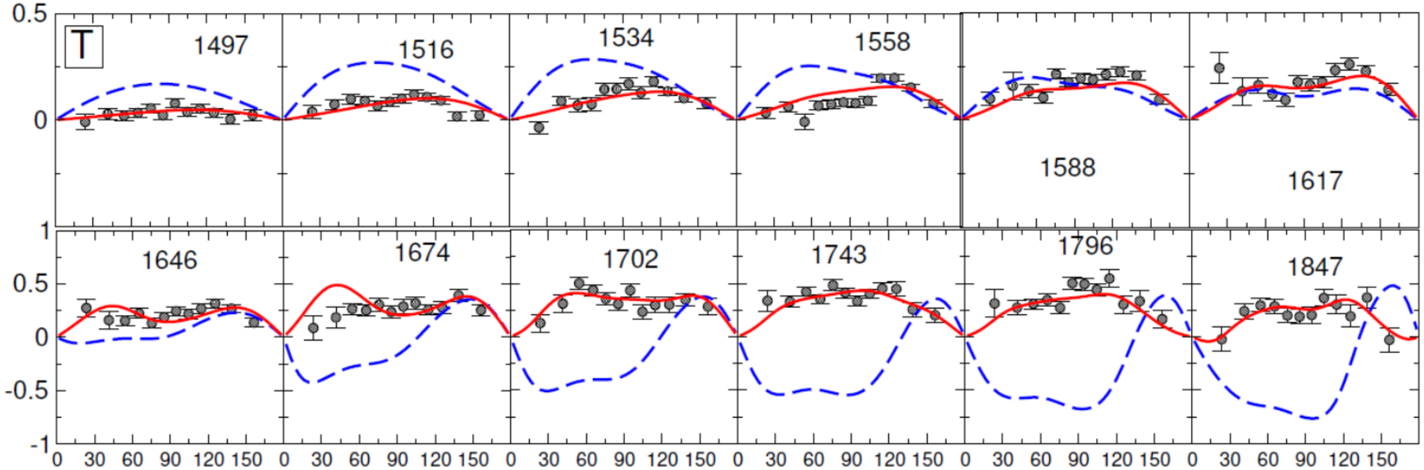

prediction

fit

Beam	Target	Recoil
0	$+y$	0
0	$-y$	0

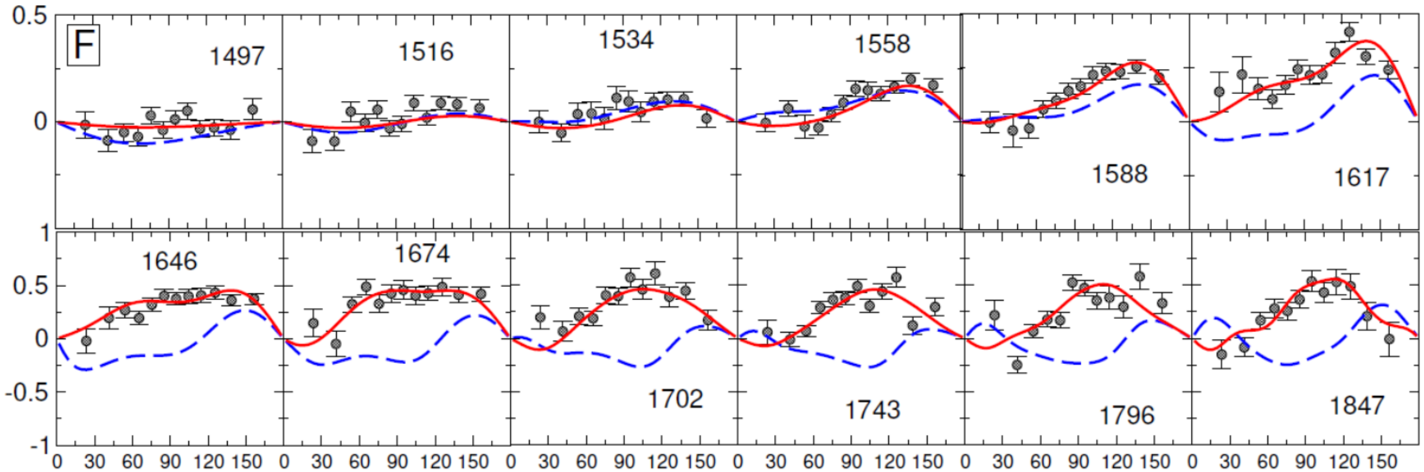

Beam	Target	Recoil
$+1$	$+x$	0
-1	$+x$	0

Older, more incomplete Chiral unitary prediction

[Jido, M.D., Oset, PRC77 (2008)]

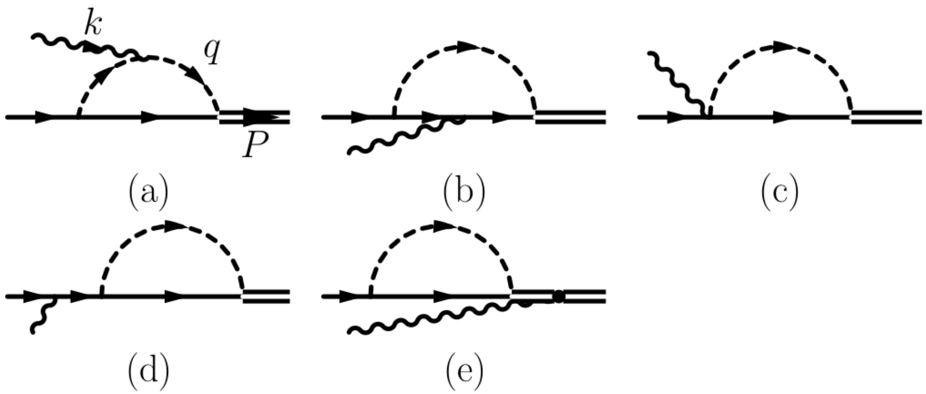

$\pi N,\ \eta N,\ K\Lambda,\ K\Sigma$ channels

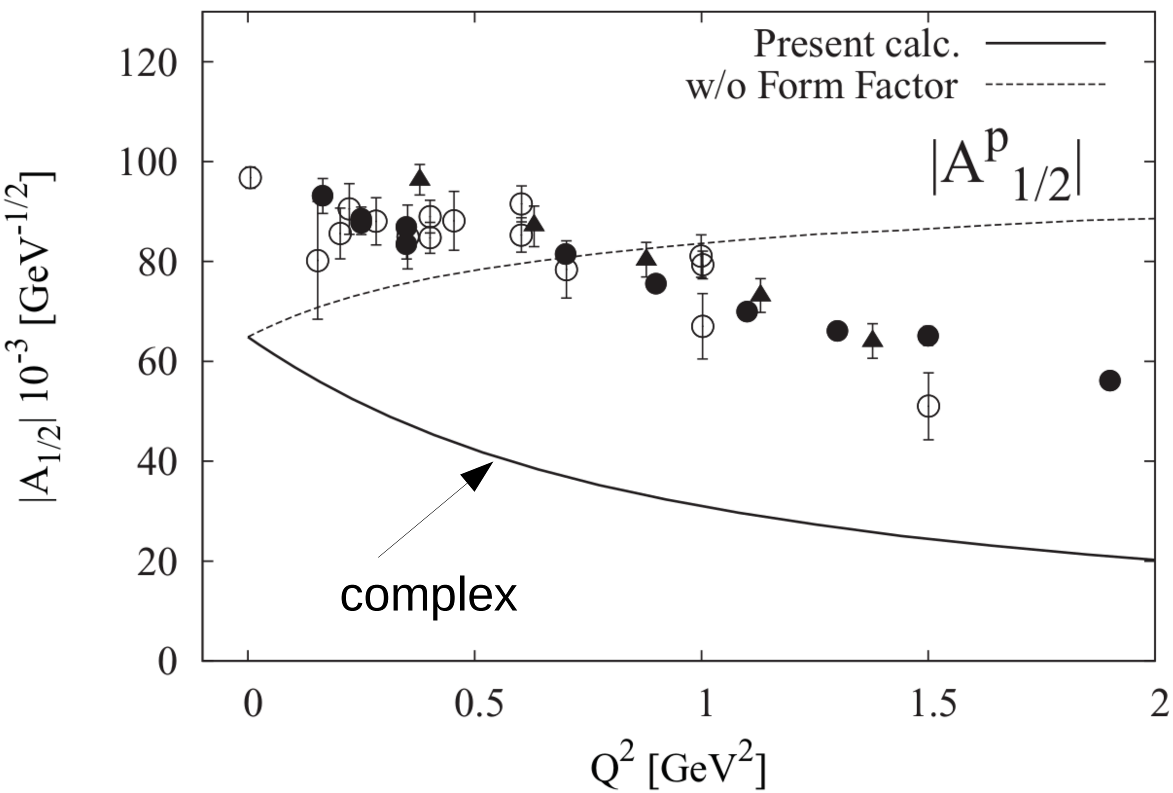

Discrepancy: Genuine problem
or due to different definitions?

This workshop: remarkable progress
On complex helicity couplings
by ANL-Osaka group.

Input parameters and their stability

Eur. Phys. J. A (2013) 49: 44

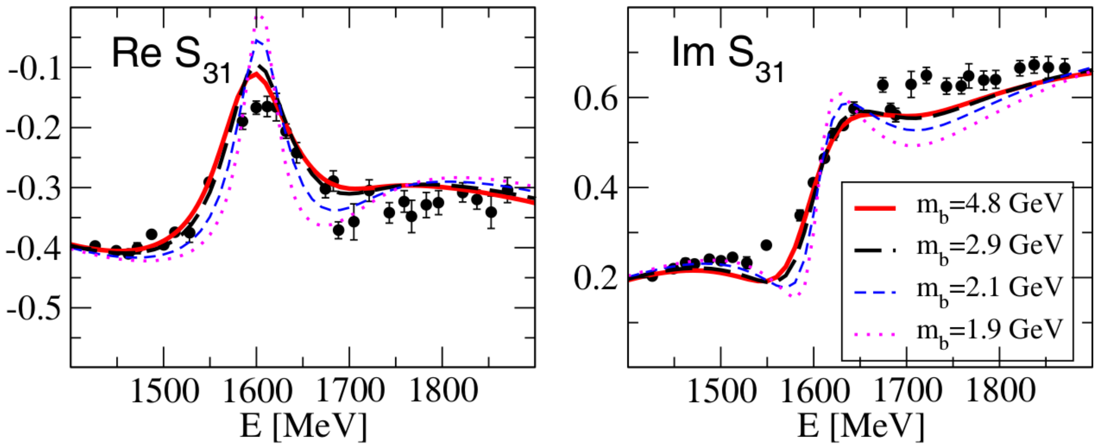

Force bare mass of $\Delta(1600)$
to fixed value; refit full data base

$$\pi N \to \pi N,\ \eta N,\ K\Lambda,\ K\Sigma$$

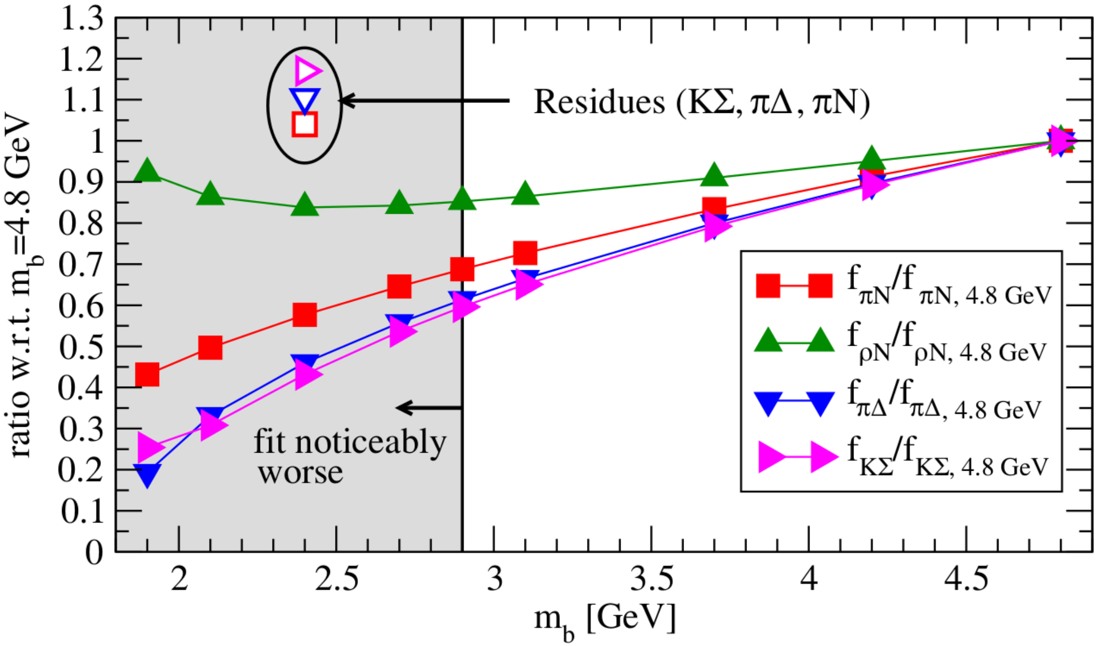

Self energy:

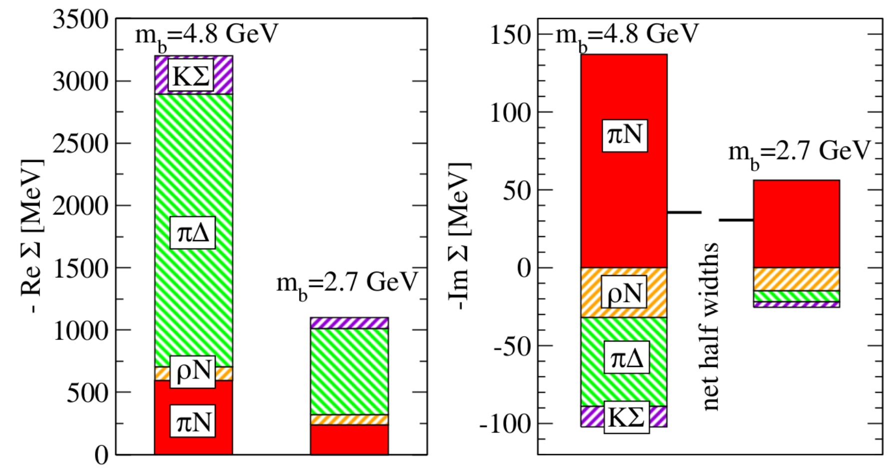

How to quantify the impact of new measurements?

Consider correlations of helicity couplings extracted from experiment

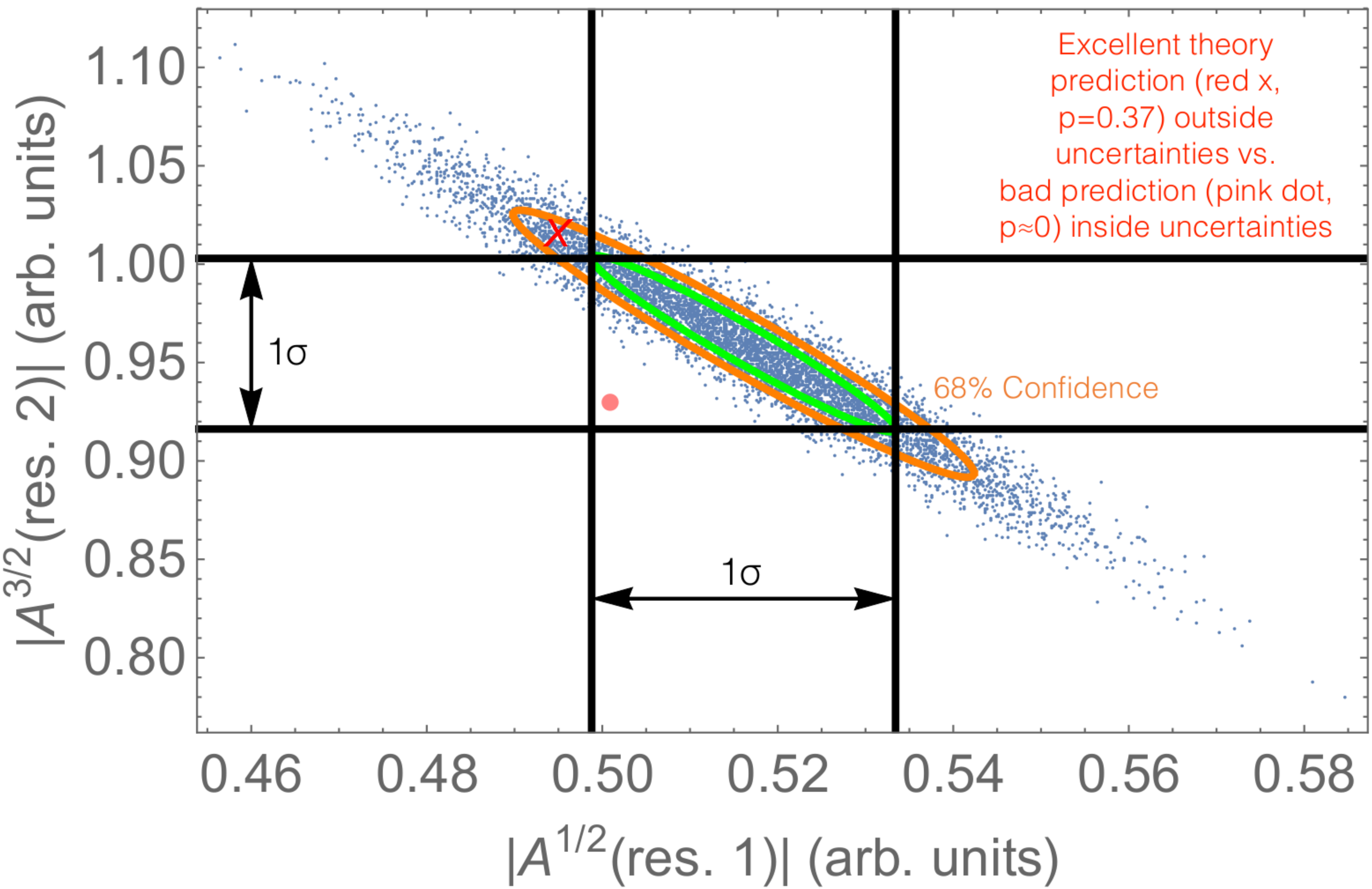

Results from analysis of world data of η photoproduction

[M.D., D. Sadasivan, in preparation]

Here $A = |A|e^{i\phi}$ defined at the resonance pole.

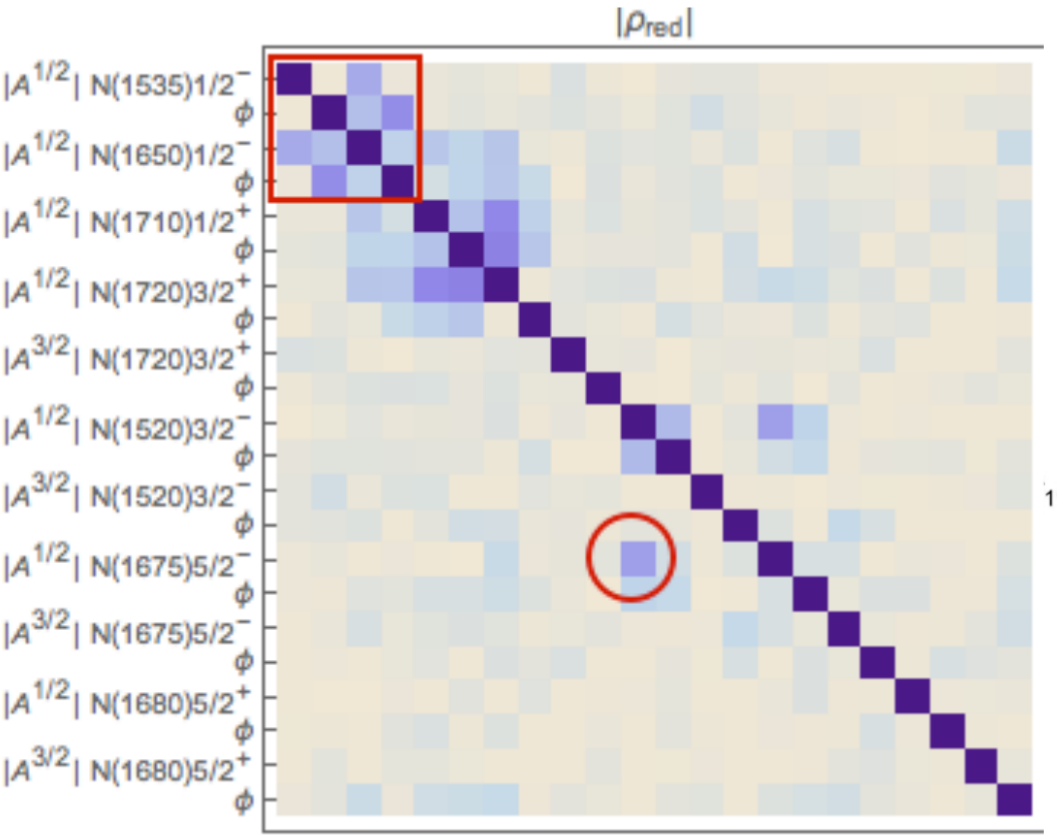

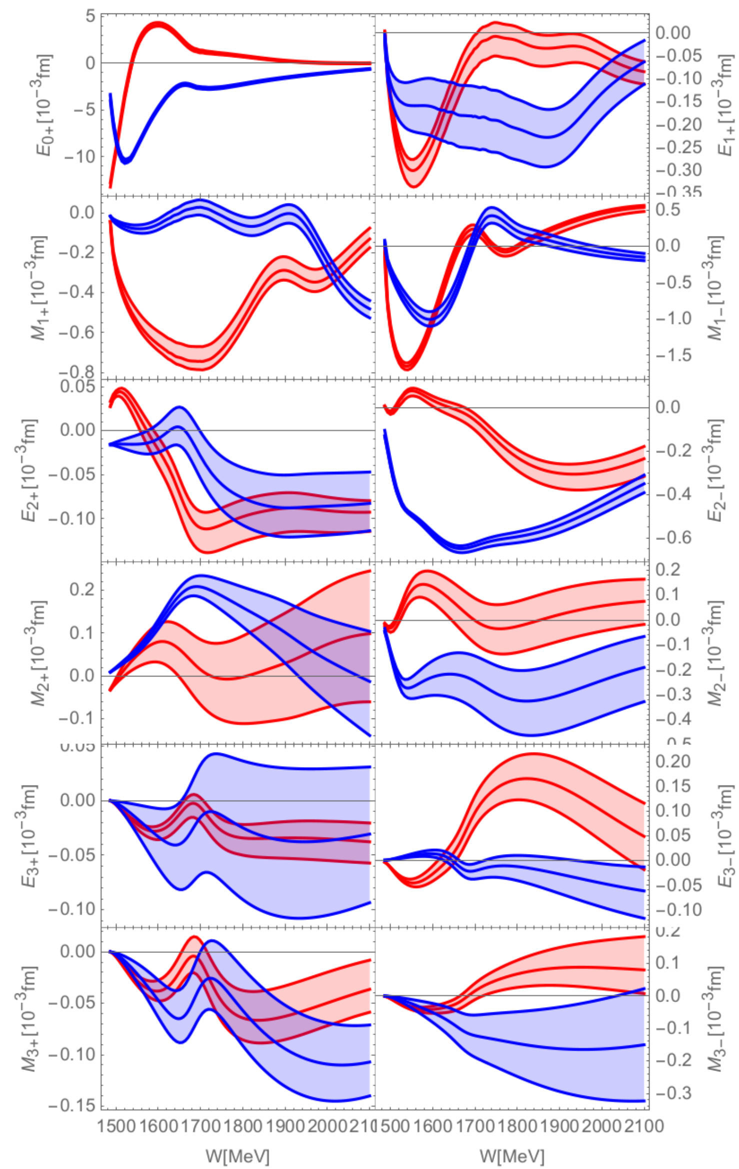

Bulk properties of uncertainties from different data sets

Helicity Coupling	All	No E	No F	No T	No Σ
Number of Data Points	6425	6369	6281	6281	6022
Generalized Variance	0.0494	0.0521	0.1288	0.1239	6.664
$\sqrt{\mathrm{Tr}\, C}$	10.4965	10.51	12.00	11.423	19.85
Multicollinearity	8.173	8.203	9.280	9.5323	10.371
Condition number	133.61	132.10	173.664	164.1	322.66

C=Covariance Matrix

Generalized Variance = Det[C] ~Volume of the Error Ellipsoid

Helicity Coupling	No artificial data	Cx	Cz	Cx and Cz
Number of Data Points	6425	6569	6569	6713
Generalized Variance	0.0494	0.03758	0.0362	0.0132
$\sqrt{\mathrm{Tr}\, C}$	10.4965	10.72	10.487	10.102
Multicollinearity	8.173	7.599	6.770	6.157
Condition number	133.61	112.47	109.69	107.683

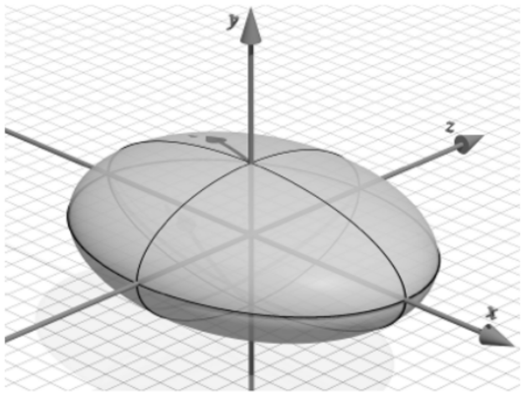

- Allows to trace quantitatively the impact of data sets and observables
- Helpful in design of new measurements
- Correlations allow to assess quality of theory predictions

Field-theoretical approach; TOPT unitarized; implemented on supercomputers.
Example:

$$\gamma N \ (\pi N) \to K\Sigma$$